



**Identification and Functional Study of Potential Receptors Involved in
Vitellogenesis of Female Banana Shrimp *Fenneropenaeus merguensis***

Manita Nonsung

**A Thesis Submitted in Partial Fulfillment of the Requirements for the
Degree of Master of Science in Molecular Biology
and Bioinformatics (International Program)**

Prince of Songkla University

2021

Copyright of Prince of Songkla University



**Identification and Functional Study of Potential Receptors Involved in
Vitellogenesis of Female Banana Shrimp *Fenneropenaeus merguensis***

Manita Nonsung

**A Thesis Submitted in Partial Fulfillment of the Requirements for the
Degree of Master of Science in Molecular Biology
and Bioinformatics (International Program)**

Prince of Songkla University

2021

Copyright of Prince of Songkla University

Thesis Title Identification and functional study of potential receptors involved in vitellogenesis of female banana shrimp *Fenneropenaeus merguensis*

Author Miss Manita Nonsung

Major Program Molecular Biology and Bioinformatics

Major Advisor

.....
(Asst. Prof. Dr. Ponsit Sathapondecha)

Examining Committee:

.....Chairperson
(Assoc. Prof. Dr. Apinunt Udomkit)

.....Committee
(Asst. Prof. Dr. Ponsit Sathapondecha)

Co-advisor:

.....
(Asst. Prof. Dr. Unitsa Sangket)

.....Committee
(Asst. Prof. Dr. Unitsa Sangket)

.....Committee
(Asst. Prof. Dr. Warapond Wanna)

The Graduate School, Prince of Songkla University, has approved this thesis as partial fulfillment of the requirements for the Master of Science Degree in Molecular Biology and Bioinformatics

.....
(Prof. Dr. Damrongsak Faroongsarng)
Dean of Graduate School

This is to certify that the work here submitted is the result of the candidate's own investigations. Due acknowledgement has been made of any assistance received.

.....Signature
(Asst. Prof. Dr. Ponsit Sathapondecha)
Major Advisor

.....Signature
(Asst. Prof. Dr. Unitsa Sangket)
Co-advisor

.....Signature
(Miss Manita Nonsung)
Candidate

I hereby certify that this work has not been accepted in substance for any degree, and is not being currently submitted in candidature for any degree.

.....Signature

(Miss Manita Nonsung)

Candidate

ชื่อวิทยานิพนธ์ การระบุและศึกษาหน้าที่ของยีนรีเซพเตอร์ที่เกี่ยวข้องกับกระบวนการพัฒนารัง

ไขในแม่กุ้งแชบ๊วย

ผู้เขียน นางสาว มานิตา โนนสูง

สาขาวิชา ชีววิทยาโมเลกุลและชีวสารสนเทศ

ปีการศึกษา 2563

บทคัดย่อ

ยีนตัวรับสัญญาณเป็นหนึ่งในปัจจัยสำคัญที่มีบทบาทแรกเริ่มโดยการส่งสัญญาณต่าง ๆ ที่เกี่ยวกับการควบคุมกระบวนการทางสรีระร่างกายที่สำคัญ เช่น กระบวนการสืบพันธุ์ ในสิ่งมีชีวิต ในงานวิจัยนี้มีวัตถุประสงค์ที่จะระบุและศึกษาบทบาทหน้าที่ของยีนตัวรับสัญญาณที่เกี่ยวข้องต่อกระบวนการพัฒนารังไขในแม่กุ้งแชบ๊วยโดยอาศัยการวิเคราะห์ลำดับดีเอ็นเอจำนวนมากด้วย Illumina RNA sequencing และการวิเคราะห์ทางชีวสารสนเทศ ผลการศึกษาพบว่าสามารถสร้างทรานสคริปโตมจากรังไขกุ้งแชบ๊วยเพศเมียในแต่ละระยะการพัฒนารังไขได้ยีนทั้งหมด 53,763 ยีน โดยระบุเป็นยีนตัวรับสัญญาณจำนวน 663 ยีน การวิเคราะห์การแสดงออกของยีนในแต่ละระยะการพัฒนารังไขพบว่ายีนตัวรับสัญญาณจำนวน 185 ยีน จากยีนที่แสดงออกแตกต่างกันในการศึกษานี้ตัวรับสัญญาณจำนวน 15 ยีน ที่มีการแสดงออกแตกต่างในระยะเวลาการพัฒนารังไข และเกี่ยวข้องกับกระบวนการพัฒนาระบบสืบพันธุ์ ได้ถูกเลือกมาเพื่อศึกษาการแสดงออก ด้วยวิธี qRT-PCR นอกจากนี้ได้ทำการเลือก bone morphogenetic protein receptor ประเภท 1 (BMPRI) หรือ saxophone (*FmSax*) และ BMPR ประเภท 2 (*FmBMPRII*) ในการศึกษาบทบาทหน้าที่ต่อกระบวนการพัฒนารังไข พบว่า ทั้งยีนตัวรับ *FmSax* and *FmBMPRII* ต่างก็มีการแสดงออกสูงในก้านตา เมื่อเทียบกับเนื้อเยื่อ อื่น ๆ เมื่อศึกษาการแสดงออกในรังไขและตับ พบว่ายีนตัวรับ *FmSax* มีการแสดงออกสูงระยะไข่สูงในขณะที่ *FmBMPRII* มีการแสดงออกสูงระยะกำลังพัฒนา ในการศึกษาหน้าที่ของยีนในระบบสืบพันธุ์อาศัยเทคนิค RNA interference โดยสามารถผลิตอาร์เอ็นเอสายคู่ที่จำเพาะต่อยีน *FmSax* (dsSax) จากแบคทีเรีย

Escherichia coli โดยหลังจากฉีด dsSax เข้าไปในกึ่งแซบวียเพคเมียไป 7 วัน พบว่า การแสดงออกของ *FmSax* ลดลงอย่างมีนัยสำคัญ และยังส่งผลให้การแสดงออกของยีนไวทิลโลจินิน (*FmVg*) และ *FmBMPRII* ลดลงทั้งในรังไข่และตับด้วย แต่หากการยับยั้งการแสดงออกของ *FmSax* กลับเพิ่มระดับการเจริญของเซลล์ไข่ ชี้ให้เห็นว่า *FmSax* มีบทบาทหน้าที่ควบคุมการแสดงออกของยีนไข่แดง และการเจริญของเซลล์ไข่

Thesis Title	Identification and functional study of potential receptors involved in vitellogenesis of female banana shrimp <i>Fenneropenaeus merguensis</i>
Author	Miss Manita Nonsung
Major Program	Molecular Biology and Bioinformatics
Academic Year	2020

ABSTRACT

One of several molecular factors control ovarian development in organisms is receptors which play an initial role in signaling pathways in several physiological processes, including reproduction. This study aimed to identify the potential receptors involved in the control of female banana shrimp, *Fenneropenaeus merguensis*, reproduction. The ovarian transcriptome derived from 4 developmental stages was constructed from Illumina RNA sequencing and bioinformatics analysis. A total of 53,763 transcripts was *de novo* assembled, and 663 genes were identified as receptors. Among them, 185 receptors were differentially expressed during ovarian development. The 15 differentially expressed receptor genes related to ovarian maturation were selected to validate for their expressions by qRT-PCR. In this study bone morphogenetic protein receptors (BMPR) were further characterized and studied their function in shrimp. Both saxophone (FmSax), a BMPR type I, and FmBMPR type II (FmBMPRII) were mainly expressed in eyestalks. The mRNA expression of *FmSax* was increased at the mature stage whilst expression of *FmBMPRII* was high at the late vitellogenic stage in both ovary and hepatopancreas. To study the role of FmSax, the double-stranded RNA specific to FmSax (dsSax) was produced in *Escherichia coli*. On day 7 after the injection of dsSax to female *F. merguensis* shrimps, *FmSax* expression was significantly suppressed, and vitellogenin (*Vg*) and *FmBMPRII* expressions were significantly increased in both ovary and hepatopancreas. In addition, the knockdown of *FmSax* led to induce oocyte proliferation *in vivo*. These suggested that FmSax positively controls *Vg* synthesis, but negatively regulates oocyte proliferation in shrimp.

ACKNOWLEDGEMENT

Firstly, I would like to express my sincere gratitude to my advisor, Asst. Prof. Dr. Ponsit Sathapondecha and my co-advisor, Asst. Prof. Dr. Unitsa Sangket for the continuous support of my master study and related research, and for giving me the opportunity to do research and providing invaluable guidance throughout this research and writing of this thesis. Their patience, motivation, vision, sincerity have deeply inspired me. They have taught me the methodology to proceed the research and to present the research works as clearly as possible. I am extremely grateful for what they have offered me. I am very grateful to Dr. Sukhuman Whankaew from the Faculty of Agricultural Technology and Community, Thaksin University, for her guidance helped writing this thesis. I also would like to thank the thesis examination committees for their valuable comments and suggestions.

I wish to acknowledge the research funding provided by PSU (Grant No. SCI6202049a) and the Science Achievement Scholarship of Thailand. Also, I wish to express my sincere thanks to the Center for Genomics and Bioinformatics Research, Division of Biological Science, Faculty of Science, Prince of Songkla University for providing necessary facilities for the research.

I would like to thank my lab mate, Ms. Thimpika Thepsuwan, and fellow master students for their feedback, cooperation, and of course friendship that we have had in the last years. In addition, I would like to special thanks to the staff of my department for the last-minute favors.

Finally, I must express my profound gratitude to my parents and to my brother for providing me with unfailing support and continuous encouragement throughout my study. This accomplishment would not have been possible without them. Thank you.

Manita Nonsung

CONTENTS

	Page
Approval Page	II
Certifications	III
ABSTRACT (Thai)	V
ABSTRACT (English)	VII
ACKNOWLEDGEMENTS	VIII
CONTENTS	IX
LIST OF TABLES	XIII
LIST OF FIGURES	XIV
LIST OF ABBREVIATIONS	XVI
CHAPTER 1 INTRODUCTION	1
1.1 Background and rationale	1
1.2 Literature reviews	2
1.2.1 <i>Fenneropenaeus merguensis</i>	2
1.2.2 Ovarian maturation	6
1.2.3 Receptors	8
1.2.4 Transcriptome	14
1.2.5 RNA interference	14
1.2.6 EdU assay	18
1.3 Objectives	18
CHAPTER 2 MATERIALS AND METHODS	19
2.1 Materials	19
2.1.1 Animal samples	19
2.1.2 Bacterial samples	19
2.1.3 Plasmid vectors	19
2.1.4 Culture medium	20
2.1.5 Chemical reagents	23
2.2 Methodology	25
2.2.1 Sample preparation and RNA sequencing (RNA-seq)	25

CONTENTS (cont.)

	Page
CHAPTER 2 MATERIALS AND METHODS	26
2.2.2 <i>De novo</i> transcriptome assembly	26
2.2.3 Gene functional annotation	26
2.2.4 Differentially expressed gene (DEG) analysis	26
2.2.5 Identification of candidate receptor genes involved in ovarian maturation	27
2.2.6 RNA extraction	27
2.2.7 The first stranded complementary DNA synthesis	28
2.2.8 Determination of the candidate receptor gene expression in shrimp by quantitative realtime PCR (qRT-PCR)	28
2.2.9 Determination of primer efficiency by qPCR	39
2.2.10 The qRT-PCR reaction and relative quantification of gene expression	32
2.2.11 Construction of recombinant plasmid containing an inverted repeat sequence of saxophone	32
2.2.12 Cloning of the inverted repeat sequence of <i>FmSax</i> in an expression vector	33
2.2.13 Production of receptor-specific dsRNA in bacteria	35
2.2.14 Effect of the <i>FmSax</i> knockdown on vitellogenesis in shrimp	36
2.2.15 Statistical analysis	38
CHAPTER 3 RESULTS	39
3.1 Transcriptome sequencing and analysis	39
3.2 Functional annotation of receptor genes	39
3.3 Identification of candidate receptor gene in <i>F. merguensis</i> 's ovaries	43

CONTENTS (cont.)

	Page
CHAPTER 3 RESULTS	
3.4 Determination of the candidate receptor gene expression during ovarian developmental stages	43
3.5 Expression analysis of <i>FmSax</i> and <i>FmBMPRII</i> in shrimp tissues and hepatopancreas during ovarian development	48
3.6 Sequence characteristics and phylogenetic analysis of bone morphogenetic protein receptors	49
3.7 Production of the saxophone specific double-stranded RNA	54
3.8 Effect of <i>FmSax</i> silencing on vitellogenesis in female <i>F. merguensis</i>	54
CHAPTER 4 DISCUSSION	60
CHAPTER 5 CONCLUSION	72
REFERENCES	69
APPENDICES	90
Appendix A results	90
Appendix B proceeding	105
VITAE	116

LIST OF TABLES

	Page
Table 1 Oligonucleotides used in this study	30
Table 2 Summary of statistics for the <i>de novo</i> assembly of the <i>F. merquensis</i> 's transcriptome	40
Table 3 Summary of a number of the receptor genes and the candidate receptor genes in each type of receptor	46

LIST OF FIGURES

		Page
Figure 1	Lateral view of adult penaeid prawn	4
Figure 2	Distribution view of banana shrimp and catch in 1990–2018	5
Figure 3	The ovarian development at each stage of the banana shrimp	7
Figure 4	Overview of receptor types	9
Figure 5	The structure and activated function of G protein-coupled receptors binding ligand and receptor tyrosine kinase binding ligand	10
Figure 6	The structure and activated function of ion channel and nuclear receptor	12
Figure 7	Standard workflow of an RNA-seq based transcriptome analysis	15
Figure 8	Workflow of bioinformatics analysis for transcriptome	16
Figure 9	Overview of RNAi process	17
Figure 10	Map and multiple cloning site sequence of pTG19-T vector	21
Figure 11	Map and multiple cloning site sequence of pET28a vector	22
Figure 12	Length distribution of the de novo assembled transcriptome	41
Figure 13	Gene ontology (GO) functional enrichment of receptor genes	42
Figure 14	KEGG functional enrichment of the receptor genes	4

LIST OF FIGURES (cont.)

		Page
Figure 15	Analysis of the differentially expressed receptor genes	45
Figure 16	Determination of the candidate receptor expression during ovarian developmental stages	47
Figure 17	Determination of <i>FmSax</i> and <i>FmBMPRII</i> expressions in shrimp tissues	50
Figure 18	Determination of <i>FmSax</i> and <i>FmBMPRII</i> during ovarian developmental stages in hepatopancreas	51
Figure 19	Alignment and feature of FmSax and FmBMPRII sequences	52
Figure 20	Phylogenetic tree analysis of FmSax and FmBMPRII.	55
Figure 21	The production and RNase digestion of dsSax and dsGFP	57
Figure 22	Effect of <i>FmSax</i> knockdown on <i>Vg</i> and <i>FmBMPRII</i> mRNA expression	58
Figure 23	Effect of <i>FmSax</i> knockdown on oocyte proliferation	59

LIST OF ABBREVIATIONS

°C	Degree Celsius
µg	Microgram
µl	Microliter
$2^{-\Delta\Delta CT}$	Delta-delta Ct
ANOVA	One-way analysis of variance
BLAST	Basic local alignment search tool:
BMP	Bone morphogenetic protein
BMPRI	Bone morphogenetic protein type 1 receptor
BMPRII	Bone morphogenetic protein type 2 receptor
Bn	Brain
bp	Base pair
CaCl ₂	Calcium chloride
COG/KOG	Clusters of Orthologous Groups/Eukaryotic Ortholog Groups
Ct	Cycle threshold
DAPI	4',6-Diamidine-2-phenylindole dihydrochloride
DEG	Differentially expressed gene
DEPC	Diethyl pyrocarbonate
DI water	Deionized water

LIST OF ABBREVIATIONS (cont.)

RNA	Ribonucleic acid
DNA	Deoxyribonucleic acid
DNase	Deoxyribonuclease
dNTPs	Deoxynucleotide Triphosphates
Ds	Double-strand
EDTA	Ethylenediaminetetraacetic acid
EdU	5-ethynyl-2'-deoxyuridine
EF1 α	Elongation factor 1 alpha
EGFR	Epidermal growth factor receptor
Es	Eyestalk
EtBr	Ethidium bromide
F	Forward
FastQC	Fast quality score
FBS	Fetal bovine serum
FPKM	Fragments per kilobase million
g	Gram
GC	Guanine and Cytosine
GFP	Green fluorescent protein

LIST OF ABBREVIATIONS (cont.)

Gi	Gill
GO	Gene ontology
GPCR	G protein-coupled receptor
HCl	Hydrochloric acid
Hp	Hepatopancreas
hr	Hour
IC	Ion channel
IPTG	Isopropyl β -d-1-thiogalactopyranoside
KCl	Potassium acetate
KEGG	Kyoto Encyclopedia of Genes and Genomes
KH_2PO_4	Potassium dihydrogen phosphate
M	Mole per liter
mg	Milligram
MgCl_2	Magnesium chloride
min	Minute
ml	Milliliter
mM	Millimolar
MnCl_2	Manganese chloride

LIST OF ABBREVIATIONS (cont.)

Ms	Muscle
Na ₂ HPO ₄	Disodium hydrogen phosphate
NaCl	Sodium chloride
NCBI	The National Center for Biotechnology Information
nm	Nanometer
NMDA	N-methyl-D aspartate
NR	Non-redundant protein
NR	Nuclear receptor
NT	Non-redundant nucleotide
OD	Optical density
Ov	Ovary
PBS	Phosphate-buffered saline
PCR	Polymerase chain reaction
PFAM	Protein domains and families
ppt	part per thousand
qRT-PCR	Quantitative realtime PCR
R	Reverse
RNAi	RNA interference

LIST OF ABBREVIATIONS (cont.)

RNase	Ribonuclease
RNA-seq	RNA-sequencing
ROR	Receptor tyrosine kinase-like orphan receptor
rpm	Revolutions per minute
RSEM	RNA-Seq by Expectation-Maximization
RT	Reverse transcriptase
RTK	Receptor tyrosine kinase
RYK	Receptor-like tyrosine kinase
sax	Saxophone
sec	Second
SEM	Structural equation modeling
Smo	Smoothed
st	Stage
TBE	Tris-borate
Tg	Ganglia
TGF- β 1	Transforming growth factor- β 1
ul	Unit
v/v	Volume by volume

LIST OF ABBREVIATIONS (cont.)

Vg	Vitellogenin
w/v	Weight/volume
ΔG	Gibb's free energy

CHAPTER 1

INTRODUCTION

1.1 Background and Rationale

In the international seafood trade, the marine shrimp ranked top of the exported products having high economic value. However, over the last few decades, the long-term sustainability of shrimp aquaculture has been hampered by many problems involved in shrimp reproduction. In shrimp aquaculture, the eyestalk ablation has been used to rapidly stimulate ovarian maturation in female penaeid shrimp (Uawisetwathana *et al.*, 2011) because the eyestalks of crustaceans are the source of the gonad-suppressive hormone, particularly gonad inhibiting hormone (GIH) (Feijo *et al.*, 2016; Treerattrakool *et al.*, 2008). Nonetheless, it causes high mortality and short-molt cycle duration in shrimp broodstock (Benzie, 1998), and it is a cruel and unnecessary industry practice that impacts animal cruelty laws. Therefore, the traditional technique should be replaced with more effective methods to induce shrimp ovarian maturation.

Understanding the molecular pathway is one of the promising approaches, which expands knowledge and leads to manipulating the control of ovarian maturation. Receptors are one of the important factors that play an initial role in signaling pathways involved in several physiological processes. Several types of receptors are important factors in development and reproduction that regulate target gene expression in organisms. For example, ecdysone receptor complex and ecdysteroid signaling are crucial for successful ovulation and oviposition regulating ovarian development in the female desert locust, *Schistocerca gregaria* (Lenaerts *et al.*, 2019). The ryanodine receptor regulates Ca^{2+} signals involved with several aspects of embryonic development through to the differentiation of the musculoskeletal, cardiovascular, and nervous systems in zebrafish (Wu, Brennan, and Ashworth, 2011). In crustaceans, a few receptors have been identified and studied to be involved in the reproductive process. For example, the progesterone receptor binding progesterone regulates directly vitellogenesis and ovarian development in the ovary and hepatopancreas and modulates indirectly ovarian development through nerve tissue in

Chinese mitten crab *Eriocheir sinensis* (Wu, *et al.*, 2014). Transforming growth factor- β (TGF- β) receptor type 1 (T β R1) plays roles in the early embryonic development and T β R1-mediated signaling in the morphogenesis and metamorphosis found in *Crassostrea gigas* (Herpin *et al.*, 2004) as well as in *Scylla paramamosain* (Zhou *et al.*, 2018). Epidermal growth factor receptor (EGFR) is important for the proper development of embryos and adult limbs, gonads, and eyes, and body size in the *Macrobrachium rosenbergii* (Sharabi *et al.*, 2013). Even though some receptors have been studied in crustaceans, gonad-regulating receptors have not been investigated so far.

Hence, this study aimed to identify the ovarian-regulating receptors using RNA sequencing and bioinformatics analyses in female banana shrimp, *Fenneropenaeus merguensis*. The differential gene expression of putative receptor genes among ovarian developmental stages was also investigated. The putative gonad-regulating receptors were characterized for their expressions, and bone morphogenetic protein receptor, a candidate receptor was studied for its role in the control of vitellogenesis using RNA interference.

1.2 Literature Review

1.2.1 *Fenneropenaeus merguensis*

Scientific name: *Fenneropenaeus merguensis* (De Man, 1888).

Old scientific name: *Penaeus indicus merguensis* (De Man, 1882).

FAO names: Banana prawn (En), Crevette banane (Fr), Langostino banana (Sp).

Local names: Kung chaebauy (Thailand), Jaira, Jiaro (Pakistan, also used for other species of *Fenneropenaeus*), Udang kaki merah (Malaysia), Udang putih (Indonesia), Pak ha, White prawn (Hong Kong), Banana prawn, White prawn (Australia).

Taxonomy: it is classified as domain: Eukaryota, subkingdom: Metazoa, kingdom: Animalia, phylum: Arthropoda, subphylum: Crustacea, superclass: Multicrustacea, class: Malacostraca, subclass: Eumalacostraca, superorder: Eucarida, order: Decapoda, suborder: Dendrobranchiata, superfamily: Penaeoidea, family: Penaeidae, genus: *Fenneropenaeus*, and species: *F. merguensis*. (WoRMS, 2019).

Characters: its carapace is smooth, and lack gastrofrontal and hepatic crests; no dark brown transverse bands on the carapace and abdomen; horizontally straight tip of rostrum; elevated rostral crest and broadly triangular shape (particular in fully grown female); teeth on rostrum generally with 7-8 dorsal and 5-6 ventral teeth; no lateral spines on telson; adrostral carina shorts of epigastric tooth; the maximum size of total length in the female with 35 centimeters and male with 26.3 centimeters; weight about 50.00 grams (Motoh and Kuronuma, 1980; Chong and Sasekumar, 1982; Holthuis, 1980) (Figure 1 A).

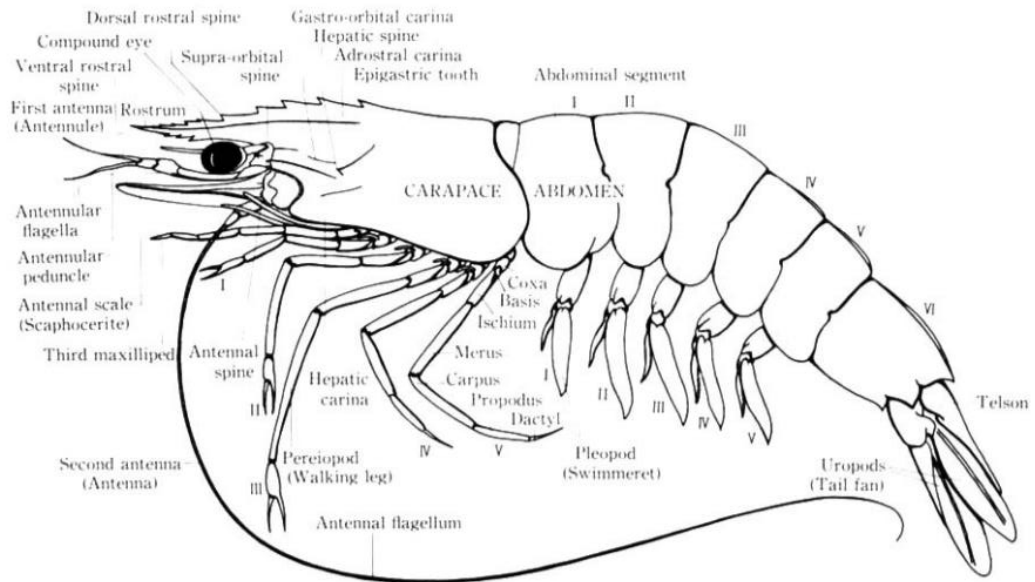
Colors: its body is semi-translucent, often yellowish to greenish and covered with numerous minutes speckled with reddish-brown or greenish dots; brown-banded antennules; yellowish legs and pleopods; combinations of yellowish-green and brownish shades in uropods; brown upper margin of the rostrum in fully grown prawn (Motoh and Kuronuma, 1980; Josileen, 2013) (Figure 1 B).

Habitat and life cycle: it usually inhabits on bottom mud and sand from the coastline and river mouths of estuarine and marine to depths of about 10 - 45 meters, mostly less than 30 meters (Siddeek *et al.*, 1999). In life cycle, similar to other penaeid prawns (Dall *et al.*, 1990), adults prawn occupies and spawns in near- and off-shore waters (Crococ and Kerr 1983; Rothlisberg *et al.*, 1985), and larvae and juvenile migrate to estuarine nurseries (Rothlisberg and Jackson, 1987) (Sheaves *et al.*, 2012).

Distribution: it is widely distributed in the western part of the Indo-Pacific Ocean from the Persian Gulf up to India, Pakistan, Sri Lanka, Kenya, Thailand, Hong Kong, Philippines, Indonesia, Singapore, Malaysia, Papua New Guinea, Australia (north of 29°S), New Caledonia and Fiji (Grey *et al.*, 1983; Pérez Farfante and Kensley, 1997; Munga *et al.*, 2012) and Turkish part of the Mediterranean Sea (Eastern Basin) (Özcan *et al.*, 2006) (Figure 2 A).

Fishery: It is an important target for commercial and subsistence fisheries. The global farm production of *F. merguensis* was 219,309 tons in 1999 (Hoang, 2001): it is raised in extensive ponds in Southeast Asia and semi-extensive ponds in Australia, Thailand, Indonesia, and elsewhere (Gundermann and Popper 1975; Holthuis, 1980; Buckworth *et al.*, 2013) (Figure 2 B).

(A)

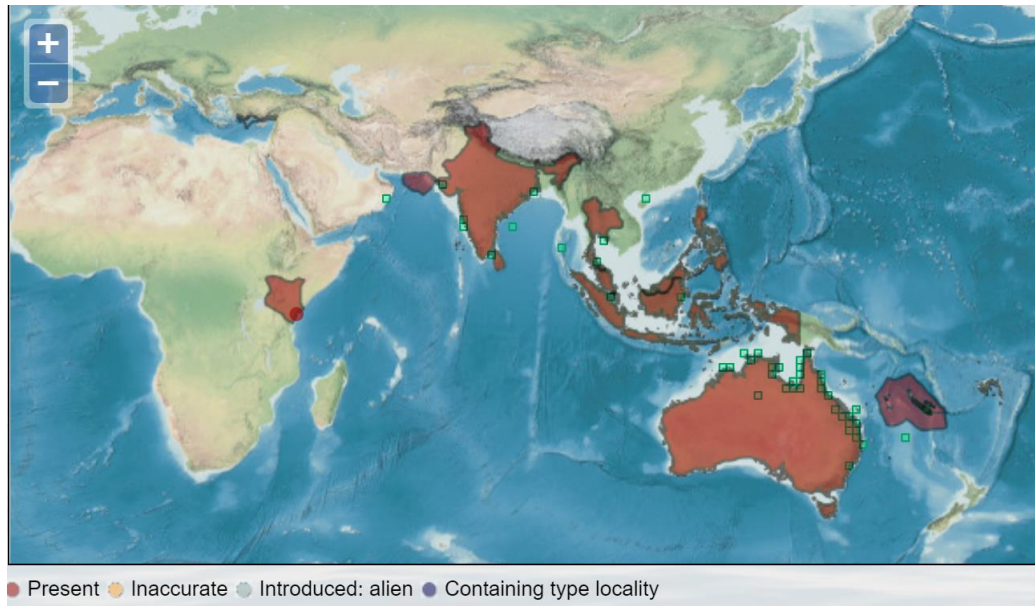


(B)



Figure 1 Lateral view of adult penaeid prawn showing technical terms for various parts of the body (Motoh and Kuronuma, 1980) (A). Lateral view of adult banana shrimp (Ratmuangkhwang, n.d.) (B).

(A)



(B)

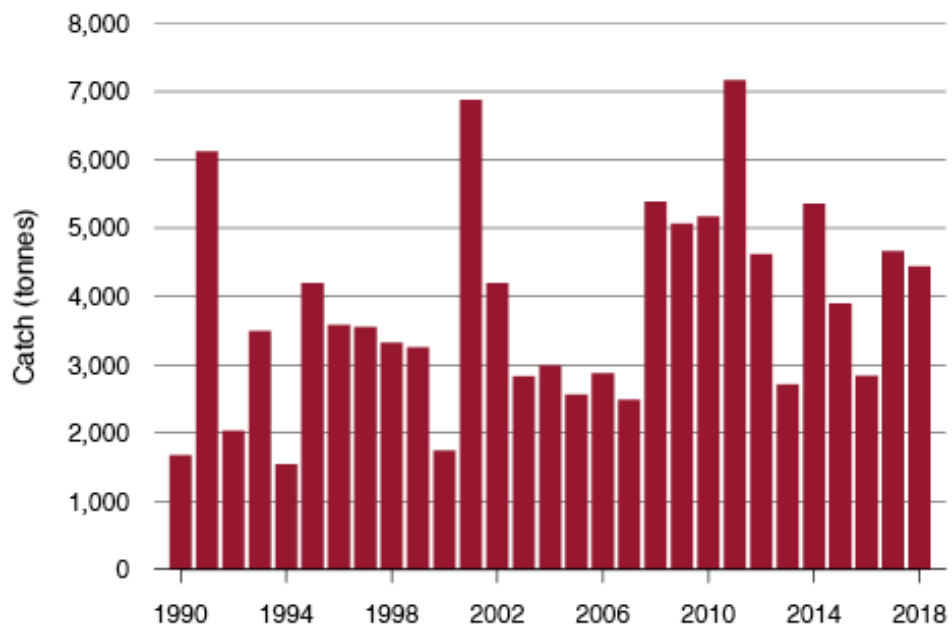


Figure 2 Distribution view of banana shrimp (WoRMS, 2019) (A). The banana shrimp catch in 1990–2018 (Parsa *et al.*, 2019) (B).

1.2.2 Ovarian maturation

During ovarian maturation in crustaceans, the ovary exhibits size and color changes. It can be visible through the transparent carapace. These changes are due to the accumulation of a vitellin (Vn) in the oocytes, resulting in a rapid increase in oocyte diameter (Sagi *et al.*, 1995; Tsukimura, 2001). The accumulation of the carotenoid components in the ovary leads to a change of the ovary's color (Arculeo *et al.*, 1995). A series of ovarian colors have changed from transparent, yellow, light green through dark green related to the ovarian developing stage, respectively (Ayub *et al.*, 2002) (Figure 3).

Vitellin is the major yolk protein accumulated in crustacean oocytes, where it provides free amino acids, lipids, carbohydrates, carotenoids, and minerals (Byrne *et al.*, 1989; Kunkel and Nordin, 1985; Niimi *et al.*, 1993; Khalaila *et al.*, 2004) to utilize the growing and developing of embryo and larva. Vitellogenin (Vg), a female-specific protein and also a major estrogen-inducible yolk precursor protein (Tsang *et al.*, 2002), is synthesized in both hepatopancreas and ovary, then circulated in the hemolymph before depositing in the ovary (Tsang *et al.*, 2003). In the oocytes, Vg undergoes a proteolytic process to produce several subunits (Meusy, 1980; Adiyodi and Subramoniam, 1983; Meusy and Payen, 1988; Tsukimura, 2001). Therefore, the synthesis and accumulation of vitellogenin are crucial for oocyte and embryo development.

The ovarian development in crustaceans can be divided into four stages (previtellogenic, early vitellogenic, late vitellogenic, and mature ovary stages) classified by ovarian histology and expression of Vg gene. In the previtellogenic stage (stage I), the ovary contains small oocyte cells including oogonia, chromatin-nucleolar oocytes, and some perinucleolar oocytes. Cellular activities in the previtellogenic stage are involved in oocyte growth and proliferation (Ayub *et al.*, 2002). The Vg expression is rarely detectable in this stage. For the early vitellogenic stage (stage II), follicular cells are surrounding perinucleolar cells, and it performs an initiation of oocyte cells to accumulate yolk protein in their cytoplasm (increasing expression of Vg gene). In the late vitellogenic stage (stage III), the size of the oocyte cells has dramatically increased (120-200 μm) with a high accumulation of yolk protein, called a yolky oocyte. Finally,

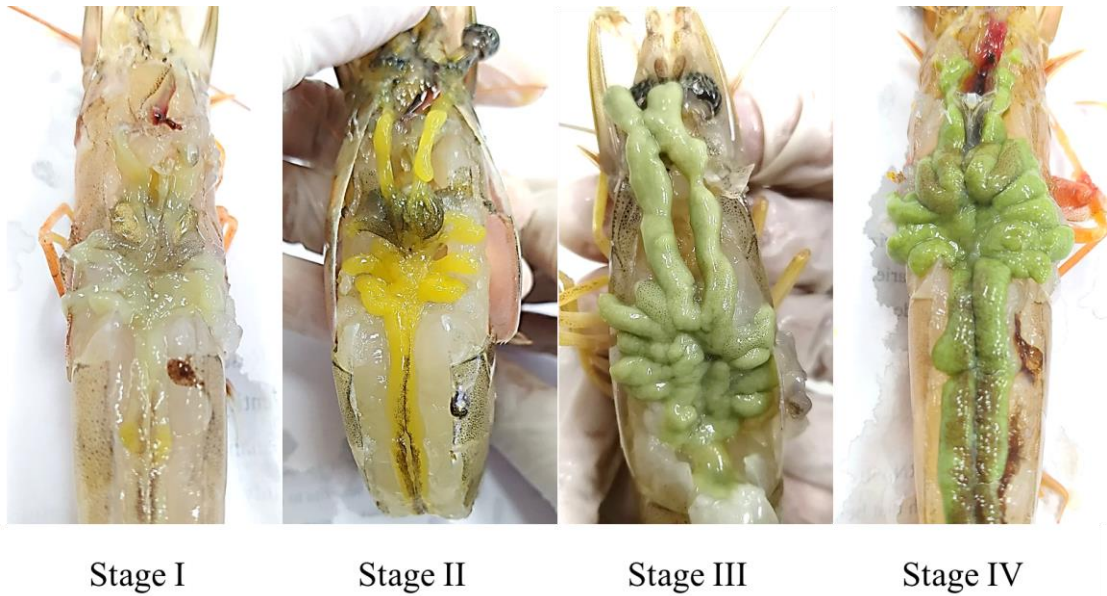


Figure 3 The ovarian development at each stage of the banana shrimp including stage I: previtellogenic, stage II: early vitellogenic, stage III: late vitellogenic, and stage IV: mature stages.

the mature ovary (stage IV) contains the yolky oocytes which form cortical rods at the edge of the ooplasm (Ayub *et al.*, 2002; Yano, 1988).

1.2.3 Receptors

Receptors are proteins or glycoproteins that receive signals by binding to signaling molecules. A molecule that binds to a receptor is called a ligand and can be a peptide or other small molecules such as a neurotransmitter, a peptide hormone, a growth factor (Cooper, 2000), a pharmaceutical drug, toxin, or parts of the outside of a virus or microbe. When a ligand binds to its specific receptor, it activates or inhibits the receptor's associated-biochemical pathway. Receptors can play several physiological regulatory roles, including cell growth and differentiation, division, and death; and can control membrane channels or regulate cell binding (Feger, 1994).

The receptors can be classified into two categories by their locations; intracellular receptors, which are found inside of the cell (in the cytoplasm or nucleus), including nuclear receptors (NRs), and cell surface/transmembrane receptors, which are found in the plasma membrane, including ion channels (ICs), G protein-coupled receptors (GPCRs), and receptor tyrosine kinases (RTKs) (Figure 4).

1.2.3.1 G protein-coupled receptors

The G protein-coupled receptors are also known as seven-(pass)-transmembrane domain receptors, 7TM receptors, or heptahelical receptors. It is the most prominent group of cell surface receptors. Its structure is an integral membrane protein that possesses seven membrane-spanning domains or transmembrane helices (Venkatakrishnan *et al.*, 2013; Hollenstein *et al.*, 2014). The extracellular parts of the receptor can be glycosylated. These extracellular loops also contain two highly conserved cysteine residues that form disulfide bonds to stabilize the receptor structure. The GPCRs are activated by binding a stimulus (or ligand) in the extracellular space and then transduce that information to the inside of the cell through conformational changes. The conformational changes activate different heterotrimeric G-proteins (Gilman, 1987), which execute the downstream signaling transduction pathways through ultimately, cellular responses (Figure 5 A). GPCRs are involved in the regulation of several physiological processes. The highly specific ligand-GPCR interaction prompts an efficient cellular response, which is vital for the health of the

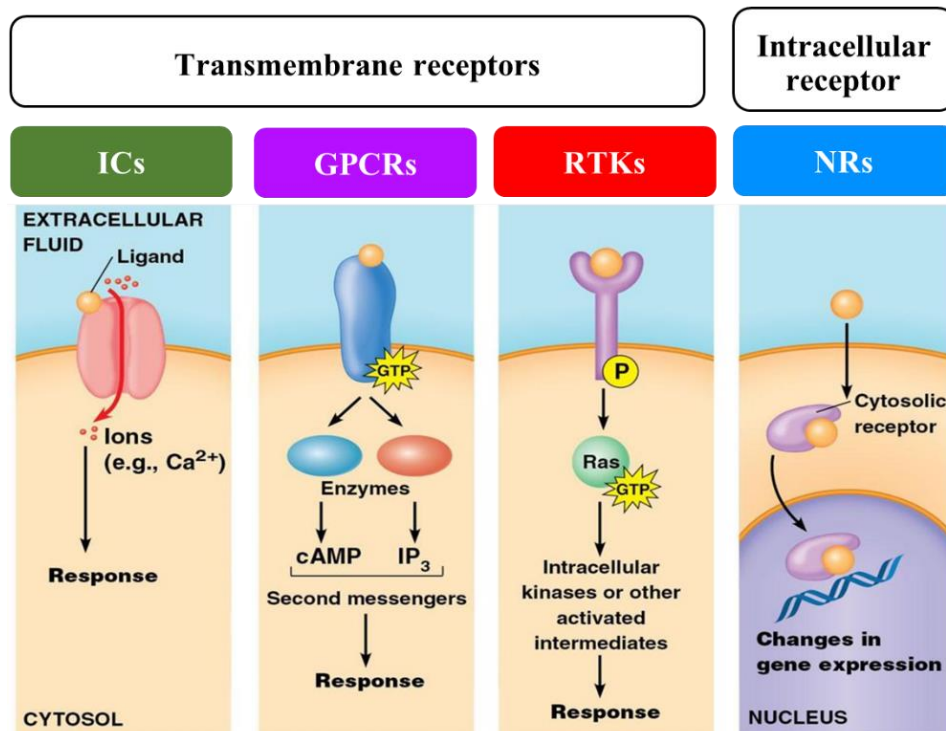
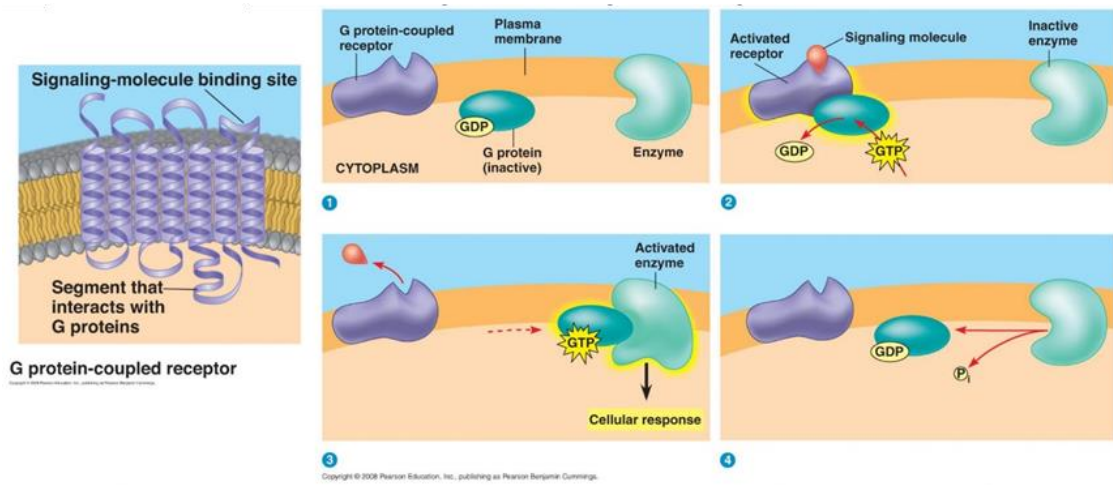


Figure 4 Overview of receptor types. The receptor was classified by their locations. In cell transmembrane including G protein-coupled receptor (GPCR), receptor tyrosine kinases (RTK), and nuclear receptor (NR). In the cytoplasm or nucleus including ion channel (IC) (Pearson education, 2006).

(A)



(B)

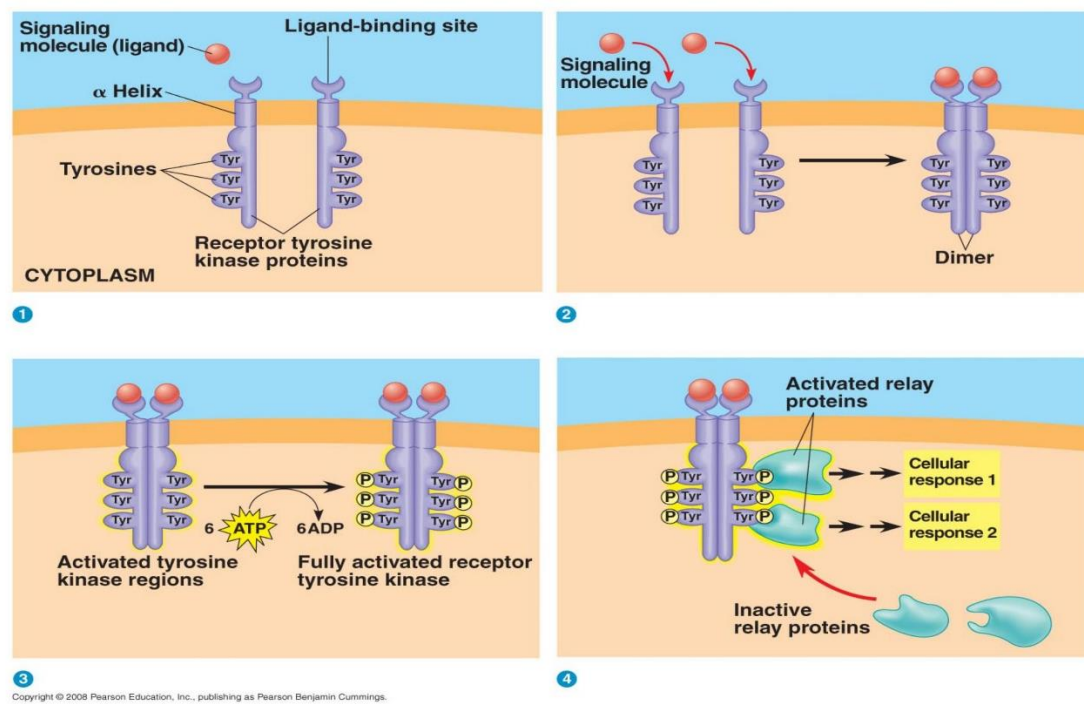


Figure 5 The structure and activated function of G protein-coupled receptors binding ligand (A) and receptor tyrosine kinase binding ligand (B) (Pearson education, 2006).

cell and organism (Hanlon *et al.*, 2015). For example, the retinoid X receptor can regulate the expression of vitellogenin and ovarian development in the mud crab (Gong *et al.*, 2016). The luteinizing hormone receptor (LHR) are essential for the regulation of the gonadal maturation in Chinese mitten crab (Nguyen *et al.*, 2018).

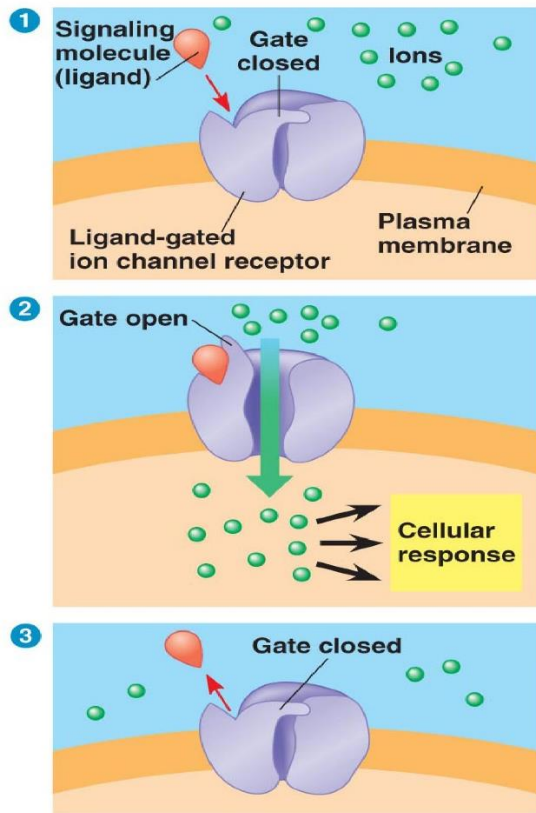
1.2.3.2 Receptor tyrosine kinase

The receptor tyrosine kinase is a class of enzyme-linked receptors and a part of the tyrosine kinases family. A kinase is a name for an enzyme that transfers phosphate groups to a protein or other target, and a receptor tyrosine kinase transfers phosphate groups specifically to the amino acid tyrosine. Generally, RTKs are activated through ligand-induced oligomerization, typically dimerization which initiates activation of the tyrosine kinase domain. This conduces autophosphorylation of regulatory tyrosine residues leading to conformational changes that serve to stabilize the active state of the kinase (Hubbard, 2004) (Figure 5 B). The RTKs and their cellular signaling pathways play important roles in normal development and homeostasis that are implicated in several biological processes including cell proliferation, differentiation, motility, and survival (Yarden and Ullrich, 1988). For example, bone morphogenetic protein (BMP) receptor in the banana shrimp *F. merguensis* (Sathapondecha and Chotigeat, 2019), The BMP signaling pathway is one of two branches of transforming growth factor- β (TGF-B) superfamily which has been implicated as playing potential roles in the regulation of gonad development. Also, the insulin-like receptor plays a growth regulatory role in the prawn *Macrobrachium rosenbergii* (Sharabi, 2001; Leever, 2001).

1.2.3.3 Ion channel

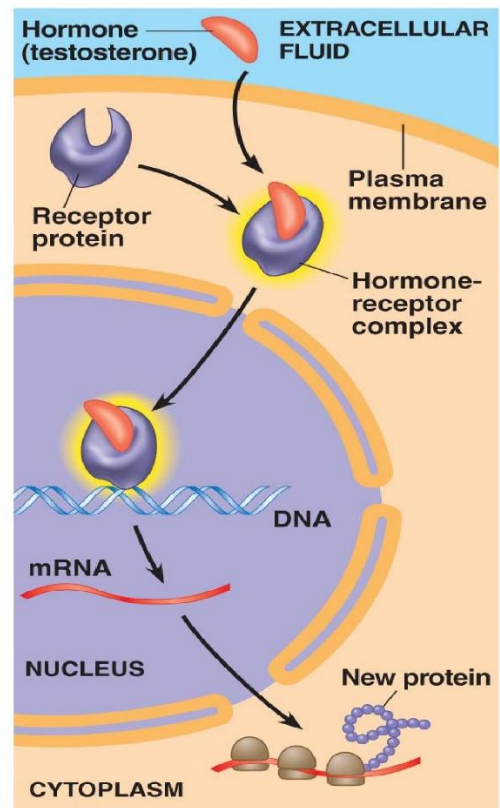
The ion channel is a pore-forming membrane protein that consists of four subunits with six transmembrane helices. Each of these proteins arranges itself to form a pore extending from one side of the membrane to the other. These pores or ion channels can open and close in response to chemical or mechanical signals. When an ion channel opens ions move in or out of the cell in a single-file fashion (Figure 6 A). The individual ion channel is specific to particular ions. Their functions include

(A)



Copyright © 2008 Pearson Education, Inc., publishing as Pearson Benjamin Cummings.

(B)



Copyright © 2008 Pearson Education, Inc., publishing as Pearson Benjamin Cummings.

Figure 6 The structure and activated function of ion channel (A) and nuclear receptor (B) (Pearson education, 2006).

establishing a resting membrane potential, shaping action potentials and other electrical signals by gating the flow of ions across the cell membrane, controlling the flow of ions across secretory and epithelial cells, and regulating cell volume. The ion channels are present in the membranes of all excitable cells (Scitable, 2014). For example, depolarizing effect of gamma-Aminobutyric acid (GABA) receptors was induced by GABA in the neurosecretory cells in crayfish's X-organ neurons (Garduño *et al.*, 2002). It participated in the control of different functions such as molting, regulation of blood sugar levels, segmentary and retinal pigment position, locomotion, and neuronal activity (García and Aréchiga, 1998); the ryanodine receptor from the zebrafish (Ht Wu *et al.*, 2011).

1.2.3.4 Nuclear receptor

The nuclear receptor is a family of ligand-regulated transcription factors that are activated by steroid hormones, such as estrogen and progesterone, and various other lipid-soluble signals, including retinoic acid, oxysterols, and thyroid hormone (Mangelsdorf *et al.*, 1995). Due to its structure contains a highly conserved DNA-binding domain (DBD) and a ligand-binding domain (LBD), it binds to specific sequences of a DNA region called hormone response element. This binding transduces specific changes in target gene expression (Figure 6 B). The nuclear receptor plays several functions as a transcriptional regulator to control the expression of genes involved in development, homeostasis, and metabolism, reproduction, and development (Laudet and Gronemeyer, 2002). The ligand binds to a nuclear receptor leading to a conformational change and dimerization. This activates the receptor and results in up-or down-regulation of target gene expression. For example, the nuclear receptors HR3 and E75 in the crustacean *Daphnia magna* serve as a mediator of ecdysteroids. They can initiate signaling along multiple pathways that regulate various aspects of development, maturation, and reproduction in arthropods (Hannas and Leblanc, 2009); the nuclear estradiol receptor is involved in the regulation of the reproduction in the Japanese mantis shrimp *Oratosquilla oratoria* (Yan *et al.*, 2017).

1.2.4 Transcriptome

Transcriptomic technology is the technique used to study an organism's transcriptome, the sum of all its RNA transcripts. The information content of an organism is recorded in the DNA of its genome and expressed through transcription (Lowe *et al.*, 2017). Transcriptome analysis has enabled the study of how gene expression changes in different organisms. The transcriptome is performed by advanced RNA sequencing and analyzed by bioinformatics. The sequencing workflow is initiated with library construction before sequencing including mRNA extraction, double-stranded cDNA synthesis, poly-A tail and adaptor addition, fragment selection and PCR, and library quality assessment (Figure 7). The bioinformatics workflow is used to analysis of raw data derived from sequencing, including quality control of the data, transcriptome *de novo* assembly, gene functional annotation with many databases, gene expression analysis, and other analyses for final target data (Figure 8). There are many studies in crustaceans such as Japanese mantis shrimp (*Oratosquilla oratoria*) (Lou *et al.*, 2019), mud crab (*Scylla paramamosain*) (Lin *et al.*, 2019), banana shrimp (*Fenneropenaeus merguensis*) (Powell *et al.*, 2015), spotted seabass (*Lateolabrax maculatus*) (Cai *et al.*, 2020), and a Korean native cow (hanwoo) (Chowdhury *et al.*, 2020), as well as in plants such as pepper fruit (*Capsicum annuum*) (Liu *et al.*, 2020), ripe peach (*Prunus persica*) fruit (Li *et al.*, 2020), and Ajowan (*Trachyspermum ammi*) inflorescence (Amiripour *et al.*, 2019).

1.2.5 RNA interference

RNA interference (RNAi) is a biological process of mRNA degradation induced by sequence-specific suppression of gene expression by double-stranded RNA, through translation or transcriptional repression (Xu and Huang, 2019) (Figure 9). There are many studies in crustaceans such *Litopenaeus vannamei* (Hou *et al.*, 2014), *Fenneropenaeus merguensis* (Zhuo *et al.*, 2017), *Scylla paramamosain* (Huang *et al.*, 2017), *Artemia franciscana* (Copf, Rabet and Averof, 2006), *Lepeophtheirus salmonis* (Eichner *et al.*, 2014), and *Tigriopus californicus* (Barreto, Schoville, and Burton, 2015).

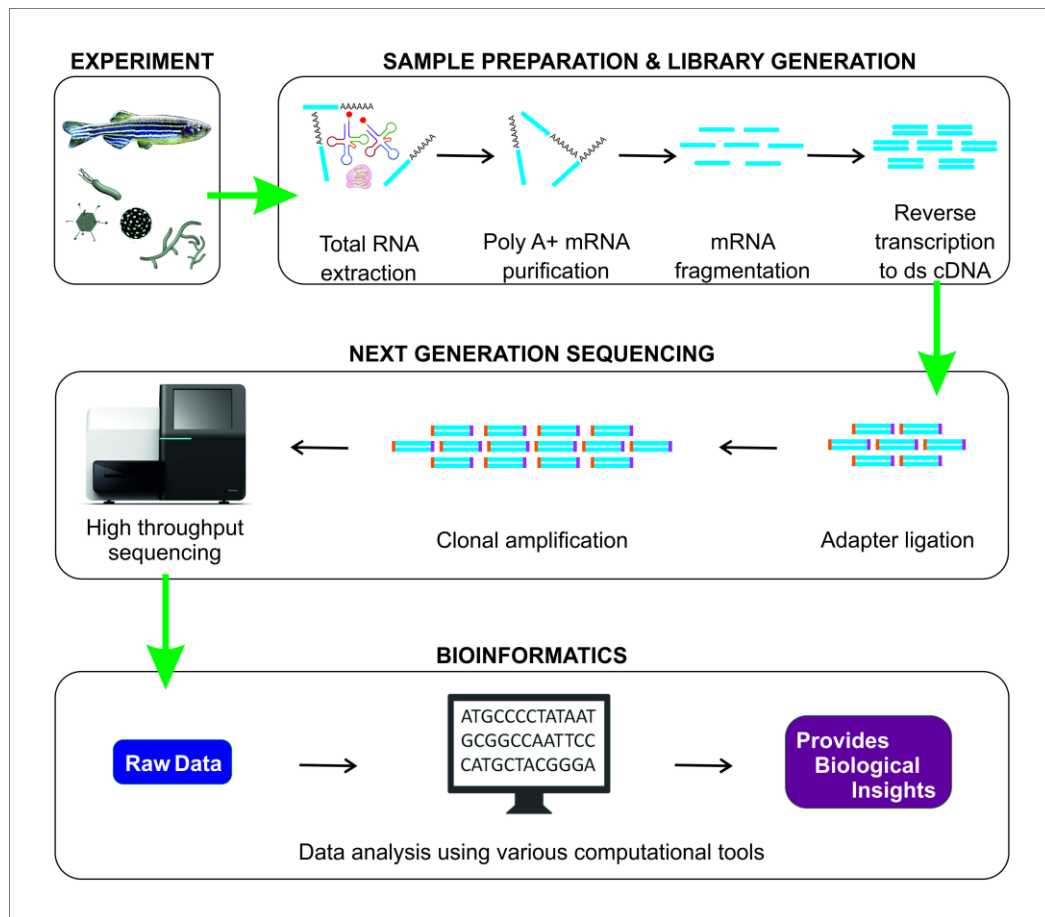


Figure 7 Standard workflow of an RNA-seq based transcriptome analysis (Sudhagar *et al.*, 2018).

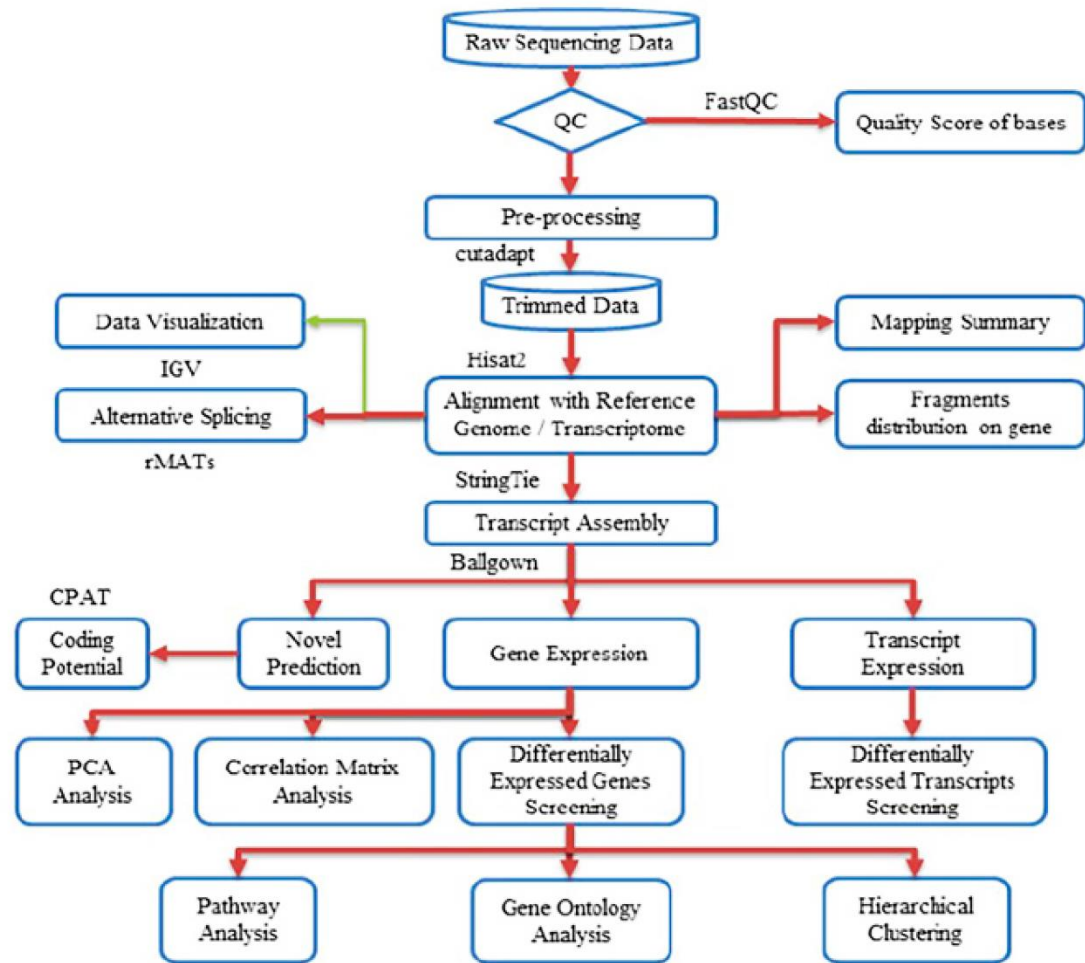


Figure 8 Workflow of bioinformatics analysis for transcriptome (Gopalakrishnan and Kumar, 2020).

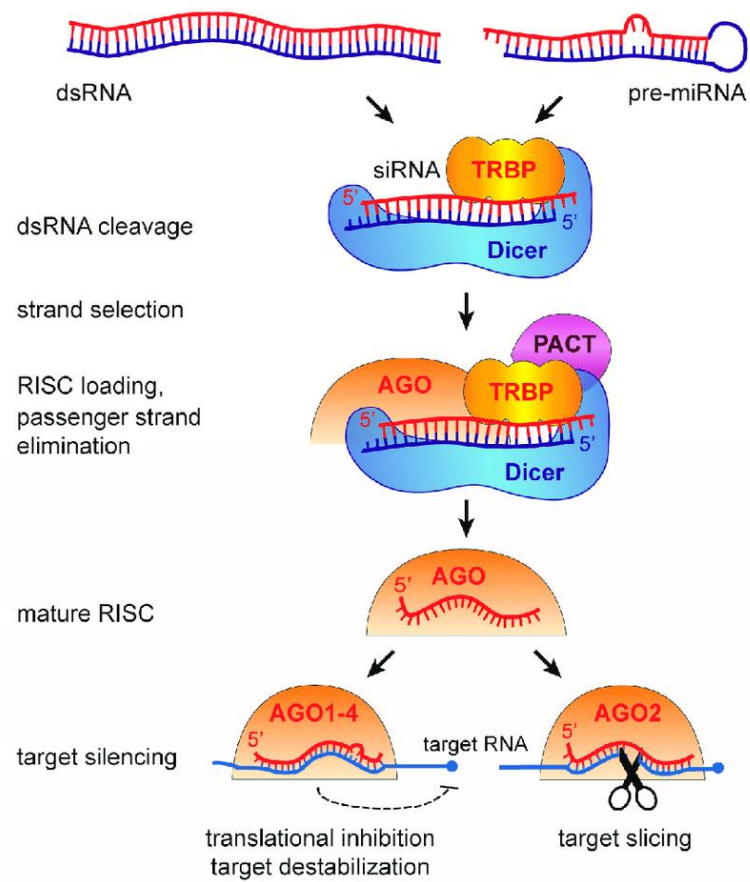


Figure 9 Overview of RNAi process (Schuster, Miesen, and van Rij, 2019).

1.2.6 EdU assay

EdU (5-ethynyl-2'-deoxyuridine) assay provides an accurate and effective method to measure cell proliferation by incorporation of EdU (thymidine analog) into DNA synthesis during the S-Phase of the cell cycle (Salic and Mitchison, 2008). EdU can be detected with a fluorescent dye or biotin for colorimetric or fluorometric detection via streptavidin- horseradish peroxidase (HRP). There are many studies such as *F. merguensis* (Sathapondecha and Chotigeat, 2019), *Cherax quadricarinatus* (Li *et al.*, 2021), *Cladonema pacificum* (Fujita, Kuranaga, and Nakajima, 2019), *Lineus ruber* (Martín-Durán, Vellutini, and Hejnol, 2015), *Juncus prismatocarpus* (Yin and Tsukaya, 2019), and *Apostichopus japonicus* (Li *et al.*, 2019).

1.3 Objectives

1.3.1 To identify and characterize candidate receptors involved in ovarian development in female banana shrimp.

1.3.2 To study an ovarian stimulating function of the candidate receptors in female banana shrimp.

CHAPTER 2

MATERIALS AND METHODS

2.1 Materials

2.1.1 Animal samples

Approximately 40-50 g of adult female banana shrimps, *F. merguensis*, were obtained from the Gulf of Thailand, Nakhon Sri Thammasat province, Thailand. The shrimp were kept in a tank containing 30 parts per thousand (ppt) salinity of seawater for 2-3 days before starting the experiment. During the experiment, they were fed with commercial food pellets (Goongbest, Thailand) twice per day and maintained under a photoperiod of 12-hour light and dark. About 50 % of seawater was changed every 2 days. The feed residues in each tank were cleaned twice per day.

2.1.2 Bacterial samples

2.1.2.1 *Escherichia coli* TOP10

The *E. coli* TOP10 was used for processes of cloning and plasmid propagation in this study. Its genotype is F- *mcrA* $\Delta(mrr-hsdRMS-mcrBC)$ $\phi 80lacZ\Delta M15$ $\Delta lacX74$ *recA1* *araD139* $\Delta(ara-leu)7697$ *galE15* *galK16* *rpsL(Str^R)* *endA1* *nupG* λ -.

2.1.2.2 *Escherichia coli* HT115

The *E. coli* HT115 was used for double-stranded RNA production in this study. This strain is a Rnase III-deficient *E. coli* strain with IPTG-inducible T7 Polymerase activity and tetracycline-resistant. Its genotype is F-, *mcrA*, *mcrB*, *IN(rrnD-rrnE)1*, *rnc14::Tn10(DE3 lysogen: lacUV5 promoter -T7 polymerase)*.

2.1.3 Plasmid vectors

2.1.3.1 pTG19-T vector

The pTG19-T was used for rapid cloning of PCR products in this study. Its features are sequence containing multiple cloning sites, *lacZ* gene for blue/white

selection, M13 primer sites for PCR screening and sequencing, and containing *BamHI* restriction enzyme for releasing the insert from the pTG19-T vector (Figure 10).

2.1.3.2 pET28a vector

The pET28a vector was used for cloning and expression of the target products in this study. It contains multiple cloning sites, T7 expression region, and other features (Figure 11).

2.1.4 Culture medium

2.1.4.1 LB (Luria-Bertani) medium 100 ml

Peptone 0.8 % w/v	0.8	g
Yeast extract 1 % w/v	1	g
NaCl 0.5 % w/v	0.5	g
Agar powder (*option) 2 % w/v	2	g

The volume of the solution was added up to 100 ml with DI water and sterilized by autoclaving at 121°C for 15 min.

2.1.4.2 2XYT medium 100 ml

Peptone 1.6 % (w/v)	1.6	g
Yeast extract 1 % (w/v)	1	g
NaCl 0.5 % w/v	0.5	g
Agar powder (*option) 2 % (w/v)	2	g

The volume of the solution was added up to 100 ml with DI water and sterilized by autoclaving at 121°C for 15 min.

2.1.4.3 2X Leibovitz's L-15 medium

The medium was composed of 2X Leibovitz's L-15 powder, 10 % v/v fetal bovine serum (FBS), 1 % w/v glucose. The medium was prepared under an aseptic technique via laminar flow.

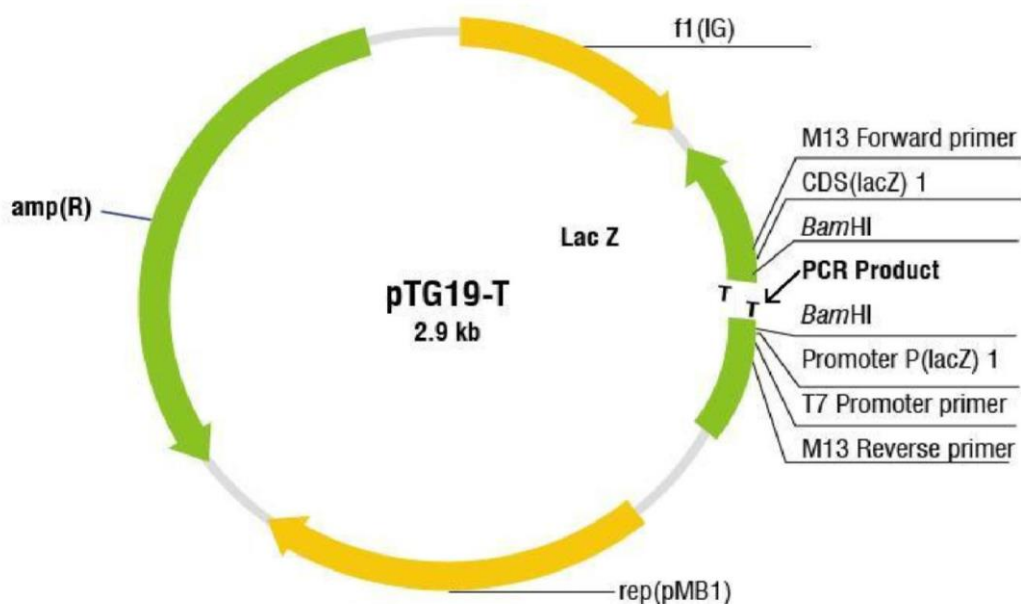
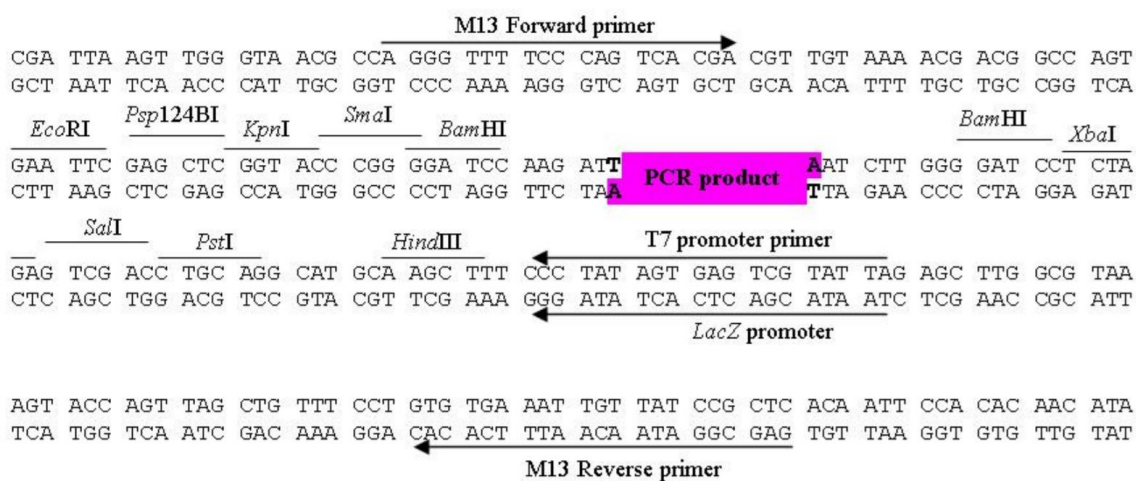


Figure 10 Map and multiple cloning site sequence of pTG19-T vector (Sinaclon: Cat. No. CL5841).

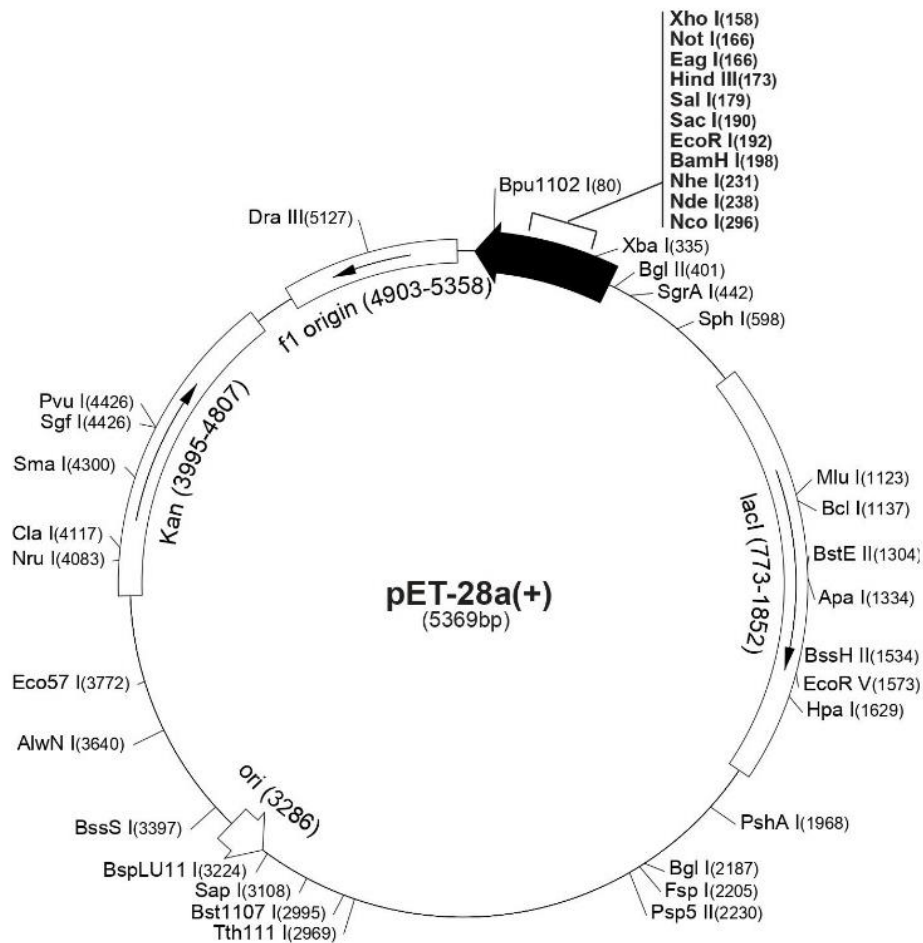
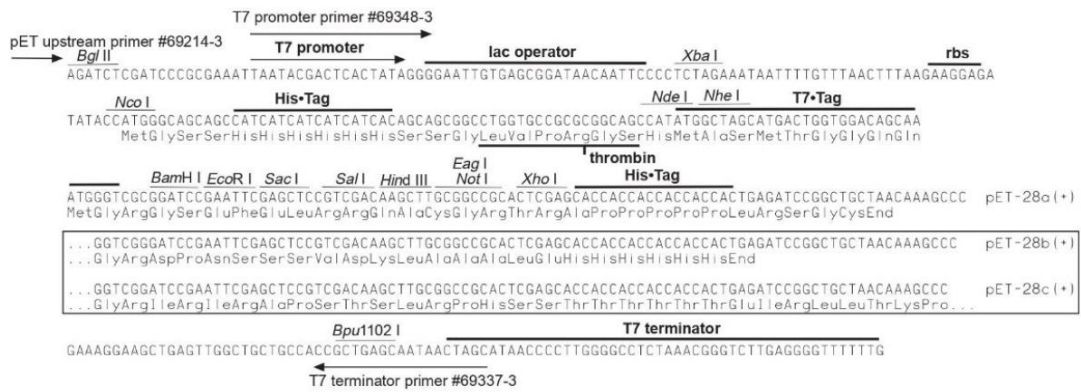


Figure 11 Map and multiple cloning site sequence of pET28a vector (Novagen: Cat. No. 69864-3).

2.1.5 Chemical reagents

2.1.5.1 RNA extraction reagents:

RNAstore reagent (Tiangen biotech)

Trizol reagent (Ambion)

Chloroform

Propan-2-ol (isopropanol)

Ethanol

2.1.5.2 cDNA synthesis reagents (Thermo Scientific):

Deoxyribonuclease I (DNase I)

DNase I buffer

10X M-MuLV reverse transcriptase (RT) buffer

200 μ M dNTP

10 nM oligo-dT primer

100 U M-MuLV

50 mM EDTA (Ethylenediaminetetraacetic acid)

2.1.5.3 PCR reagents (Thermo Scientific):

10X PCR buffer

10 mM dNTP

50 mM MgCl₂

10 U Taq polymerase

10 mM primers

2.1.5.4 Realtime PCR reagents (KAPA Biosystems):

10X KAPA SYBR® FAST universal

10X KSF low ROX

2.1.5.5 Ligation reagents (Vivantis):

10X buffer T4 ligase

10 U of T4 DNA ligase

2.1.5.6 FavorPrep Gel/PCR purification kit (Favorgen):

FADF buffer

Wash buffer

Elution buffer

2.1.5.7 GF-1 plasmid DNA extraction kit (Vivantis):

Solution 1

Solution 2

Neutralizing buffer

Washing Buffer

2.1.5.8 RNase digestion reagents:

10 U of RNase III (New England Laboratories)

10X RNase III buffer (New England Laboratories)

50 mM MnCl₂

1 µg/mL RNase A (Thermo Scientific)

2.1.5.9 Digestion reagent:

10X Fastdigest buffer (Thermo-Scientific),

10 U restriction enzyme (XbaI, XhoI, NdeI, NotI)

2.1.5.10 Other reagents:

Agarose powder

Glycerol

Bromophenol blue

Ethidium bromide (EtBr)

200 mM isopropyl β-d-1-thiogalactopyranoside (IPTG)

Sodium chloride (NaCl)

Calcium chloride (CaCl₂)

Diethyl pyrocarbonate (DEPC)

Tris-borate

Boric acid

DNA marker

Liquid nitrogen

Potassium acetate (KCl)

Disodium hydrogen phosphate (Na_2HPO_4)

Potassium dihydrogen phosphate (KH_2PO_4)

Ampicillin

Kanamycin

Penicillin

Streptomycin

Peptone

Yeast extract

2X Leibovitz's L-15 powder

10 % v/v Fetal bovine serum (FBS)

Glucose

Alexa Fluor™ 488 azide

Cupric sulfate (CuSO_4)

L-Ascorbic acid

5 $\mu\text{g}/\text{ml}$ 4',6-Diamidino-2-phenylindole dihydrochloride (DAPI)

Triton X-100

N-propyl gallate

Hydrochloric acid (HCl)

2.2 Methods

2.2.1 Sample preparation and RNA sequencing (RNA-seq)

The ovarian development was classified into 4 stages, including previtellogenic, early vitellogenic, late vitellogenic, and mature stages by ovarian histology and ovarian color (Ayub and Ahmed, 2002). The 3 ovarian pieces from 3 individual shrimp with the same ovarian development stage were isolated and pooled together in a 500 μl RNASTore reagent (Tiangen Biotech, China). The 4 pooled sample in each stage of ovarian development was sent to Novogene, Hongkong to analyze for their transcriptome with the Illumina HiSeq2500 platform.

2.2.2 *De novo* transcriptome assembly

Raw reads derived from RNA-seq in different stages of ovarian development were recorded in FASTQ files. The quality of raw reads was analyzed by FastQC program v 0.11.8 with (1) per base sequence content: difference between A and T, or G and C was less than 20% in any position; (2) per sequence GC content: the sum of the deviations from the normal distribution showed more than 30% of the reads and (3) overrepresented sequences: any sequence showed more than 1% of the total (Andrews, 2010). Due to a reference genome of *F. merguensis* has not been available so far, *de novo* assembly of the ovarian transcriptome was generated using Trinity software v2.11.0 (Grabherr et al., 2011) via Conda v4.8.4 (miniconda3) (Anaconda, 2020) with an assembled contig length at least 200 bp. The assembled transcripts then were hierarchically clustered and removed their redundant sequences using CD-HIT software v4.8.1 (Li and Godzik, 2006; Fu et al., 2012) by setting the identity threshold at 90 % and word length at 10 bp, obtaining the longest transcript in each gene as a unigene for subsequent analysis.

2.2.3 Gene functional annotation

The unigenes were annotated for their functions by Novogene using DIAMOND software v0.8.22 to search against databases, including NR (the NCBI non-redundant protein), Swiss-Prot, and COG (Clusters of Orthologous Groups)/KOG (Eukaryotic Ortholog Groups) (Tatusov et al., 2003). Also, the unigenes were matched up NT (the NCBI non-redundant nucleotide) from NCBI blast software v2.2.28+, KEGG (the Kyoto Encyclopedia of Genes and Genomes) (Kanehisa and Goto, 2000) from KAAS software r140224, PFAM (protein domains and families database) from hmmscan software HMMER3, and Gene Ontology (GO) (Bada et al., 2004) from blast2go software b2g4 pipe_v2.5.

2.2.4 Differentially expressed gene (DEG) analysis

To obtain normalized expression values, the clean reads in each stage of ovarian development were aligned to the unigenes from section 2.2 and estimated for the abundance using the Trinity package including Bowtie v1.3.0 and RSEM v1.3.3 software via Conda, respectively. For samples without biological replicates, trimmed

mean of M-values (TMM values were analyzed for differentially expression levels using NOISeq software v2. 26. 1 via R Studio v1. 1. 463 software. Furthermore, fragments per kilobase million (FPKM) values were converted to a term of \log_2 values. The data was created a hierarchical clustering heatmap with BioVinci software v2. 8. 3 (BioTuring Inc., USA).

2.2.5 Identification of candidate receptor genes involved in ovarian maturation

To find out the candidate receptor, the unigenes derived from the transcriptome were filtered with several keywords such as gene family, class, and specific names in each receptor type, including G protein-coupled receptor (GPCR), receptor tyrosine kinase (RTK), nuclear receptor (NR), and ion channel (IC) (Appendix 1). Subsequently, the receptor genes were analyzed for their DEGs' result in different stages of ovarian development by thresholds of \log_2 - FoldChange ≥ 1 as an up-regulation or ≤ -1 as a down-regulation. Also, the receptor genes that were differentially expressed analyzed from section 2.4 were analyzed for their gene functions with KAAS (<https://www.genome.jp/kegg/kaas/>) exploring in KEGG pathways, and the receptors annotated to be involved in reproductive pathways were the candidate receptor genes.

2.2.6 RNA extraction

2.2.6.1 Total RNA extraction

Total RNA extraction was performed using a Trizol reagent (Ambion, USA). Briefly, 20-30 mg of shrimp tissue was homogenized in 1 ml of Trizol reagent and then added with 200 μ l of chloroform, mixed vigorously, and incubated on ice for 15 min before centrifuging at 12,000 rpm, 4 °C for 15 min. For RNA precipitation, the aqueous phase was carefully transferred to a new tube, then added with 500 μ l of propan- 2- ol, mixed gently, and incubated at room temperature for 5 min before centrifuging at 12,000 rpm, 4 °C for 15 min. The RNA pellet was washed with 75 % v/v ethanol. After centrifugation, the pellet was dried and then dissolved with 10-50 μ l DEPC-treated water.

2.2.6.2 Measurement of DNA/RNA concentration by spectrophotometer

The total RNA or DNA was measured by the Nanodrop 2000c spectrophotometer (Thermo Scientific, USA) for its quantity and purity at absorbance ratios of OD_{260/280} and OD_{260/230}. Also, the RNA sample was evaluated integrity level using agarose gel electrophoresis with 1X TBE buffer (45 mM Tris-borate, 1 mM EDTA). The RNA sample was maintained at -80°C.

2.2.6.3 Determination of DNA/RNA by agarose gel electrophoresis

Agarose gel was prepared by weighing a w/v percentage solution of agarose powder and 1X TBE buffer into the flask. The concentration of agarose in a gel depended on the sizes of the DNA fragments to be separated. The agarose/buffer was melted using a microwave. Then, the dissolve agarose in buffer was poured into a gel mold and set at room temperature. The solid gel was placed on a gel box containing the running buffer. The DNA/RNA sample was added with a final concentration of 1X DNA loading dye (1 mM Tris pH 8.0, 5 % w/v glycerol, and 0.04 % w/v bromophenol blue) before loading. The sample was carefully loaded into wells of gel and run electrophoresis at 100-120 volt until the dye migrated to an appropriate distance. An appropriate DNA size marker loaded along with the sample as well. For detection of DNA/RNA, the gel was stained with ethidium bromide (EtBr) and then destained with distilled water and visualized under a UV light source.

2.2.7 The first stranded complementary DNA synthesis

Before cDNA synthesis, the RNA sample was treated with Deoxyribonuclease I (DNase I) to eliminate DNA contamination. Briefly, 1 µg of total RNA was mixed with, 1X DNase I buffer, and 1 U of DNase I (Thermo Scientific, USA), and up to a total volume of 10 µl with DEPC-treated water. The mixture was incubated at 37 °C for 20 min, then added with 0.5 µl of 50 mM EDTA before heat at 65 °C for 5 min. After placed on ice for 2-3 min, the DNase I-treated RNA was added with a mixture of 1X M-MuLV reverse transcriptase (RT) buffer, 200 µM dNTP, 0.5 µM oligo-dT primer, 100 U M-MuLV, and up to the total volume of 15 µl with DEPC-treated water. The reaction condition was initiated at 25 °C for 5 min, 42 °C for 60 min, and 70 °C for 10 min. The cDNA was kept at -20 °C until used.

2.2.8 Determination of the candidate receptor gene expression in shrimp by quantitative realtime PCR (qRT-PCR)

2.2.8.1 Experimental samples

The 5-6 ovaries from individual shrimp corresponding to each stage of ovarian development was used to determine for gene expression during ovarian maturation, while the shrimp tissues, including eyestalk, brain, thoracic ganglia, gills, hepatopancreas, muscle, and ovary, isolated from 3 previtellogenic female shrimp were used for tissue distribution experiment.

2.2.8.2 Designation of gene-specific primers for qRT-PCR

The candidate receptor gene primers (Table 1) were design corresponding to the coding region from transcriptome NCBI Primer- BLAST (<https://www.ncbi.nlm.nih.gov/tools/primer-blast/>) with the setting parameters of 1) the amplicon size of 100-250 bp, 2) 50-60 % GC content, and 3) melting temperature of 58-60 °C. Then, the resulted candidate primer was analyzed for its characteristics by OligoAnalyzer program (<https://sg.idtdna.com/calc/analyzer>) with the criteria of 1) Gibb's free energy (ΔG) of self-hairpin greater than -0.5, 2) ΔG of self-dimer greater than -0.5 and no more than 4-base paring, and 3) ΔG of a heterodimer between forward and reverse primers greater than -0.5 and no more than 4-base paring.

2.2.9 Examination of specificity and efficiency of the specific primer

2.2.9.1 Polymerase chain reaction

The specificity of primers was performed by conventional PCR. The ovarian cDNA was used as a template in a PCR reaction. The PCR mixture was composed of a template DNA and a final concentration of 1X PCR buffer, 2 mM MgCl₂, 0.2 mM primer pair, 0.2 mM dNTP, and 1 U Taq polymerase. The temperature profile was at 94 °C for 3 min, followed by 35 cycles of 94 °C for 30 sec, 55 °C for 30 sec, and 72 °C for 45 sec, and a final extension at 72 °C for 10 min. The PCR product was analyzed for its quality by agarose gel electrophoresis as mentioned in 2.6.3.

Table 1 Oligonucleotides used in this study.

Primer name	Forward sequence (5'→3')	Purpose
oligo-dT	CCGGAATTCAAGCTTCTAGAGGAT CCTTTTTTTTTTTTTTTTTT	cDNA synthesis
qFm-Vg-F	TCCATCTGCAGCACCAATCTTCGC	qRT-PCR
qFm-Vg-R	GCAACAGCCTTCATTCTGATGCCA	qRT-PCR
qFm-EF1 α -F	GAACTGCTGACCAAGATCGACAGG	qRT-PCR
qFm-EF1 α -R	GAGCATACTGTTGGAAGGTCTCCA	qRT-PCR
qFm-EGF receptor-F	CAGTGTCAGTAGCAATGGAG	qRT-PCR
qFm-EGF receptor-R	CGTTGTAATACTCGTGAGCC	qRT-PCR
qFm-ROR-F	GGTAGTGTGTCTGGTCATTC	qRT-PCR
qFm-ROR-R	GAGTATTGGAGGAGAGGTTG	qRT-PCR
qFm-RYK-F	GGCAAATAACCACTCAGG	qRT-PCR
qFm-RYK-R	ATATCCCACCGACTTCTCC	qRT-PCR
qFm-GRL101 receptor-F	CAACATGGGCGAGAGTTT	qRT-PCR
qFm-GRL101 receptor-R	ACGATGGAAGGCTTACTGTC	qRT-PCR
qFm-Smo receptor-F	CTCACTAGACTCGCAGATGT	qRT-PCR
qFm-Smo receptor-R	GGGTATCTTGGTTCATGGTG	qRT-PCR
qFm-Glycine α receptor-F	GGTATTCGGTCAGTTGTAGG	qRT-PCR
qFm-Glycine α receptor-R	GTCTTTACACAGACCACGAG	qRT-PCR
qFm-Glycine β receptor-F	GGATCATGGTCGCTCTAAC	qRT-PCR
qFm-Glycine β receptor-R	GTGTGTGGGATTGACTCG	qRT-PCR
qFm-Glutamate receptor-F	CGCCGCCGCCGCCCTTCTTC	qRT-PCR
qFm-Glutamate receptor-R	CTCTCCTTGGTGATGACTTC	qRT-PCR
qFm-Insulin receptor-F	TAAGGCTTCAGGGCGGGGTC	qRT-PCR
qFm-Insulin receptor-R	AGGTTGTGTTGGAGGACGGG	qRT-PCR
qFm-NMDA receptor-F	GAACACCTCAGCCTCAAG	qRT-PCR
qFm-NMDA receptor-R	CTTTGTCGTAGGGGATGCTC	qRT-PCR
qFm-BMPRII-F	CCACCATTACAGCCCCACCA	qRT-PCR
qFm-BMPRII-R	GCCTGAAACACTGAGTTCCTG	qRT-PCR
qFm-Renin receptor-F	GTGTGGGGAGGTGACTGTGG	qRT-PCR

Primer name	Forward sequence (5'→3')	Purpose
qFm-Renin receptor-R	AATGGGCAGGTTGAAGGGGG	qRT-PCR
qFm-Notch receptor-F	GCCCTGACTCCGCCGCAG	qRT-PCR
qFm-Notch receptor-R	CCGTCCTTGTCGTCCTCGTC	qRT-PCR
qFm-TGF- β 1 receptor-F	GCTTTGGGAAGGCACAGT	qRT-PCR
qFm-TGF- β 1 receptor-R	GGGGGTTTGTAAATCGGGAGG	qRT-PCR
qFm-Sax receptor-F	CTGCCTTGCCGTTACCTCAT	qRT-PCR
qFm-Sax receptor-R	GTTTGGCAAGAGTTCGCTGG	qRT-PCR
XbaI-stem-Sax receptor-F	GCC-TCTAGA-AACATTGCCCT CTCAGCCAT	Cloning
NdeI-stem-Sax receptor-R	GCC-CATATG-TGGGTCATTGG GAACTACATC	Cloning
XhoI-stem-loop-Sax receptor-F	GCC-CTCGAG-AACATTGCCCT CTCAGCCAT	Cloning
NdeI-stem-loop-Sax receptor-R	GCC-CATATG-AGGGTTCTGGT GCCAACATT	Cloning
XbaI-stem-GFP-F	GCG-TCTAGA-AGCAGACTATG GACCTGACC	Cloning
NdeI-stem-GFP-R	GCT-CATATG-ATCTTCTCGGTA CTGGG CTC	Cloning
NotI-stem-loop-GFP-F	AA-GCGGCCGC-AGCAGACTATGG ACCTGACC	Cloning

2.2.9.2 Determination of primer efficiency by qPCR

The efficiency of primer was determined by amplification with 2-fold serial diluted cDNA in a qPCR reaction, which was mentioned in section 2.8.4. To calculate the primer efficiency, a slope value of regression between sample Ct value (y-axis) and \log_{10} value of serial dilution (x-axis) was calculated into the equation, $\text{efficiency} = [10^{(-1/\text{slope})} - 1]$ (Appendix 2). Also, all primers were PCR amplified using agarose gel electrophoresis to ensure each candidate receptor gene having a single band and correct size.

2.2.10 The qRT-PCR reaction and relative quantification of gene expression

In the realtime PCR reaction, the 2 μl of 1:10 diluted cDNA was added in a mixture of 1X KAPA SYBR® FAST universal (KAPA Biosystems), 1X KSF low ROX, 0.5 μM primer pairs, and up to a final volume of 15 μl with deionized (DI) water. The sample was subjected to a realtime PCR machine (Agilent Technologies Stratagene MX3000P, USA). The temperature profile for amplification was at 95 °C for 1 min, followed by 40 cycles of 95 °C for 15 sec and 60 °C for 30 sec. Subsequently, the dissociation curve was generated by heating the PCR product at 95 °C for 1 min, 60 °C for 30 sec, and 95 °C for 30 sec. Elongation factor 1 α gene (EF1 α) was used as an endogenous control. After the PCR reaction finished, a threshold cycle (Ct) value from each reaction was obtained. The PCR product which represented a single peak of the melting curve was further used to analyze for relative expression. The relative expression was calculated by the delta-delta Ct ($2^{-\Delta\Delta\text{CT}}$) method (Livak and Schmittgen, 2001). Statistical analysis was performed using one-way analysis of variance (ANOVA).

2.2.11 Construction of recombinant plasmid containing an inverted repeat sequence of saxophone

The RNA interference (RNAi) was proceeded to study the function of the candidate receptor gene using receptor-specific doubled stranded RNA (dsRNA).

2.2.11.1 Amplification and purification of PCR product

According to the nucleotide sequence of saxophone (FmSax) receptor retrieved from the transcriptome, the FmSax-specific primers tagged with restriction

enzyme site at 5' ends were designed (Table 1 and Figure 19 A). The ovarian cDNA was used as the template to amplify with the specific primers to obtain stem and stem-loop fragments by PCR as mentioned in 2.8.3.1. The PCR product separated in an agarose gel as mentioned in 2.6.3 was excised with a clean blade. The PCR product in the gel was purified using a FavorPrep Gel/PCR purification kit (Favorgen). Briefly, the piece of gel was added with 500 μ l FADF buffer and then incubated at 55 °C until it dissolved completely. The sample mixture was then transferred to the FADF column and centrifuged at 12,000 rpm for 1 min. After discarded the flow-through, the column was added with 750 μ l washing buffer (ethanol added). After centrifuging and discarding the flow-through, the column was spun again for 3 min to dry the column matrix. Then, 15-20 μ l DI water was added to dissolve the DNA sample. The DNA sample was eluted with 15-20 μ l DI water and centrifuged. The purified PCR product was determined for its quantity by Nanodrop as mentioned in 2.6.2.

2.2.12 Cloning of the inverted repeat sequence of FmSax in an expression vector

To construct a recombinant plasmid carrying the inverted repeat sequence of the FmSax, a molecular cloning method was performed.

2.2.12.1 Restriction enzyme digestion

The stem and stem-loop fragments were digested with restriction enzymes (RE). The 10 μ l of digestion reaction was composed of the purified PCR product, 1X FastDigest buffer (Thermo-Scientific), and 1 U of corresponding REs such as *Xba*I, *Eco*RI, or *Xho*I (as Table 1). The sample was incubated at 37 °C for overnight before being cleaned up using FovarPrep Gel/PCR purification kit as mentioned in 2.9.1. The pET28a was used as an expression vector to produce dsRNA in a bacterial system. It was digested with the same REs as the stem fragment.

2.2.12.2 DNA ligation

The 10 μ l of the ligation reaction was composed of 1X buffer T4 ligase, 1 U of T4 DNA ligase (Vivantis), 15 ng of digested plasmid, and appropriated digested DNA fragment. The molar ratio of vector to insert was 1:3. The reaction was incubated at 4 °C overnight.

2.2.12.3 Competent cell preparation

The *Escherichia coli* TOP10 or HT115 was prepared for competent cells by the calcium chloride method. Briefly, 80 ml of LB broth was inoculated with 3 ml of LB broth containing cultured *E. coli* and then incubated at 37 °C, 200 rpm until the OD_{600 nm} of 0.4-0.5. A total of the bacteria was harvested in a flat bottom centrifuge bottle by centrifuging at 4,000 rpm, 4 °C for 15 min. After removing the supernatant, the bacterial pellet was gently resuspended in 10 ml of 0.1 M ice-cold CaCl₂ and still on ice for 10 min. After spinning, the pellet was resuspended in 30 % v/v glycerol with 1 ml of 0.1 M CaCl₂. The competent cells were aliquot 50 µl of competent cells to each microcentrifuge tube and stored at -80 °C until used.

2.2.12.4 Plasmid transformation

The ligation reaction or recombinant plasmid was transformed in the competent *E. coli* cells using the heat shock method. The 50 µl of the competent cell was mixed with 5 µl of ligation reaction or 1 µl of recombinant plasmid and incubated on ice for 20 min. Then, the sample was heated at 42 °C for 75 sec and immediately placed on ice for 5 min before being added with 950 µl of LB medium. The sample was further incubated at 37°C, 250 rpm for 1-1.5 hr before being spread on LB agar containing both 50 µg/mL kanamycin and 10 µg/mL tetracycline. The plate was incubated at 37°C overnight.

2.2.12.5 Plasmid extraction

A single bacterial colony was cultured in 3 ml of LB broth at 37 °C, 180 rpm overnight. The plasmid was extracted using the GF-1 plasmid DNA extraction kit (Vivantis, Malaysia). Briefly, the bacterial culture in the microcentrifuge tube was centrifugated at 12,000 rpm for 1 min. After removing the supernatant completely, the pellet was added with 250 µl solution 1 and resuspended. The tube was then added with 250 µl of solution 2 and gently mixed at room temperature for no longer than 5 min. The add 400 µl neutralizing buffer was added and gently mix by inverting the tube until a white precipitate form. After centrifuging for 1 min, the 650 µl of supernatant was transferred into a column and then spun for 1 min. When discarding flow through, the column was washed with 650 µl of wash buffer and centrifuged. Removing flow

through, the column was spun again to remove residual ethanol. The column was placed into a clean microcentrifuge tube, added 15-30 of DI water and stood for 1 min, and then spun for 1 min to elute DNA. The DNA was stored at -20 °C before used. The plasmid was measured for its concentration by Nanodrop as mentioned in 2.6.3.

2.2.12.6 Preparation of plasmid carrying the inverted repeat sequence of FmSax in *E. coli* HT115

The pET28a harboring the stem fragment of FmSax was then digested with the same REs as the stem-loop fragments (mentioned in 2.9.2.1). After purification of the digested recombinant plasmid (as described in 2.9.1), the ligation of the stem-loop fragment and the stem-inserted pET28a was performed as described in 2.9.2.2. After transformation in *E. coli* TOP10, a single bacterial colony was cultured and extracted for the inverted repeat sequence of FmSax harbored plasmid (as described in 2.9.2.5). The nucleotide sequence of FmSax was analyzed by DNA sequencing (Ward medic, Thailand). In addition, the recombinant plasmid was validated by double restriction enzyme digestion as described in 2.9.2.1 and visualized on agarose gel electrophoresis as described in 2.6.3. Finally, the recombinant plasmid was transformed into incompetent *E. coli* HT115 DE3 cells and then spread on LB agar containing 50 µg/mL kanamycin as described in 2.9.2.4. Besides, a green fluorescent protein (GFP) from pHMGFP plasmid was used to construct an inverted repeat sequence to produce GFP-specific dsRNA as a non-specific dsRNA. Both dsRNAs were maintained in 30 % glycerol at -80 °C until use.

2.2.13 Production of receptor-specific dsRNA in bacteria

2.2.13.1 Induction of dsRNA expression in bacteria

A single bacterial colony of *E. coli* HT115(DE3) containing the recombinant plasmid was cultured in LB broth containing 50 µg/ml kanamycin at 37 °C, 180 rpm overnight. Then, the bacterial starter was inoculated in a fresh LB broth (volume of LB medium to a flask for optimal aeration of 1 to 5) and cultured at 37 °C, 180 rpm until mid-exponential bacterial growth phase with OD₆₀₀ was reached between 0.4-0.8 measuring by GENESYS 10S UV-Vis spectrophotometer (Thermo Scientific, USA). Next, the culture was added with a final concentration of 0.2 mM of isopropyl

β -D-1-thiogalactopyranoside (IPTG) was further incubated for 2-3 hours at the same conditions. The total bacteria were harvested by centrifuge at 12,000 rpm, 4 °C for 15 min. After discarding the supernatant, the bacterial pellet was kept at -20 °C until use in dsRNA extraction.

2.2.13.2 Extraction of receptor-specific dsRNA

The dsRNA was extracted from the bacteria using the ethanol method (Posiri et al., 2013). Shortly, the bacterial pellet was resuspended vigorously in 75 % ethanol in PBS and incubated at room temperature for 10 min. After centrifuged at 12,000 rpm, 4 °C for 15 min, the supernatant was removed, and the bacterial pellet was resuspended in 150 mM NaCl. The pellet was incubated at room temperature for 1 hr. The supernatant was cautiously transferred to a new tube. To increase the concentration of dsRNA, the dsRNA sample was precipitated by mixed with isopropanol (volume of 1 to 1) and stored at -20 °C for 30 min to precipitate the RNA. After centrifuged at 12,000 rpm, 4 °C for 30 min, the dsRNA pellet was carefully washed in 70 % ethanol and centrifuge at 12,000 rpm, 4 °C for 5 min. The pellet was air-dried for 5 min before being dissolved in 150 mM NaCl. The dsRNA was stored at -20 °C and used within 1 week after production. Before used in the experiments, the concentration of the extracted dsRNA was evaluated comparing the integrity of the dsRNA and DNA marker by agarose gel electrophoresis as described in 2.6.3.

2.2.13.3 Determination of dsRNA by RNase digestion

The purified dsRNA was confirmed for its dsRNA characteristic by RNase digestion assay. The 10 μ L of the RNase III digestion reaction was composed of 1 μ l from 1:10 dilution of dsRNA, 0.5 μ l from 1 U of RNase III (New England Laboratories), 1X RNase III buffer, and 1X MnCl₂. In addition, the 1 μ l of 1:10 diluted dsRNA sample was treated with 1 μ g/mL RNase A (Thermo Scientific, USA). The reactions were incubated at 37 °C for 5 min and then visualized on an agarose gel by electrophoresis as described in 2.6.3.

2.2.14 Effect of the FmSax knockdown on vitellogenesis in shrimp

2.2.14.1 Determination of FmSax knockdown by the dsRNA injection

To silence the *FmSax* expression, the experiment was set into three groups; shrimp injected with the 2.5 $\mu\text{g/g}$ body weight dsGFP, *FmSax* receptor-specific dsRNA (dsSax), or 150 mM NaCl. Seven shrimp were used in each group. The dsRNA was intramuscularly delivered into the 2nd ventral abdominal segment of each previtellogenic female shrimp using a 0.5 mL insulin syringe with a needle (Nipro, Indonesia). After the injection for 7 days, ovary, and hepatopancreas were isolated and extracted for the total RNA extraction as described in 2.6, and subsequently used to generate cDNA as described in 2.7. The determination of *FmSax* expression was performed by qRT-PCR as described in 2.8.4. The one-way ANOVA was used to analyze statistics.

2.2.14.2 Effect of the *FmSax* knockdown on gene expression in shrimp

After the determination of the *FmSax* knockdown by the dsRNA injection, the effect of *FmSax* silencing on vitellogenesis was investigated by determination of vitellogenin (*Vg*) and *FmBMPRII* expressions and oocyte proliferation. The ovaries and hepatopancreas derived from cDNA were used to determine for *Vg* expression by qRT-PCR as described in 2.8.4.

2.2.14.3 Effect of the *FmSax* knockdown on oocyte proliferation

The oocyte proliferation was determined by 5-ethynyl-2-deoxyuridine (EdU) assay. The ovaries were freshly collected from shrimp in each experimental group and cut into small pieces under an aseptic condition. The ovarian pieces were serially washed for 30 sec/step in 500 μl of a culture medium (2X Leibovitz's L-15 (Gibco, UK), 10 % v/v fetal bovine serum (FBS) (Gibco, South America), and 1 %w/v glucose) containing 10X, and 20X penicillin/streptomycin (Gibco, USA), respectively, in a 24-well plate. After washed, each ovarian piece was transferred in 150 μl of the culture medium containing 1X penicillin/streptomycin in a 96-well plate. Then, each sample was added with a final concentration of 10 μM 5-EdU (Abcam). The ovarian explant was cultured at 28 °C for overnight. Then the ovarian pieces were fixed in absolute methanol at -20 °C until used. The fixed tissues were sonicated at 40 % amplitude for 1 sec on/off until the supernatant was turbid. The supernatant was transferred to a new tube and stood at room temperature until the oocyte cells were

precipitated. The supernatant was carefully removed, and the oocyte cells were rehydrated with a serial dilution of methanol in PBS, 70 %, 50 %, and 1X PBS, respectively. During each step, the oocyte cells were precipitated to the bottom by standing at room temperature. For EdU detection, the oocyte cells were blocked in 500 μ l of a blocking solution (10 % FBS in PBS) and incubated at room temperature for 1 hr. After discarding the supernatant, the oocytes were incubated with 50 μ l of a staining solution (100 mM Tris (pH 7.5), 10 μ M Alexa Fluor™ 488 azide (Molecular probes, USA), 1 mM CuSO₄, and 100 mM L-Ascorbic acid in the blocking solution) in dark for 20 min. After discarding the supernatant, the oocyte cells were incubated with a washing buffer (0.05 % Triton X-100 in PBS) containing 5 μ g/ml 4',6-Diamidino-2-phenylindole dihydrochloride (DAPI) (PanReac AppliChem) to counterstain all nuclei for 3-5 min. After removing the supernatant, the oocytes were rinsed with the washing buffer three times. The oocyte cells were mounted with a mounting medium (0.02% w/v n-propyl gallate, 10 mM Tris pH 8.0, and 90% v/v glycerol) on a glass slide covered with a coverslip and sealed sample with nail polish before kept at 4 °C until used. The sample was observed under a fluorescence microscope (Olympus BX51), and images were captured using with cellSens Standard software (Olympus). The EdU index was calculated as a percentage of the numbers of EdU-positive cells to the total counted oocyte cells (n = 100-150).

2.2.15 Statistical analysis

The data were statistically analyzed by one-way ANOVA and pair-wise comparison by Sheffe's test or t-test.

CHAPTER 3

RESULTS

3.1 Transcriptome sequencing and analysis

A total of 44,153,692, 42,514,922, 44,704,814, and 47,240,232 raw reads were obtained from the paired-end Illumina sequencing of *F. merguensis*'s ovaries at the ovarian developmental stage of 0, 1, 2, and 3, respectively. These raw reads were *de novo* assembled by Trinity to construct the transcriptome resulting in a total of 58,343 transcripts. After hierarchically clustered and removed for the redundant transcripts, the 53,763 longest transcripts of each cluster were obtained with an average length of 1,060 bp, a 43 % GC content, and an N50 length of 2,380 bp (Table 2). Also, the length distribution of unigenes was analyzed, and the result showed that 72.7 % of the transcriptome contained their length less than 1,000 bp (Figure 12).

3.2 Functional annotation of receptor genes

In the functional annotation, the unigenes were annotated against the databases as follows: NR, NT, Swiss-Prot, COG/KOG, KEGG, Pfam, and GO databases. Using several keywords of receptor to filter the annotated unigenes, a total of 663 receptor genes were obtained. The functional distribution analyzed by the GO annotation of the receptor genes revealed that 50 %, 26 %, and 24 % of the receptors represented their roles as the biological process, the cellular component, and the molecular function, respectively (Figure 13). The most represented classifications were cellular process and metabolic process; membrane and membrane part; and binding and catalytic activity (Figure 13). Some receptor genes were classified in more than one domain giving a total of 3,013 gene classifications. In addition, the receptor genes analyzed by blast KEGG orthology and links annotation (BlastKOALA) (Kanehisa, Sato, and Morishima, 2016) revealed that most

Table 2 Summary of statistics for the *de novo* assembly of the *F. merguensis*' s transcriptome.

Transcriptome assembly statistics for <i>F. merguensis</i>	
Raw reads of stage 0 (bp)	44,153,692
Raw reads of stage 1 (bp)	42,514,922
Raw reads of stage 2 (bp)	44,704,814
Raw reads of stage 3 (bp)	47,240,232
Number of transcripts	58,343
Number of unigenes	53,736
• GC (%)	43.14
• Longest contig length (bp)	22,232
• Shortest contig length (bp)	189
• Average contig length (bp)	1,060
• Contig N10 (bp)	6,988
• Contig N20 (bp)	5,219
• Contig N30 (bp)	4,005
• Contig N40 (bp)	3,116
• Contig N50 (bp)	2,380
• Total bases	56,998,612

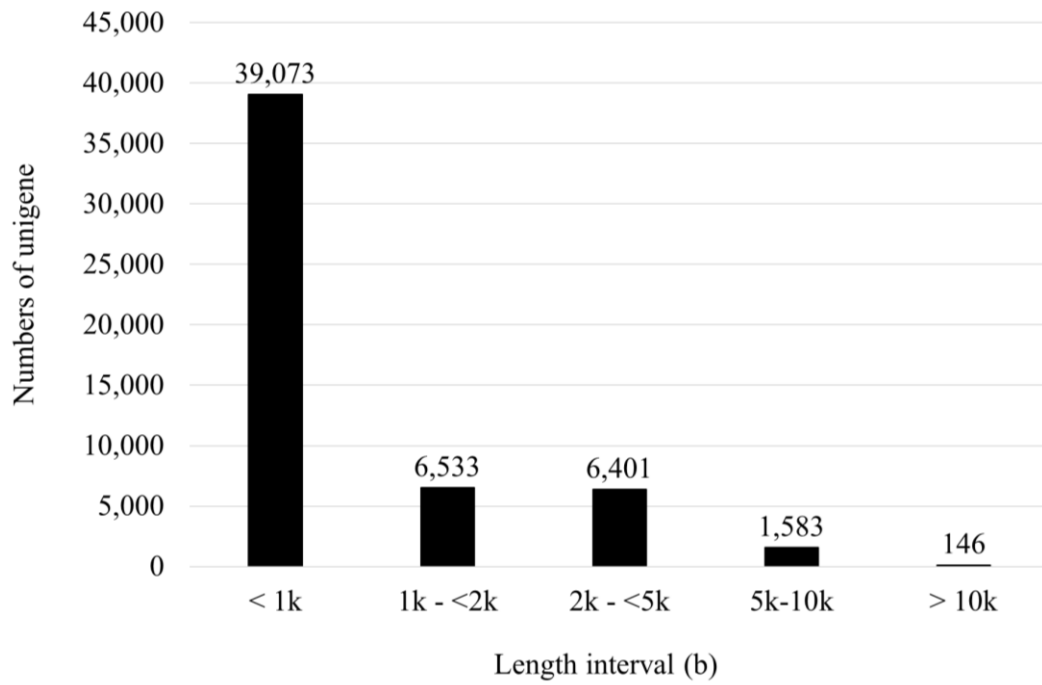


Figure 12 Length distribution of the *de novo* assembled transcriptome. The X- and- Y-axis indicate the interval of unigene length and. the frequency of unigenes in each interval.

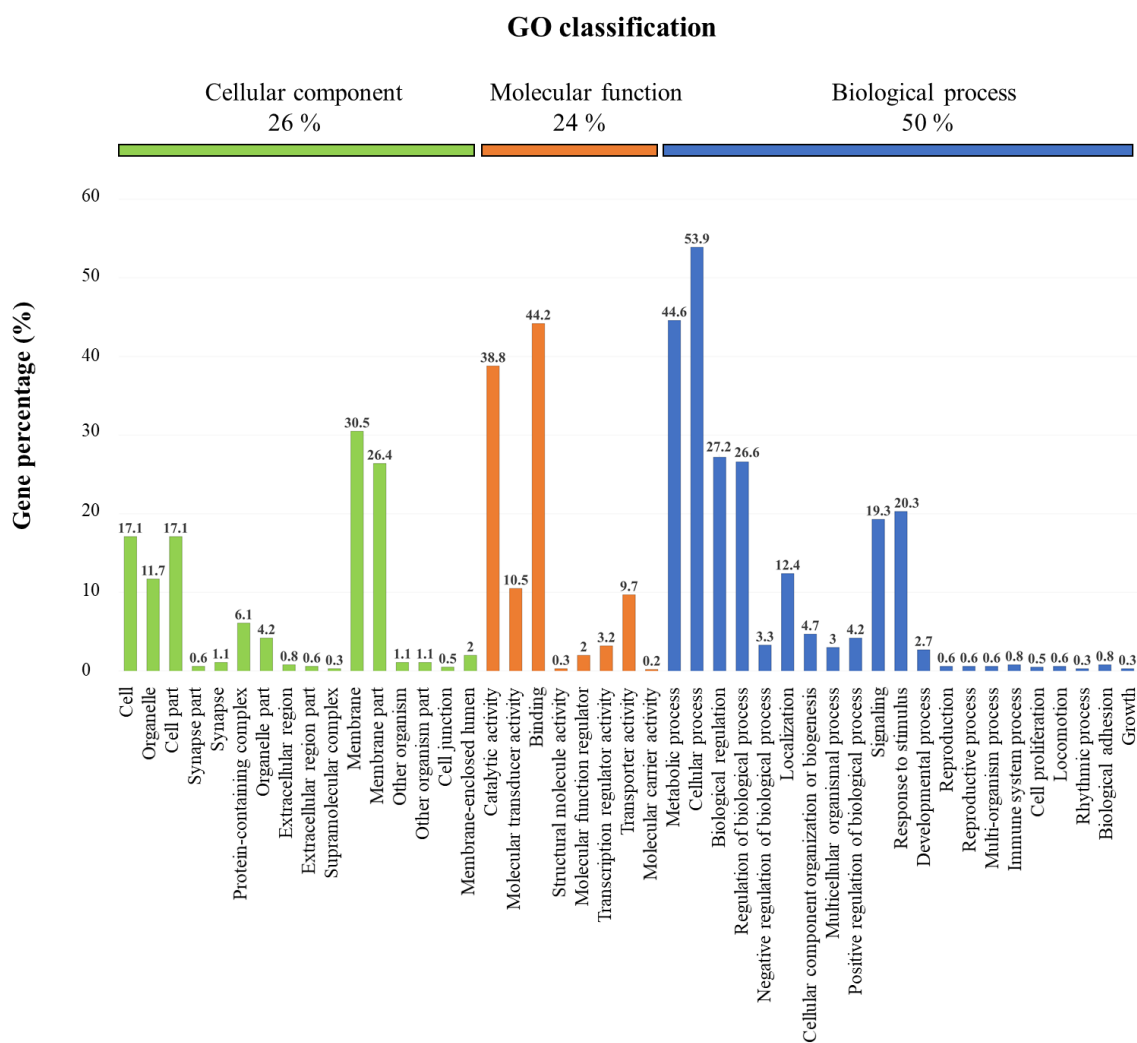


Figure 13 Gene ontology (GO) functional enrichment of receptor genes. The X-axis represents the GO term under the three main GO domains and the ratio between the number in this pathway and the total number of annotated genes. The Y-axis was the percentage of the genes annotated in the term.

ovarian receptors were involved in human diseases (39%), and less in organismal systems (26 %). The smallest group of the receptors was metabolism (1 %) (Figure 14). Furthermore, the FPKM values derived from the DEG prediction of the receptor genes, were generated a heatmap using BioVinci (Figure 14 5) and plotted mean-centered expression clusters using the R package.

3.3 Identification of candidate receptor gene in *F. merguensis*'s ovaries

According to the receptor identification, the 663 receptor genes were obtained using several receptor keywords. They were composed of 160 GPCRs, 263 RTKs, 65 NRs, and 175 ICs as shown in Table 3. Among those, 185 receptors were at least 2-fold differentially expressed during ovarian development stages. In this study, a total of 15 candidate receptor genes were selected including 3 GPCRs, 8 RTKs, and 4 ICs (Table 3). Most candidate receptor genes were considered based on the reproductive pathways analyzed via KEGG, and their differential expression profile were plotted as mean-centered expression patterns into clusters 3, 4, and 7, respectively (Figure 15 B). All expression patterns were separated into 36 patterns (Appendix 3).

3.4 Determination of the candidate receptor gene expression during ovarian developmental stages

The 15 candidate receptor genes were selected based on KEGG annotation and differential expression during ovarian development. Then, they were determined for their expression profiles during ovarian development stages including previtellogenic (st0), early vitellogenic (st1), late vitellogenic (st2), and mature stages (st3), respectively, by qRT-PCR. The results showed 5 expression patterns among those genes:

1. The expression of the NMDA receptor gene was a significant peak at the previtellogenic stage. Then it dramatically went down at the early vitellogenic stage and steadily fluctuated at the mature stage (Figure 16).

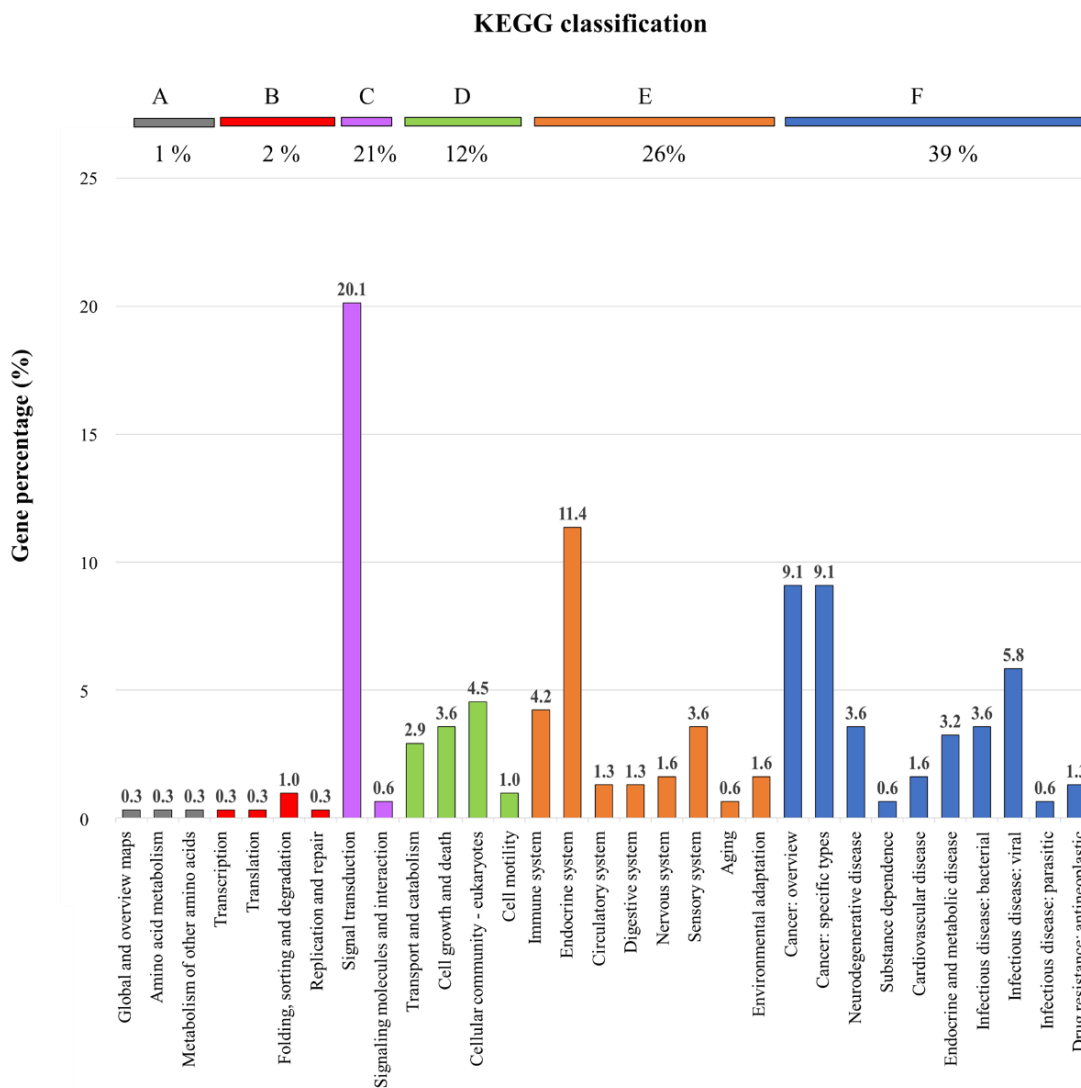
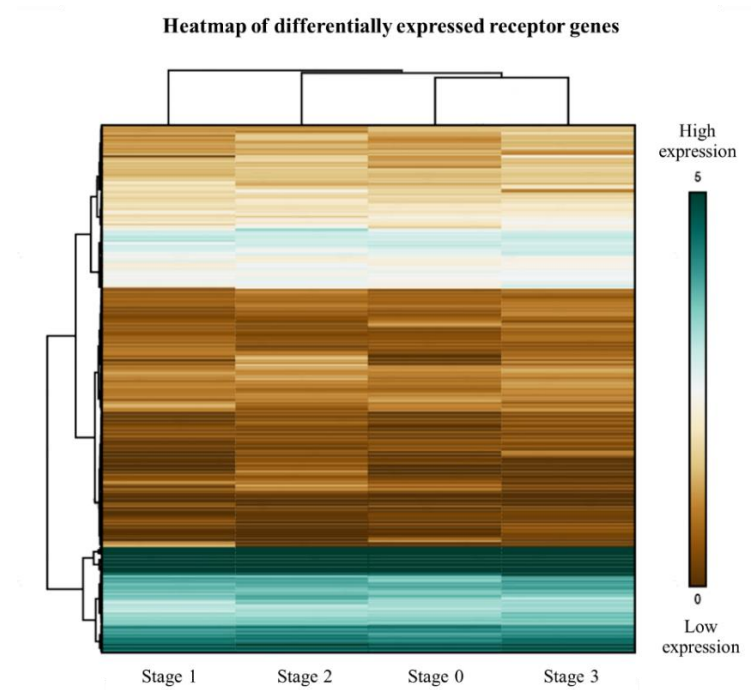


Figure 14 KEGG functional enrichment of the receptor genes. The KEGG pathway analysis was performed via BlastKOALA. The KEGG pathways gene were divided into 6 branches: A: Metabolism B: Genetic information processing, C: Environmental information processing, D: Cellular processes, E: Organismal systems, and F: Human diseases. The bars represented the number of the genes annotated in the pathway under the four main KEGG domains and the ratio between the number in this pathway and the total number of annotated genes.

(A)



(B)

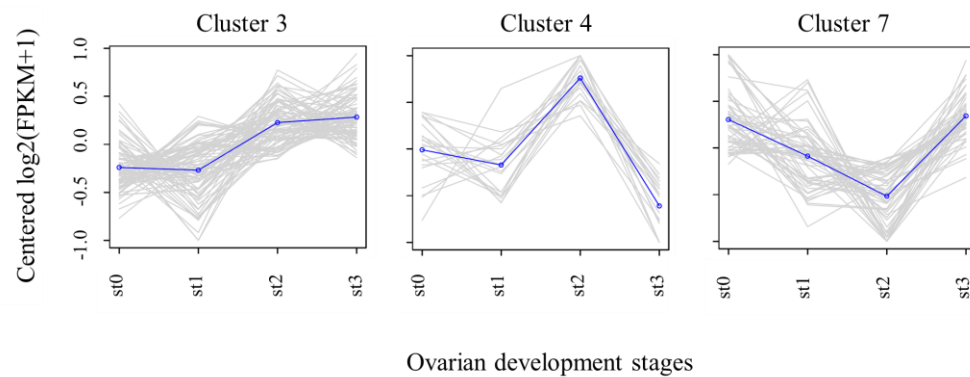


Figure 15 Analysis of the differentially expressed receptor genes. The heatmap (A) and some dendrogram (B) analyses were generated from the results of differentially expressed receptor genes using the $\log_2(\text{FPKM}+1)$ value. In the heatmap, the range of colors from green to brown denoted the $\log_2(\text{FPKM}+1)$ value from high to low expression (A). In the dendrogram, the expression patterns were analyzed into subclusters. Each grey line in a subplot represented the relative expression value of a gene cluster under ovarian development stages, and the blue line represented the mean value (B).

Table 3 Summary of a number of the receptor genes and the candidate receptor genes in each type of receptor.

Receptor types	No. of differentially expressed receptors	Number of candidate receptor genes
G protein-coupled receptor (GPCR)	160	3
<ul style="list-style-type: none"> • Smoothened (Smo) receptor • G-protein coupled receptor GRL101 (GRL101) • Renin receptor 		
Receptor tyrosine kinase (RTK)	263	8
<ul style="list-style-type: none"> • Epidermal growth factor receptor (EGFR) • Receptor tyrosine kinase-like orphan receptor (ROR) • Receptor-like tyrosine kinase (RYK) • Transforming growth factor-β 1 (TGF-β 1) receptor • Bone morphogenetic protein type 1 receptor (BMPRI) or saxophone (sax) • Bone morphogenetic protein type 2 receptor (BMPRII) • Notch receptor • Insulin receptor 		
Ion channel (IC)	175	4
<ul style="list-style-type: none"> • Glycine-α receptor • Glycine-β receptor • Glutamate receptor • N-methyl-D aspartate (NMDA) receptor 		
Nuclear receptor (NR)	65	0
Total genes	663	15

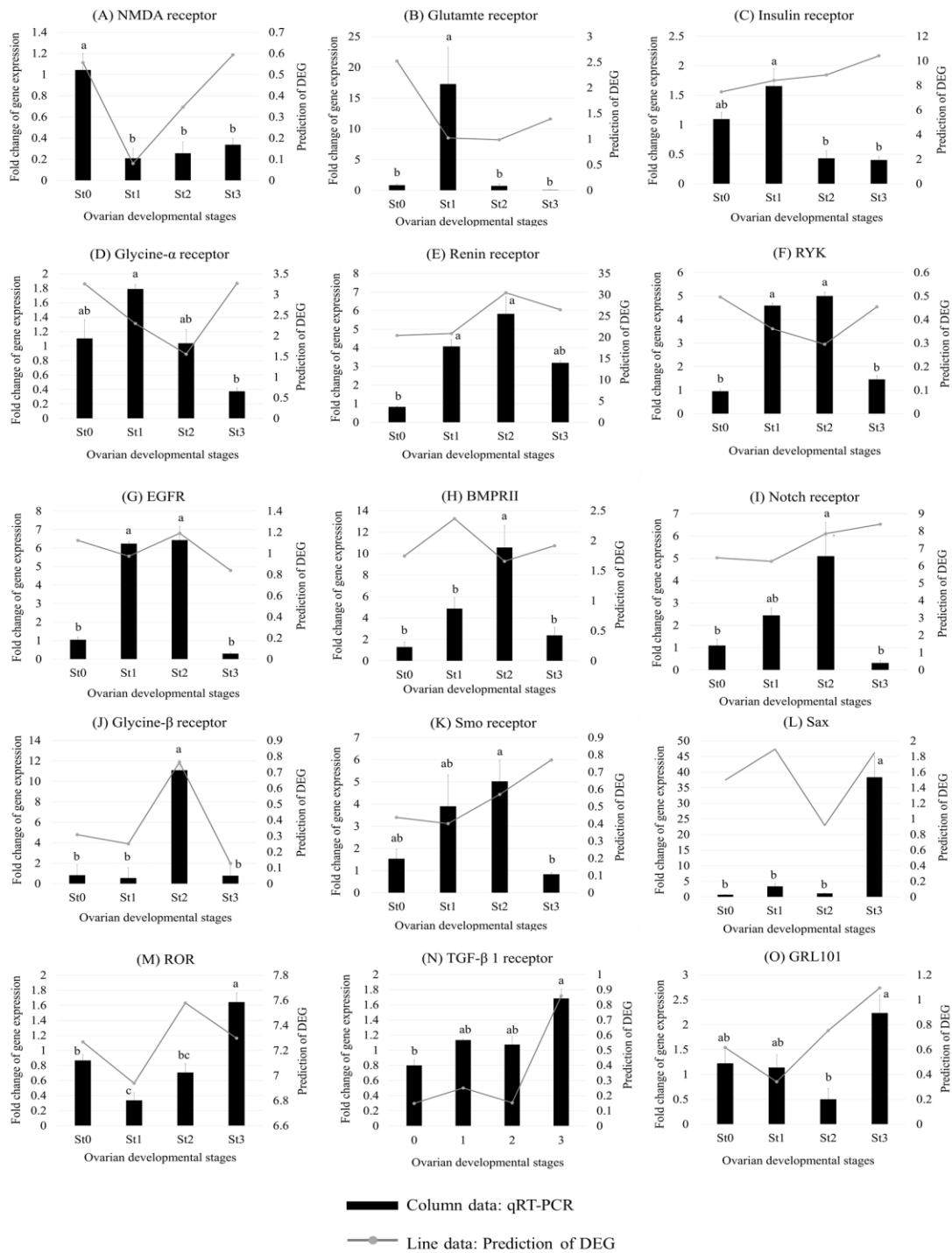


Figure 16 Determination of the candidate receptor expression during ovarian developmental stages. The ovaries from shrimp corresponding to 4 stages of ovarian development, including previtellogenic (st0), early vitellogenic (st1), late vitellogenic

(st2), and mature stages (st3), were determined for gene expression. The bars and the lines denote the relative expression derived from qRT-PCR and in silico analysis, respectively. The 7 individual shrimp were used in each group. Bars and error bars represent means and SEM, respectively. Alphabets indicated significant differences between groups analyzed by one-way ANOVA ($p < 0.05$) followed by pair-wise comparison by Scheffe's test.

2. The expression of glutamate receptor, insulin receptor, and glycine- α receptor, were low at the previtellogenic stage. Then the expressions were significantly rose at the early vitellogenic stage and dropped at the mature stage (Figure 16 B-D).
3. The expressions of renin receptor, EGFR, and RYK, were decrease at the previtellogenic stage. Then their expressions were rapidly increased at both early vitellogenic and late vitellogenic stages before suddenly declined at the next stage (Figure 16 E-G).
4. The expressions of BMPRII, notch receptor, glycine- β receptor, and Smo receptor, were low at both previtellogenic and early vitellogenic stages. Then they gradually grew up until they considerably peaked at the late vitellogenic stage, and quickly fell at the mature stage (Figure 16 H-K).
5. The expressions of sax, ROR, TGF- β 1 receptor, and GRL101, were low at the previtellogenic stage. Then they slightly fluctuated at later stages and suddenly increased at the mature stage (Figure 16 L-O).

However, only expression profiles of 3 receptors (renin, glycine- β , and TGF- β 1 receptors) from qRT-PCR showed similar profiles to the predicted DEG derived from transcriptome analysis genes (Figure 16 E, J, and N).

3.5 Expression analysis of *FmSax* and *FmBMPRII* in shrimp tissues and hepatopancreas during ovarian development

According to the previous study, we demonstrated that the glass bottom boat, a BMP ortholog, plays a stimulatory role in vitellogenesis in *F. merguensis* (Sathpondecha and Chotigeat, 2019). Also, the expression of the BMP receptors, BMPRII

(*FmBMPRII*) and saxophone (*FmSax*) were differentially expressed during ovarian development (Figure 16 H and L). Therefore, *FmSax* and *FmBMPRII* were selected for further investigation. The expression of *FmSax* and *FmBMPRII* were determined in shrimp tissues, including eyestalks, brain, thoracic ganglia, gill, hepatopancreas, muscle, and ovary, by qRT-PCR. The results indicated that the expression of *FmSax* was mainly found in eyestalks and gills and less in other tissues (Figure 17 A). The *FmBMPRII* was also highly expressed in eyestalks and brain, and less in thoracic ganglia and gills, while the very low expression level was found in muscles, hepatopancreas, and ovary (Figure 17 B). Furthermore, the expression of *FmSax* and *FmBMPRII* in hepatopancreas during ovarian development stages were determined. The result revealed that *FmSax* expression was eventually increased along ovarian developmental stages and had the highest level in the mature stage, while *FmBMPRII* expression was significantly increased in the late vitellogenic stage before being dropped at the mature stage (Figure 18 A and B).

3.6 Sequence characteristics and phylogenetic analysis of bone morphogenetic protein receptors

The 1,707 and 3,021 bp of *FmSax* and *FmBMPRII* coding sequences were obtained and encoded for 569 and 1,007 amino acid residues, respectively. Alignment of *FmSax* with *FmBMPRII* amino acid sequences using NCBI blastp showed coverage of blast hits of 51 %, identity of 37.25 %, and e-value of 1e-54. Also, domain annotation of BMPRs with Pfam database showing protein kinases, catalytic domain (PKc_like superfamily), transforming growth factor-beta type I GS-motif (TGF_beta_GS), activin types I and II receptor domain (Activin_recp), and Ly-6 antigen / uPA receptor-like domain (LU superfamily) were found in *FmSax* sequence, while *FmBMPRII* found only PKc_like superfamily (Figure 19 B and C).

Phylogenetic analysis of BMPRs showed that the *FmSax* was clustered in the BMPR type I separated from the *FmBMPRII*, which was in the BMPR type II. The *FmSax* was close related to TcSax of *Tribolium castaneum* and it was clustered to sax and

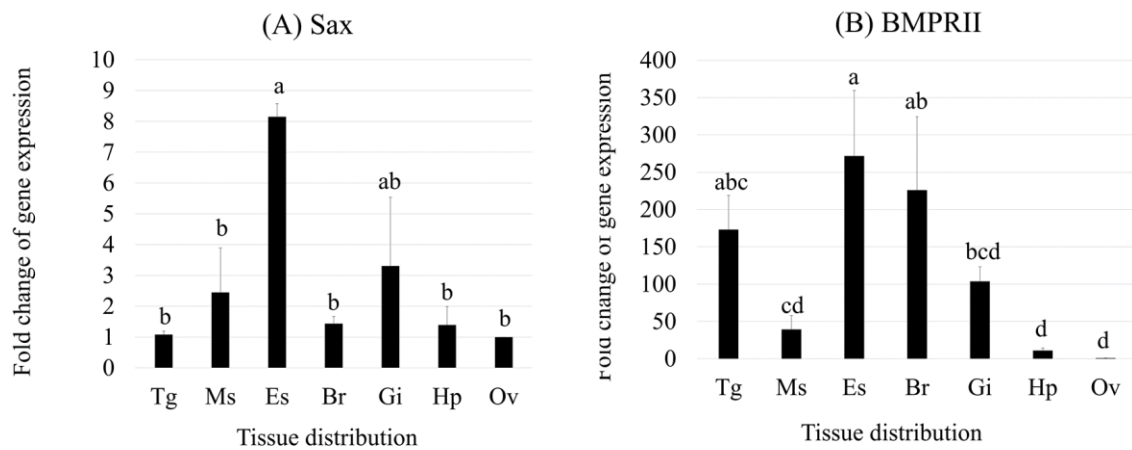


Figure 17 Determination of *FmSax* and *FmBMPRII* expressions in shrimp tissues. The relative expressions of *FmSax* (A) and *FmBMPRII* (B) were determined in shrimp tissues, including thoracic ganglia (Tg), muscle (Ms), eyestalk (Es), brain (Bn), gill (Gi), hepatopancreas (Hp), and ovary (Ov) by qRT-PCR. The tissues were isolated from 3 previtellogenic female shrimps. Bars and error bars represent means and SEM, respectively. Alphabets indicate significant differences between groups ($p < 0.05$) analyzed by one-way ANOVA followed by pair-wise comparison by Scheffe's test.

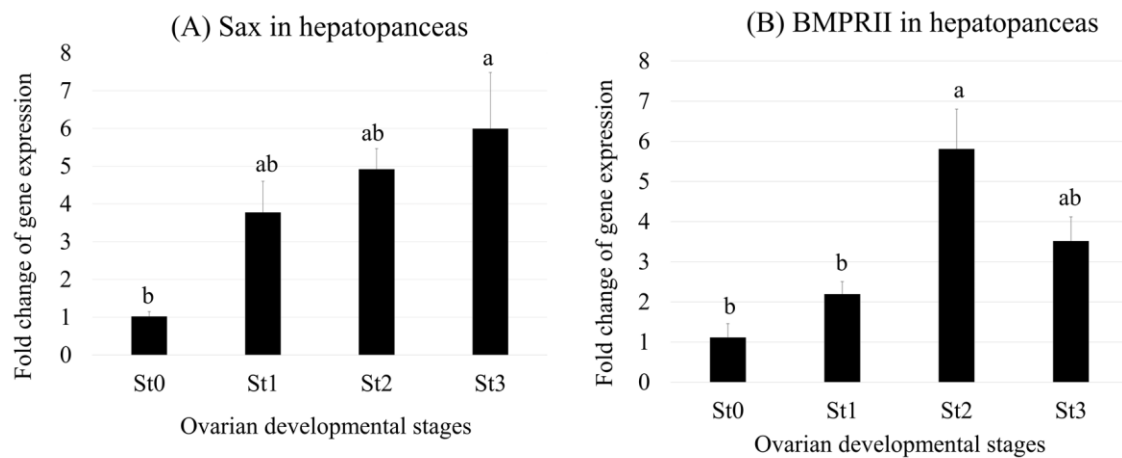


Figure 18 Determination of *FmSax* and *FmBMPRII* during ovarian developmental stages in hepatopancreas. Both *FmSax* (A) and *FmBMPRII* (B) expressions were determined in hepatopancreas isolated from female shrimp corresponding to different ovarian development stages (previtellogenic (st0), early vitellogenic (st1), late vitellogenic (st2), and mature stages (st3)) by qRT-PCR. The 5 individual shrimp were used in each stage. Bars and error bars represent means and SEM, respectively. Alphabets indicated significant differences between groups analyzed by one-way ANOVA ($p < 0.05$) followed by pairwise comparison by Scheffe's test.

(A)

dsFmSax-F

```

FmSax : CAG-----ACCTGACCAT-----CCCTCCCT-----TGGACACACACACATAAT-----TACATTGCCCT-----CT : 1105
FmBMPRII : CATTAGAAATCCATGACCAATTAATGCCATCCCTAAATGAGACATGCAACACAGCTGCTGTGGTACACAGCCAGGCCAAGCCACTTCCCG : 2070
    
```

dsFmSax-F

```

FmSax : GAGCCCTGATGCGATGCTCT---TCCTTTGCTACAGAAATTTTGGTACACAGGAAACCCAGCCATT-----GCCCTTGGT : 1179
FmBMPRII : GACCCATCTTACTGCGACGGGATCCACAGTACACAGATGAGTGGTTCCATTGACCAACCAGCCAAAAAGACAGAAATACGCTGTTCGA : 2160
    
```

```

FmSax : GA-----CATCAAAAGAAAGAAC---TTTGGTAAGG-----CTG---AACGG-----GACATGTC---GATTTGCCGATTTTG- : 1240
FmBMPRII : GAGGAAGAGRATCATATAAATACAGAGATGCTGGGAACGGAACTCATGGACACGGTGGCGTAGACATGGCAAGATGCCCTTAACTCT : 2250
    
```

```

FmSax : ---GCTCGCCGAGGAGCCCACTCA--------ACTACAGGGAAATCAA---GATAGCGAATAATC----- : 1294
FmBMPRII : CTCATTCCTCGCCGTCGACACAAATAGTGAAGATGAGGACACACAGAGATTTAATACACCACAGTGTGATGCTGTGAGAACCA : 2340
    
```

```

FmSax : CCAG---ACTACGACAAAGCCCTTCATG---AGCCTGCAAC---TTTCAATGATGTCAT---CAGAGGATCTGC----- : 1359
FmBMPRII : CCAACTCCAGTTCACAAAGCCAGTCCATAGCAGTCAATACAGCCACATGCCAATCCAGACAGAGCGGCTACTTACCAATGCTGGACCC : 2430
    
```

```

FmSax : -----TTCGATCTCTTC-----CCTAATGTCGATCTTGGCTTG---CTTGGTTCTGCGAATTTGC-----CGAAG : 1424
FmBMPRII : CATACTGTGATCTCTGCGATCTCACTTTAAACACGACACAGTTCATGATGGCGAATTAATTCAGACACAGAAATTTGCCATAGCAAA : 2520
    
```

dsFmSax-R (stem sequence)

```

FmSax : ATCCATATCCA---ATGAAAT---CATACACAGATCAAG---CTCTCTCTATGATGATCTCCCAATGCGCCAG---CTTTGAA : 1500
FmBMPRII : TTTCAATATCCAGATGGATTTGGCAGCTATATATAGATCAAGGCAAGGATCAATATGATAGTGGATTAATTAATCTAGTGAGAACGCTTT : 2610
    
```

```

FmSax : GGCATCCAGAGAGCTGCG---AGTGGCGATCAGTATCGACCTG---TCATCC-----CCAAATGGTGGCAACTGAT- : 1566
FmBMPRII : AGCTTTCAGATAGTGAATCTCTGTGAGAACTAAGAGACCAACAACACTGCTCTCCAGAGAGGCCAAATCAGAGCCCTTTTGAAT : 2700
    
```

dsFmSax-R (stem loop sequence)

```

FmSax : ---CCGGAATTAACAGG---AAGGTCAGAT-----CATCTCCTAATGTTG---GCCACGAA--- : 1616
FmBMPRII : AAAAGCCATATACATAAGCTAAATCAGACCCAGATCCAAGACACAAAAACACACAGCGAATCGAAAATGCTCCAGCCAGCAGATGATGAA : 2790
    
```

dsFmSax-R (stem loop sequence)

```

FmSax : -----CCCT-----ACCTGC-----CGACTAACAG---CCCTC-----AGAGTC : 1647
FmBMPRII : GAATCTCCACCCATACGGAAAGCAAAGCATACAGTGAAGACACCTCGACGACCAATGAACCCCGCTCTTCACTGTATGATGATCCGATC : 2880
    
```

(B)

```

FmSax : MYGSGSEKALVMSQGTKESSKVSDEKADVDGVLQVLLQNTGGKSESSGSGSGSSTSETRNWPVRLWNEVYDR-ISKIKLRPH : 89
FmBMPRII : ---MAGFVITLACWAAVITGAVGEAAASTHTQCAVHISTTATDSEKTSBVIIVDGRSVIRCLETTNGSYWRYEVDNVIKWKIAGG : 87
    
```

```

FmSax : CNOIECHNALMCKAKTFREHGEENSRGCIKVPQVEMOCASKETHKNFEMDCCRTNYCNNGSFFVLPPTVTHCEDSEIMSVLVHH : 179
FmBMPRII : CWGASKIQNQSSGVANSNR-----NHSYFCCTGDMQNEDEVSVFVVEEKPTSLVKVDPEPQTELSPFMLIKILVCGG----- : 160
    
```

```

FmSax : VVPVLLVVIHAILVLIQLQHAEKRRMEAYASAAAAASALPLPHMYRDELATAGDSTLREIFNDSITSGSGSLPLLIQRTIAKQIWL : 269
FmBMPRII : -----FEWVAVLGVSATLGWKR-SRPSNFPVPIEETPSPCHDLSIRILES----- : 207
    
```

```

FmSax : EVICKGRYGVVMDGHWQGSVAVKIFSRDEASARETHLYSTVLLRHHNILEVYGS-LMISRCACTQLWVTHHEFCSTHLYLNHLY : 358
FmBMPRII : --LCKGRYCTAFRAIVQGEVAVRMEFQHHKSSMNERVLYSLHLEESNDLRYLGSERVEQDGSYYQLVLSYQEMCRSLTYLSENY : 295
    
```

```

FmSax : DHTSLINIALSANGILHLHTETL-CTQSKHATAHRDIKTKNLLVRLNGTGVHAEGLAVMHTQTTEIN-----IGNNERVGRKRYM : 440
FmBMPRII : SWPQCHIVLSATRGLHLSLIRKGLIVKGLISHRDENTRNLLKDNMTCCVSLGLGAAHTQGAKYFINGEEQHAETSSLSDVGLDRYM : 385
    
```

```

FmSax : SPEVLNESTINMTVPS-FRRVDIYALGLVLWVCRRC--LSNGLID-EYKHPFYDVPNEPSEDMKKVVCVDQYREVHPNRWTS-DEVL : 525
FmBMPRII : APEVLGAVNLRDCAALNGLIDIYALGLVLWVCAARCHLYCGLQTPSYMIPQEEIQLFPTFERVQVLRARRRARELHPVWKRDNFAI : 475
    
```

```

FmSax : TQSKITRECHWQNPVRLTAFVKKSLVKVAQEEKIKLEFDC----- : 569
FmBMPRII : RLKKEITRECDWDEAEARLSAMVGEGLGEHPVLWRYVSSLVGVNGVSPPTINFMNSLVYQRQEMFSGLAGNGKVISNALTPREKESV : 565
    
```

(C)

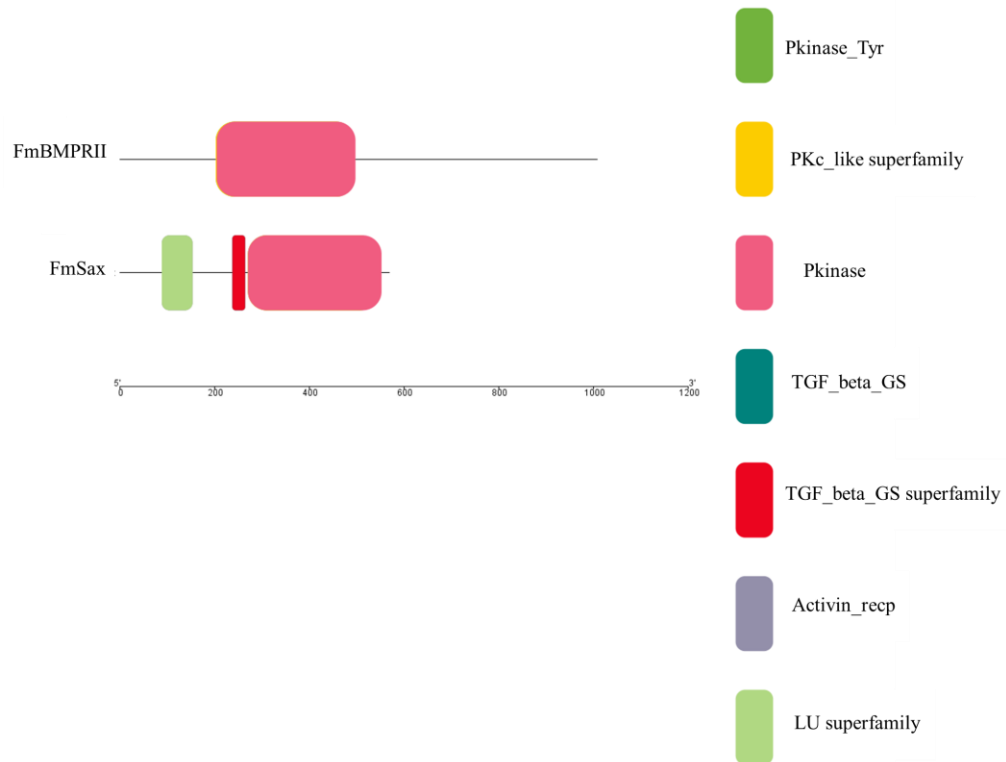


Figure 19 Alignment and feature of FmSax and FmBMPRII sequences. Alignment of FmSax and FmBMPRII nucleotide sequences showed primer regions for dsRNA specific to FmSax (dsSax) but not to FmBMPRII sequence (A). Amino acid sequences of FmSax and FmBMPRII were aligned using ClustalW showed similar regions (B). Domain proteins were found in FmSax and FmBMPRII (C).

BMPRI from the other organisms whilst the FmBMPRII was similar to BMPRII from other organisms (Figure 20).

3.7 Production of the saxophone specific double-stranded RNA

In this study, the inverted repeat sequence of *FmSax* was cloned in the pET28a plasmid and subsequently transformed in *E. coli* HT115 (DE3). The dsRNA specific to *FmSax* (dsSax) and *FmGFP* (dsGFP) were successfully produced in the bacterial system. Both dsSax and dsGFP were verified for dsRNA characteristic by RNase digestion assay. The results showed that both dsSax and dsGFP were completely digested with RNase III, but not with RNase A (Figure 21).

3.8 Effect of *FmSax* silencing on vitellogenesis in female *F. merguensis*

Previtellogenic female shrimps were injected with dsSax or dsGFP. On days 7 after the injection, their ovaries and hepatopancreas were isolated and determined for the expression of *FmSax*, vitellogenin (*Vg*), and *FmBMPRII* by qRT-PCR. In the ovary, the results showed that the expression level of *FmSax* was significantly decreased about 2-fold in dsSax-injected shrimp compared with that in dsGFP-injected shrimp, while the approximately 4-fold decrease of *Vg* expression was found in dsSax-injected shrimp. Also, the *FmBMPRII* expression seemed to decrease in *FmSax* knockdown shrimp (Figure 22 A). Similarly, *FmSax*, *Vg*, and *FmBMPRII* expression levels were significantly dropped in hepatopancreas of the shrimp injected with dsSax compared with that injected with dsGFP (Figure 22 B). In addition, the oocyte proliferation was determined in the ovaries by EdU assay. The result revealed that the EdU index was significantly increased in the ovarian explants isolated from dsSax-injected shrimp compared with that from dsGFP-injected shrimp (Figure 23).

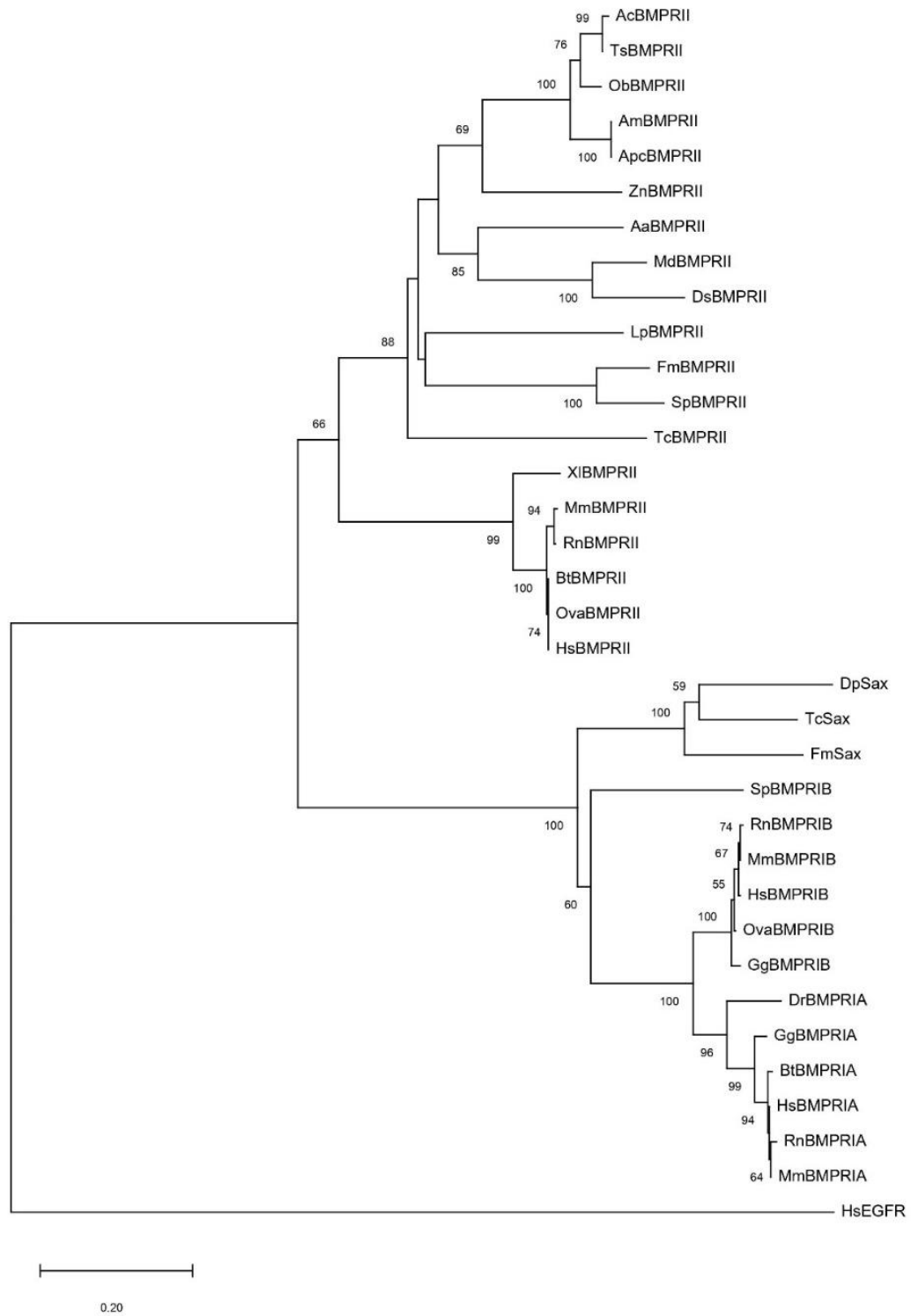


Figure 20 Phylogenetic tree analysis of FmSax and FmBMPRII. The tree of FmSax and FmBMPRII amino acid sequences and other BMPRI and BMPRIA from organisms

including crustaceans, insects, and vertebrates, was constructed using the Neighbor-Joining method within MEGA X. The optimal tree with the sum of branch length = 5.65173274 was shown. Numbers indicated the percentages of the bootstrap test (1000 replicates). The evolutionary distances were computed using the Poisson correction method and were in the units of the number of amino acid substitutions per site. This analysis involved 35 amino acid sequences. All positions containing gaps and missing data were eliminated (complete deletion option). There was a total of 274 positions in the final dataset. The BMPRII sequences obtained from GenBank as follows: *Atta colombica* (KYM88349.1), *Trachymyrmex septentrionalis* (KYN33300.1), *Ooceraea biroi* (EZA50862.1), *Apis mellifera* (XP_016773438.1), *A. cerana* (XP_016922687.1), *Zootermopsis nevadensis* (XP_021920323.1), *Aedes aegypti* (XP_021698357.1), *Musca domestica* (XP_011290781.1), *Drosophila serrata* (XP_020801528.1), *Limulus polyphemus* (XP_013784087.1), *Scylla paramamosain* (KU985444), *Tribolium castaneum* (XP_974821.1), *Xenopus laevis* (NP_001081659.1), *Mus musculus* (NP_031587.1), *Rattus norvegicus* (NP_536332.1), *Bos taurus* (NP_001291214.1), *Ovis aries* (NP_001293052.1), and *Homo sapiens* (NP_001195.2). The saxophone sequences were as follows: *Daphnia pulex* (EFX65169.1), and *T. castaneum* (EFA07576.2). The BMPRIIB sequences were as follows: *S. paramamosain* (KU985443), *R. norvegicus* (NP_001019430.1), *M. musculus* (NP_001341972.1), *H. sapiens* (NP_001243723.1), *O. aries* (NP_001009431.1), and *Gallus gallus* (NP_990463.1). The BMPRIA sequences were as follows: *Danio rerio* (NP_571696.2), *G. gallus* (NP_990688.1), *B. taurus* (NP_001070268.1), *H. sapiens* (NP_004320.2), *R. norvegicus* (NP_110476.1), and *M. musculus* (NP_033888.2). The outgroup was the EGFR of *Homo sapiens* (P00533).

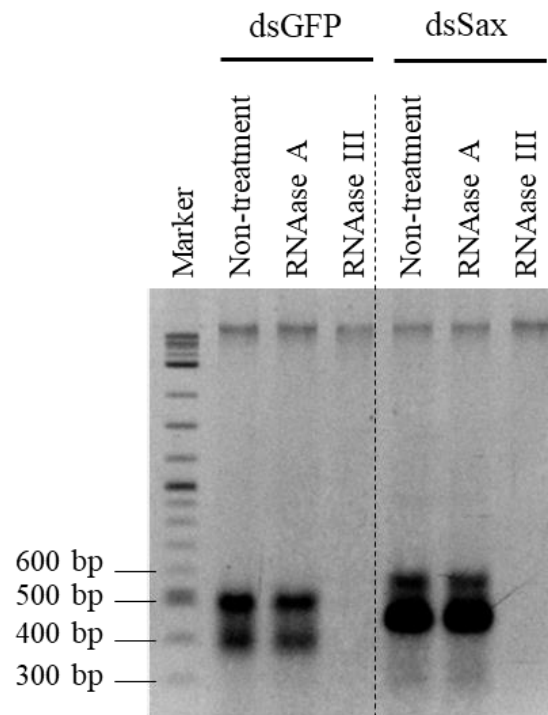


Figure 21 The production and RNase digestion of dsSax and dsGFP. Both dsSax and dsGFP produced from *E. coli* were digested with RNase A or RNase III. The result of the digestion was analyzed by agarose gel electrophoresis. The left lane was a DNA ladder.

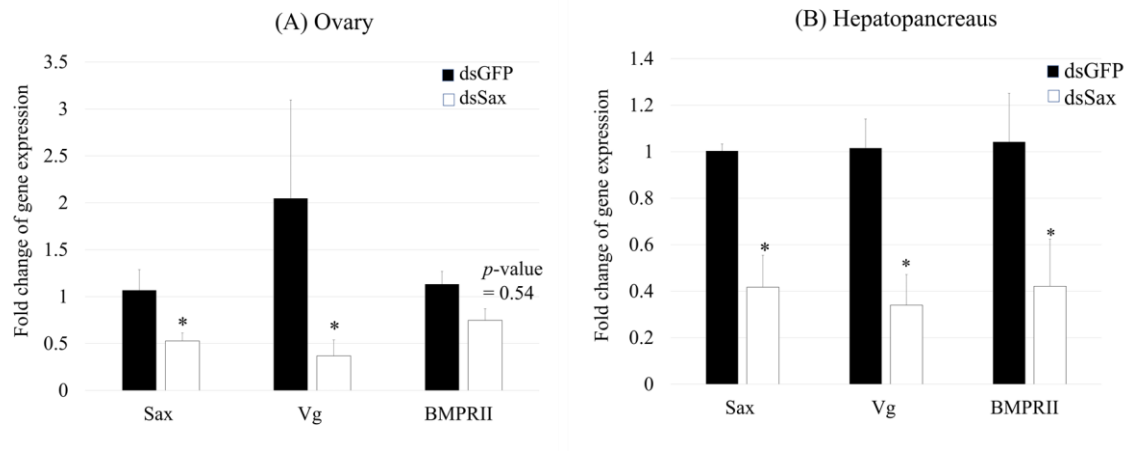


Figure 22 Effect of *FmSax* knockdown on *Vg* and *FmBMPRII* mRNA expression. The previtellogenic female shrimps (n=5) were injected with dsSax or dsGFP for 7 days. The ovary (A) and hepatopancreas (B) were determined for *FmSax*, *Vg*, and *FmBMPRII* expressions by qRT-PCR. The 2 independent experiments were performed. Bars and error bars represent means and SEM, respectively. Asterisks indicates significant differences between groups ($p < 0.05$) analyzed by one-way ANOVA using random complete block design followed by pair-wise comparison by Scheffe's method.

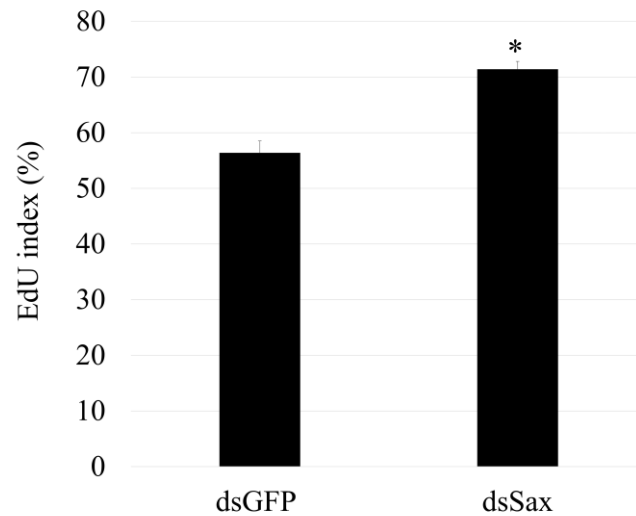


Figure 23 Effect of *FmSax* knockdown on oocyte proliferation. On days 7 after the injection, the ovarian pieces were isolated and cultured in the culture medium, subsequently incubated with EdU overnight. After staining with Alexa 488 azide and DAPI, the oocyte cells (n=100-150) were counted and calculated for the EdU index. Bars and error bars represent means and SEM, respectively. An asterisk indicates significant differences between groups ($p < 0.05$) analyzed by t-test.

CHAPTER 4

DISCUSSION

In the present study, RNA sequencing (RNA-seq) platform and bioinformatics analysis were used to generate the transcriptome of banana shrimp, *Fenneropenaeus merguensis*, from ovarian samples at each ovarian developmental stage. Over 40 million raw sequences at stages of ovarian development were *de novo* assembled for its transcriptome resulted in 58,343 unigenes, and the raw data was available at the NCBI Sequence Read Archive (SRA). The total unigenes were then annotated function to NR, NT, Swiss-Prot, COG/KOG, KEGG, PFAM, and GO databases, and analyzed for the level of differentially expressed gene (DEG). To obtain the candidate of receptor genes, the total of 663 receptor genes derived from the filter of all unigenes with many receptor keywords, was screened by KEGG's pathway associated with reproductive processes, and had a DEG's level of each ovarian developmental stage with the difference of 2-fold at least, resulting in the total candidate of 15 receptor genes in this study (Table 3). Similarly, some studies have been reported the transcriptome analysis of *F. merguensis*. For example, Saetan *et al.* (2016) reported the transcriptome of ovary's *F. merguensis* at the vitellogenic and the non-vitellogenic stages providing a total of 41,877 unigenes and identification of candidate genes involved in ovarian maturation via KEGG's pathway and DEG's analysis for validation of their gene expression between qRT-PCR and predicted DEG (Saetan *et al.*, 2016). Wang *et al.* (2017) reported the transcriptomic changes of gill's *F. merguensis* in response to ammonia stress providing a total of 106,996 unigenes and identification of candidate genes related to cytoskeleton remodeling and immune response using the DEG's analysis for validation of gene expression as well (Wang *et al.*, 2017). Jiang *et al.* (2019) reported the transcriptome of *Macrobrachium rosenbergii* eyestalk between ovary undeveloped juvenile and ovary maturing adults providing a total of 53,878 unigenes and identification of candidate genes involved in ovarian maturation with DEG analysis. Qian

et al. (2020) reported the transcriptome of adult *Apriona germari* antennae providing a total of 36,834 unigenes and identification of olfactory receptor genes providing a total of 42 genes, using transmembrane prediction of receptor genes by TMHMM Server v. 2.02 online software. Wang *et al.* (2018) reported the transcriptome of different tissues from females and male's Asian citrus psyllid, *Diaphorina citri* providing a total of 297,614 unigenes and identification of G protein-coupled receptors for neuropeptides using DAS-TMfilter server (<http://mendel.imp.ac.at/sat/DAS/>) for transmembrane domains of receptors, Pfam (<http://pfam.xfam.org>), and conserved domains (<https://www.ncbi.nlm.nih.gov/Structure/cdd/wrpsb.cgi?>), resulting in a total of 42 genes. These identification approaches were not similar to our study because the prediction of transmembrane servers was used for GPCR characterization, but the other receptors were not, and the identification approaches of the other receptors were little known. For the selection of candidates, the criteria of these studies were similar to our study using DEG analysis and KEGG pathway.

In this study, the 15 candidate receptor genes, including GPCRs, ICs, and RTKs, were chosen to determine for their expression profiles during ovarian development. The 3 candidate GPCRs, including Smo receptor, GRL101, and PRR, were differentially expressed among ovarian development (Figure 16).

1. The Smo receptor

The expression of FmSmo had an increased expression at the early- and late vitellogenic stages of ovarian development (Figure 16 K). A little known of the Smo receptor was studied. It has been studied that its expression was mostly found in the ovary of mouse (Nguyen *et al.*, 2009) and *Locusta migratoria* (Zheng *et al.*, 2020). It is involved in the activation of transcriptional factors in the critical mechanisms for embryonic development and tissue homeostasis via the hedgehog signaling pathway (Isberg *et al.*, 2015; Stone *et al.*, 1996; Alcedo *et al.*, 1996; van den Heuvel and Ingham, 1996). Suggesting the possible roles in the growth and development. However, its role in the ovarian development of crustaceans has not been investigated so far.

2. The GRL101

The expression of FmGRL101 mainly increased at the vitellogenic stage (Figure 16 O) suggesting the involvement in vitellogenesis. Similarly, the GRL101 had been reported about its reproductive roles such as the controls of neuronal communication and maturation of the accessory sex glands in *Lymnaea stagnalis* (Cox *et al.*, 1993) and physiological processes such as pregnancy and lactation in rat (Nilaweera *et al.*, 2008). The GRL101 in *Acanthaster planci* had female-biased expression within the sensory tentacles, indicating possible reproductive significance (Roberts *et al.*, 2018). Even though its structure contains several low-density lipoprotein (LDL) receptor repeats and leucine-rich repeats (LRR), its specific ligands are still unclear (Cox *et al.*, 1993).

3. The (pro)renin receptor (PRR)

The PRR expression was significantly high at the early-, late vitellogenic stages, and less at the mature stage (Figure 16 E), suggesting its role in vitellogenesis. The PRR is involved in embryonic development and cell survival by acting as an adaptor between the Wnt receptor complex and the vacuolar H⁺-ATPase (V-ATPase) (Cruciat *et al.*, 2010). The mutation of *ATP6ap1/Ac45* and *ATP6ap2/PRR* resulted in central nervous system (CNS) necrosis and embryonic lethality in zebrafish (Amsterdam *et al.*, 2004; Nuckels *et al.*, 2009). Also, the knockout of *ATP6ap2/PRR* led to death after birth within 3 weeks caused by the severe heart failure in cardiomyocytes of mice (Kinouchi *et al.*, 2010). Silencing of *vha-11* gene in V-ATPase affected impairment of ovulation and embryogenesis in *Caenorhabditis elegans* (Oka and Futai, 2000). These suggest that FmPRR controls vitellogenesis via Wnt and V-ATPase pathways.

Then, the 4 IC, including glycine receptor alpha and beta, glutamate receptor, and NMDA were differentially expressed among ovarian development (Figure 16).

4. Glycine receptors

the glycine receptors are ligand-gated chloride channels consisting of α and β subunits. The function of the glycine receptors with their ligands plays an important role in mediating inhibitory neurotransmission distributed in the CNS, especially in the spinal

cord and brain stem (Betz, 1991; Moss & Smart 2001; Lynch, 2004). In this study, the expression of the glycine- α receptor was rose at the early vitellogenic stage and fell gradually in the next stages during ovarian development (Figure 16 D), while the expression of the glycine- β receptor was rapidly great at the late vitellogenic stage and suddenly low at the mature stage (Figure 16 J). This may because the function of the glycine receptor α subunit has binding sites for native glycine receptor whilst the glycine receptor β subunit promoters and stabilizers of glycine receptor assembly (Sato, Tucker, and Meizel, 2002) and may not specifically colocalize with the α subunit indicating independent roles of each glycine receptor subunit (Waxham, 2014). Moreover, Nishizono et al., (2020) reported that the defect of glycine receptor alpha-4 subunit (*Glr4*) affected the inhibition of embryonic development to the blastocyst stage in mouse fertilized eggs by a decrease of the number of cells in the blastocysts. Suggesting the regulatory role of the glycine receptors in the development of preimplantation (Nishizono *et al.*, 2020). Mutant of glycine receptor alpha and beta subunits caused defect of their ability to undergo the sperm acrosome reaction initiated in vitro, which is essential for fertilization by glycine and by solubilized egg zona pellucida from mouse eggs (Sato *et al.*, 2000). However, the reproductive function of glycine receptor subunits has been unclear so far, and our result could be the first report of glycine receptors involved in ovarian maturation in crustaceans.

5. Glutamate receptor

The glutamate receptor and its ligand mediate most excitatory neurotransmission in the CNS as similar as the glycine receptors. Here, the glutamate receptor had dramatic expression at the early vitellogenic stage and a dropped expression in other stages during ovarian development (Figure 16 B), suggesting a specific role in vitellogenesis. The glutamate receptor plays roles in the control of reproduction, hormone secretion, and neuroendocrine regulation. For example, the mutants of glutamate receptor AMPA-1 (GRIA1) led to the decrease of immature ovarian follicles before undergoing the ovulation and slowing down the releasing of luteinizing hormone (LH) among *Bos taurus* (Sugimoto *et al.*, 2010). The glutamate receptor subunits and Fos in gonadotrophin-

releasing hormone (GnRH) neurons were expressed involved in the delay and fade of the LH surge in estrous of rats (Bailey, Centers, and Jennes, 2006).

6. N-methyl-D aspartate (NMDA) receptor

The NMDA receptor is another subtype of glutamate receptors that widely distributes in the CNS (McBain and Mayer, 1994; Huang *et al.*, 2015). In this study, the NMDA receptor was highly expressed at the previtellogenic stage and had low expression at the later stages (Figure 16 A). The NMDA receptor has been reported to be associated with physiological and biological processes such as mediating juvenile hormone (JH) biosynthesis (Chiang *et al.*, 2002; Geister *et al.*, 2008; Huang *et al.*, 2011). Urbanski and Ojeda (1990) revealed that the interruption of NMDA receptors using specific antagonists can prevent the development of induced LH secretion in female rats during sexual maturation. The blockade of NMDA receptor using antagonist MK-801 inhibits vitellogenesis in the flesh fly *Neobellieria bullata* and in the desert locust *Schistocerca gregaria* (Begum *et al.*, 2004). These suggest that the NMDA receptor is involved in the early ovarian developmental process such as oocyte growth and follicular development in crustaceans.

Furthermore, the expression profile of 8 candidate RTKs including EGFR, ROR, RYK, notch receptor, insulin receptor, TGF β receptor, and 2 BMP receptors, were determined during ovarian maturation.

7. Epidermal growth factor receptor (EGFR)

EGFR has been known to play several physiological processes in organisms such as cell proliferation, migration, differentiation (Burrows *et al.*, 1997). It controls growth in arthropods such as *Drosophila melanogaster* (Shilo, 2003), *Apis mellifera* (Kamakura, 2011), and *Gryllus bimaculatus* (Dabour *et al.*, 2011). Several studies have been reported that the functions of EGFR are involved in reproductive processes including sexual maturation, ovulation, fertilization, and embryo implantation via epidermal growth factor signal transduction pathway (Schneider and Wolf, 2008). In this study, the expression of FmEGFR was greatly expressed at the early- and late vitellogenic stages of ovarian development (Figure 16 G). Similarly, the EGFR expression was most in the ovary

and significantly increased at the early- and late vitellogenic stages during ovarian development in *Scylla paramamosain* (Lu *et al.*, 2020). EGFR was predominantly expressed in gonad (ovary and testis) of zebrafish and the expression of EGFR was increased at the previtellogenic stage, then maintained at the early vitellogenic and midvitellogenic stages, and further increased to a higher level at the full-grown follicles (Tse and Ge, 2010). Suggesting it involved in the promotion of ovarian development in shrimp.

8. Receptor tyrosine kinase-like orphan receptor (ROR)

ROR is one of the orphan RTKs that has little knowledge about its ligands and also reproductive function. In this study, FmROR expression was decreased at the early vitellogenic stage but increased in the mature stage of ovarian development (Figure 16 M). This may suggest that ROR is involved in the negative regulation of vitellogenesis but required in ovarian maturation in the later phase. ROR controls several physiological roles via Wnt signaling pathway by acting as a Wnt5a receptor, which is involved in the developmental processes and had a high expression in the nervous system of the early embryogenesis in *Drosophila* (Wilson, Goberdhan, and Steller, 1993), *Caenorhabditis elegans* (Forrester *et al.*, 1999), and human (Al-Shawi *et al.*, 2001). Also, mutant of ROR1 or/and ROR2 caused abnormal phenotypes in *C. elegans*, nematodes, and mice and caused genetic skeletal disorders in human (Yoda, Oishi, and Minami, 2003).

9. Receptor-like tyrosine kinase (RYK)

The RYK is also one of a class of orphan RTKs. Like ROR, it also acts as a Wnt receptor to activate a Wnt signaling pathway. Both RYK and ROR can be a coreceptor along with Frizzled receptors linked to many Wnt signaling pathways (Wang *et al.*, 2004; Povinelli and Nemeth, 2014). In this study, FmRYK was highly expressed at the early- and late vitellogenic stages of ovarian development (Figure 16 F), suggesting the possible role in ovarian development. Its function has been studied in many organisms. For example, the silencing of RYK expression resulted in a defect of axon guidance in mice (Lu *et al.*, 2004). Knockout of RYK in mice led to the lethal effect after birth and displayed an abnormal secondary palate and craniofacial appearance (Halford *et al.*, 2000). The RYK

was mainly expressed in the embryonic CNS and regulated cell migration during cortical development in rat (Kamitori *et al.*, 2005). Besides, a homolog of *C. elegans*'s RYK, *lin-18*, is required for vulva development (Inoue *et al.*, 2004). A homolog of *Drosophila*'s RYK, *derailed*, is crucial for axon guidance and neurite outgrowth (Lu *et al.*, 2004; Keeble and Cooper 2006; Green, Nusse, and van Amerongen, 2014). These indicate crucial roles of RYK in the control of development in several organisms, and it may be involved in the regulation of ovarian development.

10. Notch receptor

The notch receptor and its ligands through notch signal pathway are essential for embryogenesis and postembryonic development, including proliferation, cell fate, differentiation, and apoptosis in several organisms (Artavanis-Tsakonas, Rand, Lake, 1999; Rangarajan *et al.*, 2001; Demehri *et al.*, 2008; Ramain *et al.*, 2001). In this study, we found that its expression was significantly increased at the late vitellogenic stage of ovarian development (Figure 16 I), suggesting the vitellogenesis regulatory role in shrimp. Similarly, expression of notch receptor was increased in mouse mammary gland including puberty and pregnancy leading to lactation and subsequently involution (Raafat *et al.*, 2011). Also, notch receptors and their ligands were expressed in the ovary during embryonic ovarian development (Vanorny and Mayo, 2017). The notch signaling pathway via its receptor serves several physiological processes. For example, the notch signal activation induces the early T cell development in mice (Radtke *et al.*, 1999; Bellavia *et al.*, 2000) and human (Van de Walle *et al.*, 2009, 2011, 2013). It also rescues the cells from apoptosis (Deftos *et al.*, 1998; Jehn *et al.*, 1999). Moreover, it maintains hematopoiesis in the early hematopoietic development in mice (Walker *et al.*, 2001). The mutant of notch receptor results in the tumorigenic mechanisms (Stransky *et al.*, 2011; Agrawal *et al.*, 2011). Therefore, the notch receptor is one of the potential receptors that is involved in the stimulation of ovarian development in shrimp.

11. Insulin receptor

The insulin receptor is a member of the ligand-activated receptor and tyrosine kinase family, the interaction of the insulin receptor with its insulin ligand via the

insulin signaling pathway regulates organismal glucose homeostasis, also play critical regulatory roles in development, cell division, and metabolism (Fantl, Johnson, and Williams, 1993; Schlessinger and Ullrich, 1992; Ullrich and Schlessinger, 1990; Lee and Pilch, 1994). In this study, the insulin receptor expression was increased at the early vitellogenic stage and then dropped at the late vitellogenic and mature stages of ovarian development (Figure 16 C), suggesting the role in vitellogenesis. Many reports indicated the vital roles of the insulin receptor and its signaling pathway in several organisms. For example, insulin signaling acts as an endocrine factor for primary follicle transition in oogenesis (Kezele, Nilsson, and Skinner *et al.*, 2002). Mutant of *Drosophila* insulin receptor increased lifespan and impairing neuroendocrine function (Tatar *et al.*, 2001). Insulin signaling was involved in the regulation of neuronal growth and differentiation (Heidenreich, 1993; Robinson *et al.*, 1994). A knockout of the insulin receptor in mice affected the regulation of embryonic β -cell growth (Kitamura *et al.*, 2001). A neuron-specific disruption of the insulin receptor gene (NIRKO) in mice resulted in impairment of spermatogenesis and ovarian follicle maturation (Brüning *et al.*, 2000). A mutant insulin receptor in *Drosophila* was involved in the regulation of growth and body size during development (Chen, Jack, and Garofalo, 1996) and caused severe growth retardation (Brogiolo *et al.*, 2001).

Last 3 candidate RTKs are belonged to the transforming growth factor- β 1 (TGF- β 1) receptor family, including TGF- β 1 receptor, bone morphogenetic protein type 1 receptor (BMPRI or saxophone (sax)), and BMPRII. The members of the TGF- β receptor family are involved in the transmission of the TGF- β signaling pathway and subsequently perform several roles in biological and physiological processes, including cell proliferation, differentiation, apoptosis, and reproduction (Knight and Glister, 2006; Wanger *et al.*, 2010).

12. TGF- β 1 receptor

The TGF- β 1 receptor or ALK5 is a serine/threonine kinase receptor that belongs to the TGF- β receptor family, the interaction of the TGF- β 1 receptor and its TGF- β ligands via in TGF- β signaling pathway involved in many cellular processes in both the

adult organism and the developing embryo including cell growth, cell differentiation, cell proliferation, apoptosis, cellular homeostasis (Attisano *et al.*, 1994). In this study, the expression of FmTGF- β receptor was gradually increased over ovarian development (Figure 16 N). Likewise, TGF- β 1 receptor expression is highly expressed in the early follicular development in collared peccary (*Pecari tajacu*) (Viana *et al.*, 2020). In addition, the high expression of the TGF- β 1 receptor was found in the early embryonic and larval development, and at the postmolt stage during the molt cycle of *S. paramamosain* (Zhou *et al.*, 2018). It is required for female reproductive tract integrity and function. The knockout of TGFBR1 led to the defect of structure and function in the oviduct and uterus in mice (Li *et al.*, 2011). These suggest the TGF- β 1 receptor has participated in reproduction such as development and growth.

While the other TGF- β receptor family, the BMPRs, were also investigated for their expressions in this study. There are two types of BMPR: BMPR type I and type II. They usually work together by forming heterodimerization and binding with their specific ligands such as BMPs, which belonging to the TGF- β superfamily.

13. BMPR type I and II

The BMPR type I and II are a highly similar structure including ligand-binding domain, serine/threonine kinase domain but only BMPR type I receptor has GS domain. The interaction of BMPRs and BMP ligands is involved in many processes including osteogenesis, cell growth, and cell differentiation, oocyte development (Sanchez-Duffhues *et al.*, 2020). In this study, the expression level of *FmSax* was high in the vitellogenic stage of ovarian development (Figure 16 L), while the expression of *FmBMPRII* was gradually increased to the late previtellogenic stage (Figure 16 H). This was similar to the expression of BMPRI in *S. Paramamosain*, which high expression was found at the late vitellogenic stage whilst the BMPRII was increased expression at the early vitellogenic stage (Shu *et al.*, 2016). Furthermore, the BMPRI expression was rose during the follicle development in pig (Quinn *et al.*, 2004), cattle (Chen *et al.*, 2009), hamster (Wang and Roy, 2009), and zebrafish (Li and Ge, 2011). Also, the BMPRII expression

was increased during the follicle growth in zebrafish's ovaries (Li and Ge, 2011). These suggested that BMPRs were involved in ovarian maturation.

In our previous study, Sathpondecha and Chotigeat (2019) revealed that the glass bottom boat, a BMP ortholog, is highly expressed in the developing stages of ovarian development and plays role in the regulation of vitellogenesis in *F. merguensis* (Sathpondecha and Chotigeat, 2019). This relates to the expression profiles of both *FmSax* and *FmBMPRII* that highly expressed in the developing stage of ovarian maturation (Figure 16 H and L). Thereby, the BMPRs were chosen to further study for their characteristics and reproductive function in the banana shrimp. The 1,707 and 3,021 bp of full-length cDNA of both receptors contain the signal peptide, ligand-binding domain, kinase domain, and only *Fmsax* contains GS domain (Figure 19 C) corresponding to the BMP type II receptor lacks the GS domain but found in BMP type I receptor (Schmierer and Hill, 2007). The alignment of *FmSax* and *FmBMPRII* found coverage of blast hits of 51 %, and identity of 37.25 % that was little similar to each other because of its protein kinases domain. The *dsSax* primers used in this study were specific to *FmSax* sequence both stem and stem loop but not to *FmBMPRII* sequence (Figure 19 A).

The *FmSax* and *FmBMPRII* were determined their relative expressions in various tissues, including eyestalks, brain, thoracic ganglia, gill, hepatopancreas, muscle, and ovary using qRT-PCR. As the results, both BMPRs expression distributed in many tissues, and significantly abundant in the eyestalks more than other tissues (Figure 17 A and B). However, the expression of *Sp-BMPRI* and *Sp-BMPRII* are mainly found in the ovary and very low level in the eyestalks of *S. paramamosain* (Shu *et al.*, 2016). Also, BMPR and BMP ligands expressions were high level in the ovary of mammals such as goat (Lima *et al.*, 2012), hamster (Lima *et al.*, 2012), and swine (Zhao *et al.*, 2014). Crustaceans' eyestalks are a source of several peptide hormones and other proteins that play a key role in various physiological activities including ovarian maturation such as gonad inhibiting hormone (Brady *et al.*, 2012; Jung *et al.*, 2013). High expression of *FmBMPRs* in eyestalks may suggest the functions of the BMPRs via regulation of the TGF- β signaling pathway in the secretory sites of the peptide hormones.

Both ovary and hepatopancreas are the sources of vitellogenin (*Vg*) synthesis shrimp (Puengyam, Tsukimura, and Utarabhand, 2013), the *FmSax*, and *FmBMPRII* were also determined for their relative expressions in the hepatopancreas during ovarian developmental stages. The results showed that the expression of *FmSax* was eventually increased during ovarian development and reached the highest level at the mature stage, whereas the expression of *FmBMPRII* was gradually raised at the late vitellogenic stage (Figure 18 A and B). These were similar to the expression of both *FmSax* and *FmBMPRII* in the ovary during ovarian development (Figure 16 L and H) suggesting that both *FmSax* and *FmBMPRII* were associated with vitellogenesis regulation in ovarian maturation.

The role of *FmSax* was investigated using the RNAi technique. The dsRNA specific to the *FmSax* and GFP sequences were successfully produced in *E. coli* HT115 and examined for their dsRNA characteristic by RNase digestion assay. The result revealed that *FmSax* expression was suppressed in both ovaries and hepatopancreas of shrimp injected with dsSax (Figure 21). The *FmSax* silencing affected the decrease of *Vg* expression but not changed the expression of *FmBMPRII* in the ovaries (Figure 21 A) and increased the oocyte proliferation (Figure 22). Similar results were found in hepatopancreas but the silence of *FmSax* led to a decrease in both *Vg* and *FmBMPRII* expressions (Figure 21 B). Based on data the ovaries at the previtellogenic stage contained mostly oogonia and previtellogenic oocytes and small yolk. Even though the *FmSax* knockdown were no large changes *Vg* expression, but it during previtellogenic stage was probably involved in the accumulation and preparation of substances such as yolk, mRNA, and proteins which necessary for early ovarian development or involved in activities in cell cycle (Jiang *et al.*, 2018; Kang, Sultana, and Wilder, 2021). However, these findings suggested that *FmSax* is involved in the regulation of vitellogenesis. Likewise, the knockdown of *Sp-BMPRII* in the ovary of *S. paramamosain* (Shu *et al.*, 2016). The BMPRII have been studied in several organisms. For example, the mutant of BMPRII caused the abnormal granulosa cell differentiation and maturation of ovulatory follicles in *Booroola*

Merino ewes (Mulsant *et al.*, 2001). Also, the silencing of BMPRII by siRNA inhibited porcine granulosa cell proliferation (Zhao *et al.*, 2014).

CHAPTER 5

CONCLUSION

This study investigated the transcriptome of the candidate receptors at different ovarian developmental stages in female banana shrimp, *Fenneropenaeus merguensis*, using RNA sequencing and bioinformatics analysis. The present study, we can conclude that:

1. The transcriptome results provided a total of 53,763 transcripts with an average length of 1,060 bp, a 43 % GC content, and an N50 length of 2,380 bp.
2. The 663 genes identified as receptor genes were consisted of 160 GPCRs, 263 RTKs, 65 NRs, and 175 ICs.
3. The 15 candidate receptor genes which were differentially expressed during ovarian development stages by in silico analysis were validated for their expressions using qRT-PCR.
4. The BMP receptors, saxophone or BMPRI (*FmSax*) and BMPRII (*FmBMPRII*) were mainly expressed in eyestalks and less in other tissues. In ovary and hepatopancreas, *FmSax* expression was significantly increased at the mature stage, while expression of *FmBMPRII* was high at the late vitellogenic stage.
5. The dsRNA specific to *FmSax* (dsSax) was successfully produced in *E. coli*.
6. After injection in 7 days, the silencing of *FmSax* significantly suppressed *FmVg* and *FmBMPRII* expression in ovary and hepatopancreas of female *F. merguensis*. Also, oocyte proliferation was induced in dsSax-injected shrimp.

REFERENCES

- ACNPCS, V., Freitas, J. L. S., Magalhães, L. C., Campos, L. B., Silva, A. R., Oliveira, M. F., Freitas, V. J. F., and Melo, L. M. 2020. Ovarian gene expression in collared peccary (*Pecari tajacu* Linnaeus, 1758) subjected to gonadotropin stimulation protocols. *Reproduction in Domestic Animals*, 56: 351–359.
- Adiyodi, R.G., and Subramoniam, T. 1983. Arthropoda-crustacean. Adiyodi, K.G., Adiyodi, R.G. (Eds.). *Reproductive biology of invertebrates, oogenesis, oviposition, and oosorption vol. I*. Wiley, New York, 443-495.
- Agrawal, N., Frederick, M. J., Pickering, C. R., Bettegowda, C., Chang, K., Li, R. J., Fakhry, C., Xie, T., Zhang, J., and Wang, J. 2011. Exome sequencing of head and neck squamous cell carcinoma reveals inactivating mutations in NOTCH1. *Science*, 333(6046), 1154-1157.
- Alcedo, J., Ayzenzon, M., Von Ohlen, T., Noll, M., and Hooper, J. E. 1996. The *Drosophila* smoothed gene encodes a seven-pass membrane protein, a putative receptor for the hedgehog signal. *Cell*, 86(2), 221-232.
- Al-Shawi, R., Ashton, S. V., Underwood, C., and Simons, J. P. 2001. Expression of the Ror1 and Ror2 receptor tyrosine kinase genes during mouse development. *Development Genes and Evolution*, 211(4).
- Amiripour, M., Noori, S.A.S., Shariati, V., and Howyzeh, M.S. 2019. Transcriptome analysis of Ajowan (*Trachyspermum ammi* L.) inflorescence. *Journal of Plant Biochemistry and Biotechnology*, 28(4), 496-508.
- Amsterdam, A., Nissen, R. M., Sun, Z., Swindell, E. C., Farrington, S., and Hopkins, N. 2004. Identification of 315 genes essential for early zebrafish development. *Proceedings of the National Academy of Sciences*, 101(35), 12792-12797.
- Andrews, S. 2010. FastQC: a quality control tool for high throughput sequence data. Available online at: <http://www.bioinformatics.babraham.ac.uk/projects/fastqc>.
- Arculeo, M.G., Payen, A.G., Cuttita, G.T., and Riggio, S. 1995. A survey of ovarian maturation in a population of *Aristeus antennatus* (Crustacea: Decapoda). *Animal Biology*, 4, 13-18.

- Artavanis-Tsakonas, S., Rand, M. D., and Lake, R. J. 1999. Notch signaling: cell fate control and signal integration in development. *Science*, 284(5415), 770-776.
- Attisano, L., Wrana, J. L., López-Casillas, F., and Massagué, J. 1994. TGF- β receptors and actions. *Biochimica et Biophysica Acta (BBA)-Molecular Cell Research*, 1222(1), 71-80.
- Ayub, Z., and Ahmed, M. 2002. A description of the ovarian development stages of penaeid shrimps from the coast of Pakistan. *Aqua Res.*, 33(10), 767-76.
- Bada, M., Stevens, R., Goble, C., Gil, Y., Ashburner, M., Blake, J. A., Cherry, J. M., Harris, M., and Lewis, S. 2004. A short study on the success of the Gene Ontology. *Journal of web semantics*, 1(2), 235-240.
- Bailey, J. D., Centers, A., and Jennes, L. 2006. Expression of AMPA receptor subunits (GluR1–GluR4) in gonadotrophin-releasing hormone neurones of young and middle-aged persistently oestrous rats during the steroid-induced luteinising hormone surge. *Journal of neuroendocrinology*, 18(1), 1-12.
- Barreto, F. S., Schoville, S. D., and Burton, R. S. 2015. Reverse genetics in the tide pool: knock-down of target gene expression via RNA interference in the copepod *Tigriopus californicus*. *Molecular Ecology Resources*, 15(4), 868-879.
- Begum, M., Breuer, M., Kodrik, D., Rahman, M. M., and De Loof, A. 2004. The NMDA receptor antagonist MK-801 inhibits vitellogenesis in the flesh fly *Neobellieria bullata* and in the desert locust *Schistocerca gregaria*. *Journal of insect physiology*, 50(10), 927-934.
- Begum, M., Breuer, M., Kodrik, D., Rahman, M. M., and De Loof, A. 2004. The NMDA receptor antagonist MK-801 inhibits vitellogenesis in the flesh fly *Neobellieria bullata* and in the desert locust *Schistocerca gregaria*. *Journal of insect physiology*, 50(10), 927-934.
- Bellavia, D., Campese, A. F., Alesse, E., Vacca, A., Felli, M. P., Balestri, A., Stoppacciaro, A., Tiveron, C., Tatangelo, L., and Giovarelli, M. 2000. Constitutive activation of NF- κ B and T-cell leukemia/lymphoma in Notch3 transgenic mice. *The EMBO journal*, 19(13), 3337-3348.
- Benzie, J. A. 1998. Penaeid genetics and biotechnology. *Aquaculture*, 164(1-4), 23-47.

- Betz, H. 1991. Glycine receptors: heterogeneous and widespread in the mammalian brain. *Trends in neurosciences*, 14(10), 458-461.
- Brady, P., Elizur, A., Williams, R., Cummins, S. F., and Knibb, W. 2012. Gene expression profiling of the cephalothorax and eyestalk in *Penaeus monodon* during ovarian maturation. *International journal of biological sciences*, 8(3), 328.
- Brogiolo, W., Stocker, H., Ikeya, T., Rintelen, F., Fernandez, R., and Hafen, E. 2001. An evolutionarily conserved function of the *Drosophila* insulin receptor and insulin-like peptides in growth control. *Current biology*, 11(4), 213-221.
- Brüning, J. C., Gautam, D., Burks, D. J., Gillette, J., Schubert, M., Orban, P. C., ... and Kahn, C. R. 2000. Role of brain insulin receptor in control of body weight and reproduction. *Science*, 289(5487), 2122-2125.
- Buckworth, R., Ellis, N., Zhou, S., Pascoe, S., Deng, R., Hill, F., and O'Brien, M. 2013. Comparison of TAC and current management for the White Banana Prawn fishery of the Northern Prawn Fishery. CSIRO.
- Burrows, R. C., Wancio, D., Levitt, P., and Lillien, L. 1997. Response diversity and the timing of progenitor cell maturation are regulated by developmental changes in EGFR expression in the cortex. *Neuron*, 19(2), 251-267.
- Byrne, B.M., Gruber, M., and Ab, G. 1989. The evolution of egg yolk proteins. *Prog. Biophys. Mol. Biol.*, 53, 33-69.
- Cai, L.S., Wang, L., Song, K., Lu, K.L., Zhang, C.X., and Rahimnejad, S. 2020. Evaluation of protein requirement of spotted seabass (*Lateolabrax maculatus*) under two temperatures, and the liver transcriptome response to thermal stress. *Aquaculture*, 516, p.734615.
- Chen, A. Q., Yu, S. D., Wang, Z. G., Xu, Z. R., and Yang, Z. G. 2009. Stage-specific expression of bone morphogenetic protein type I and type II receptor genes: effects of follicle-stimulating hormone on ovine antral follicles. *Animal reproduction science*, 111(2-4), 391-399.
- Chen, C., Jack, J. O. S. E. P. H., and Garofalo, R. S. 1996. The *Drosophila* insulin receptor is required for normal growth. *Endocrinology*, 137(3), 846-856.

- Chiang, A. S., Lin, W. Y., Liu, H. P., Pszczolkowski, M. A., Fu, T. F., Chiu, S. L., and Holbrook, G. L. 2002. Insect NMDA receptors mediate juvenile hormone biosynthesis. *Proceedings of the National Academy of Sciences*, 99(1), 37-42.
- Chong, V.C., and Sasekumar, A. 1982. On the Identification of Three Morphospecies of Prawns: *Penaeus merguensis* De Man, *Penaeus indicus* H. Milne Edwards and *Penaeus penicillatus* Alcock (Decapoda, Penaeidea). *Crustaceana*, 127-141.
- Chowdhury, M.M.R., Park, J., Afrin, F., Ko, Y.G., Kim, C.L., Lee, S.S., and Kim, S.W. 2020. Transcriptome profiling of in vitro-matured oocytes from a korean native cow (hanwoo) after cysteamine supplementation. *Animal Biotechnology*, pp.1-12.
- Cooper, G.M. 2000. *The cell: a molecular approach*. 2nd edition. Sunderland (MA): Sinauer associates. Functions of cell surface receptors. Available from: <https://www.ncbi.nlm.nih.gov/books/NBK9866>.
- Copf, T., Rabet, N., and Averof, M. 2006. Knockdown of spalt function by RNAi causes de-repression of Hox genes and homeotic transformations in the crustacean *Artemia franciscana*. *Developmental biology*, 298(1), 87-94.
- Cox, K. J., Van Minnen, J., Vreugdenhil, E., Van Kesteren, E. R., Spijker, J., Burke, J. F., Van Heerikhuizen, H., Tensen, C. P., and Planta, R. J. 1993. Molecular Cloning and Neuronal Expression of a Novel Type of a G-Protein-Coupled Receptor with Ldl Binding Motifs from the Pond Snail *Lymnaea Stagnalis*. *Netherlands journal of zoology*, 44(3-4), 463-472.
- Crococ, P.J., and Kerr, J.D., 1983. Maturation and spawning of the banana prawn *Penaeus merguiesis* De Man (Crustacea, Penaeidae) in the Gulf of Carpentaria, Australia. *Journal of experimental marine biology and ecology*, 69, 37-59.
- Cruciat, C. M., Ohkawara, B., Acebron, S. P., Karaulanov, E., Reinhard, C., Ingelfinger, D., Boutros, M., and Niehrs, C. 2010. Requirement of prorenin receptor and vacuolar H⁺-ATPase-mediated acidification for Wnt signaling. *Science*, 327(5964), 459-463.
- Dabour, N., Bando, T., Nakamura, T., Miyawaki, K., Mito, T., Ohuchi, H., and Noji, S. 2011. Cricket body size is altered by systemic RNAi against insulin

- signaling components and epidermal growth factor receptor. *Development, growth and differentiation*, 53(7), 857-869.
- Dall, W., Hill, B.J., Rothlisberg, P.C., and Staples, D.J. 1990. The biology of the Penaeidae. Blaxter, J.H.S., Southward, A.J. (Eds.). *Advances in marine biology*, Academic Press, London, 1-461.
- Deftos, M. L., He, Y. W., Ojala, E. W., and Bevan, M. J. 1998. Correlating notch signaling with thymocyte maturation. *Immunity*, 9(6), 777-786.
- Demehri, S., Liu, Z., Lee, J., Lin, M. H., Crosby, S. D., Roberts, C. J., Grigsby, P. W., Miner, J. H., Farr, A. G., and Kopan, R. 2008. Notch-deficient skin induces a lethal systemic B-lymphoproliferative disorder by secreting TSLP, a sentinel for epidermal integrity. *PLoS Biology*, 6(5), e123.
- Eichner, C., Nilsen, F., Grotmol, S., and Dalvin, S. 2014. A method for stable gene knock-down by RNA interference in larvae of the salmon louse (*Lepeophtheirus salmonis*). *Experimental parasitology*, 140, 44-51.
- Fantl, W. J., Johnson, D. E., and Williams, L. T. 1993. Signaling by receptor tyrosine kinases. *Annual review of biochemistry*, 62(1), 453-481.
- Feijó, R. G., Braga, A. L., Lanes, C. F., Figueiredo, M. A., Romano, L. A., Klosterhoff, M. C., Nery, L. E. M., Maggioni, R., Wasielesky, W., and Marins, L. F. 2016. Silencing of gonad-inhibiting hormone transcripts in *Litopenaeus vannamei* females by use of the RNA interference technology. *Marine Biotechnology*, 18(1), 117-123.
- Forrester, W. C., Dell, M., Perens, E., and Garriga, G. 1999. A *C. elegans* Ror receptor tyrosine kinase regulates cell motility and asymmetric cell division. *Nature*, 400(6747), 881-885.
- Fu, L., Niu, B., Zhu, Z., Wu, S., and Li, W. 2012. CD-HIT: accelerated for clustering the next-generation sequencing data. *Bioinformatics*, 28(23), 3150-3152.
- Fujita, S., Kuranaga, E., and Nakajima, Y. I. 2019. Cell proliferation controls body size growth, tentacle morphogenesis, and regeneration in hydrozoan jellyfish *Cladonema pacificum*. *PeerJ*, 7, e7579.
- García, U., and Aréchiga, H. 1998. Regulation of crustacean neurosecretory cell activity. *Cellular and Molecular Neurobiology*, 18, 81-99.

- Garduño, J., Elenes, S., Cebada, J., Becerra, E., and García, U. 2002. Expression and functional characterization of GABA transporters in crayfish neurosecretory cells. *Journal of Neuroscience*, 22(21), 9176-9184.
- Geister, T. L., Lorenz, M. W., Hoffmann, K. H., and Fischer, K. 2008. Effects of the NMDA receptor antagonist MK-801 on female reproduction and juvenile hormone biosynthesis in the cricket *Gryllus bimaculatus* and the butterfly *Bicyclus anynana*. *Journal of Experimental Biology*, 211(10), 1587-1593.
- Gilman, A.G. 1987. G-proteins: transducers of receptor-generated signals. *The Annual Review of Biochemistry*, 56, 615-649.
- Gong, J., Huang, C., Shu, L., Bao, C., Huang, H., Ye, H., Zeng, C., and Li, S. 2016. The retinoid X receptor from mud crab: New insights into its roles in ovarian development and related signaling pathway. *Scientific Reports*, 6, 23654. DOI: 10.1038/srep23654
- Gopalakrishnan, K., and Kumar, S. 2020. Whole-genome uterine artery transcriptome profiling and alternative splicing analysis in rat pregnancy. *International journal of molecular sciences*, 21(6), 2079.
- Grabherr, M.G., Haas, B.J., Yassour, M., et al. 2011. Full-length transcriptome assembly from RNA-Seq data without a reference genome. *Nature Biotechnology*, 29, 644-652.
- Green, J., Nusse, R., and van Amerongen, R. 2014. The role of Ryk and Ror receptor tyrosine kinases in Wnt signal transduction. *Cold Spring Harbor perspectives in biology*, 6(2), a009175.
- Grey, D.L., Dall, W., and Baker, A. 1983. A guide to the Australian Penaeid prawns. Department of primary production, Northern Territory, Australia, 1–140.
- Gundermann, N., and Popper, D. (1975). Experiment in growing *Penaeus merguensis* (de Man, 1888) in a fishpond in Fiji. *Aquaculture*, 6(2), 197-198.
- Halford, M. M., Armes, J., Buchert, M., Meskenaite, V., Grail, D., Hibbs, M. L., ... and Stacker, S. A. 2000. Ryk-deficient mice exhibit craniofacial defects associated with perturbed Eph receptor crosstalk. *Nature genetics*, 25(4), 414-418.

- Hanlon, C.D., and Andrew, D.J. 2015. Outside-in signaling - A brief review of GPCR signaling with a focus on the *Drosophila* GPCR family. *Journal of cell science*. DOI: 10.1242/jcs.175158
- Hannas, B., and Leblanc, G. 2009. Expression and ecdysteroid responsiveness of the nuclear receptors HR3 and E75 in the crustacean *Daphnia magna*. *Molecular and cellular endocrinology*, 315. DOI: 10.1016/j.mce.2009.07.013
- Hoang, T., 2001. The banana prawn-the right species for shrimp farming? *World aquaculture*, 40–69.
- Hoang, T., Lee, S.Y., Keenan, C.P., and Marsden, G.E. 2002. Effect of temperature on spawning of *Fenneropenaeus merguensis*. *Journal of Thermal Biology*, 27, 433-437.
- Hollenstein, K., de Graaf, C., Bortolato, A., Wang, M.W., Marshall, F.H., and Stevens, R.C. 2014. "Insights into the structure of class B GPCRs". *Trends in pharmacological sciences*, 35(1), 12–22. DOI: 10.1016/j.tips.2013.11.001
- Holthuis, L.B. 1980. FAO species catalogue. Vol. 1 Shrimps and prawns of the world. An annotated catalogue of species of interest to fisheries. FAO Fisheries Synopsis. 125(1).
- Holthuis, L.B. 1980. FAO species catalogue. Vol. 1 Shrimps and prawns of the world. An annotated catalogue of species of interest to fisheries. FAO Fisheries Synopsis. 125(1).
- Hou, F., He, S., Liu, Y., Zhu, X., Sun, C., and Liu, X. 2014. RNAi knock-down of shrimp *Litopenaeus vannamei* Toll gene and immune deficiency gene reveals their difference in regulating antimicrobial peptides transcription. *Developmental and Comparative Immunology*, 44(2), 255-260.
- Ht Wu, H. and Brennan, C., and Ashworth, R. 2011. Ryanodine receptors, a family of intracellular calcium ion channels, are expressed throughout early vertebrate development. *BMC research notes*, 4, 541. DOI: 10.1186/1756-0500-4-541
- Huang, H. C., Chang, P., Lu, S. Y., Zheng, B. W., and Jiang, Z. F. 2015. Protection of curcumin against amyloid- β -induced cell damage and death involves the prevention from NMDA receptor-mediated intracellular Ca^{2+} elevation. *Journal of Receptors and Signal Transduction*, 35(5), 450-457.

- Huang, J., Tian, L., Peng, C., Abdou, M., Wen, D., Wang, Y., Li, S., and Wang, J. 2011. DPP-mediated TGF β signaling regulates juvenile hormone biosynthesis by activating the expression of juvenile hormone acid methyltransferase. *Development*, 138(11), 2283-2291.
- Huang, X., Feng, B., Huang, H., and Ye, H. 2017. In vitro stimulation of vitellogenin expression by insulin in the mud crab, *Scylla paramamosain*, mediated through PI3K/Akt/TOR pathway. *General and comparative endocrinology*, 250, 175-180.
- Hubbard, S.R. 2004. Juxtamembrane autoinhibition in receptor tyrosine kinases. *Nature Reviews Molecular Cell Biology*, 5, 464–471.
- Huvet, A., Herpin, A., Dégremont, L., Labreuche, Y., Samain, J. F., and Cunningham, C. 2004. The identification of genes from the oyster *Crassostrea gigas* that are differentially expressed in progeny exhibiting opposed susceptibility to summer mortality. *Gene*, 343(1), 211-220.
- Inoue, T., Oz, H. S., Wiland, D., Gharib, S., Deshpande, R., Hill, R. J., Katz, W. S., and Sternberg, P. W. 2004. *C. elegans* LIN-18 is a Ryk ortholog and functions in parallel to LIN-17/Frizzled in Wnt signaling. *Cell*, 118(6), 795-806.
- Isberg, V., de Graaf, C., Bortolato, A., Cherezov, V., Katritch, V., Marshall, F. H., ... and Gloriam, D. E. 2015. Generic GPCR residue numbers–aligning topology maps while minding the gaps. *Trends in pharmacological sciences*, 36(1), 22-31.
- Jehn, B. M., Bielke, W., Pear, W. S., and Osborne, B. A. 1999. Cutting edge: protective effects of notch-1 on TCR-induced apoptosis. *The Journal of Immunology*, 162(2), 635-638.
- Jiang, Q., Min, Y., Yang, H., Wan, W., and Zhang, X. 2019. De novo transcriptome analysis of eyestalk reveals ovarian maturation related genes in *Macrobrachium rosenbergii*. *Aquaculture*, 505, 280-288.
- Josileen, J. 2013. In Training programme on taxonomy and identification of commercially important crustaceans of India. The Central Marine Fisheries Research Institute 46–47.

- Jung, H., Lyons, R. E., Hurwood, D. A., and Mather, P. B. 2013. Genes and growth performance in crustacean species: a review of relevant genomic studies in crustaceans and other taxa. *Reviews in Aquaculture*, 5(2), 77-110.
- Kamakura, M. 2011. Royalactin induces queen differentiation in honeybees. *Nature*, 473(7348), 478-483.
- Kamitori, K., Tanaka, M., Okuno-Hirasawa, T., and Kohsaka, S. 2005. Receptor related to tyrosine kinase RYK regulates cell migration during cortical development. *Biochemical and biophysical research communications*, 330(2), 446-453.
- Kanehisa, M., and Goto, S. 2000. KEGG: kyoto encyclopedia of genes and genomes. *Nucleic acids research*, 28(1), 27-30.
- Kang, B. J., Sultana, Z., and Wilder, M. N. 2021. Assessment of the effects of double-stranded RNAs corresponding to multiple vitellogenesis-inhibiting hormone subtype I peptides in subadult female whiteleg shrimp, *Litopenaeus vannamei*. *Frontiers in Endocrinology*, 12, 15.
- Keeble, T. R., and Cooper, H. M. 2006. Ryk: a novel Wnt receptor regulating axon pathfinding. *The international journal of biochemistry and cell biology*, 38(12), 2011-2017.
- Kezele, P. R., Nilsson, E. E., and Skinner, M. K. 2002. Insulin but not insulin-like growth factor-1 promotes the primordial to primary follicle transition. *Molecular and cellular endocrinology*, 192(1-2), 37-43.
- Khalaila, I., Peter-Katalinic, J., Tsang, C., Radcliffe, C.M., Aflalo, E.D., Harvey, D.J., Dwek, R.A., Rudd, P.M., and Sagi, A., 2004. Structural characterization of the N-glycan moiety and site of glycosylation in vitellogenin from the decapod crustacean *Cherax quadricarinatus*. *Glycobiology*, 14, 767-774.
- Kinouchi, K., Ichihara, A., Sano, M., Sun-Wada, G. H., Wada, Y., Kurauchi-Mito, A., Bokuda, K., Narita, T., Oshima, Y., and Sakoda, M. 2010. The (pro) renin receptor/ATP6AP2 is essential for vacuolar H⁺-ATPase assembly in murine cardiomyocytes. *Circulation research*, 107(1), 30-34.
- Kitamura, T., Kido, Y., Nef, S., Merenmies, J., Parada, L. F., and Accili, D. 2001. Preserved pancreatic β -cell development and function in mice lacking the

- insulin receptor-related receptor. *Molecular and Cellular Biology*, 21(16), 5624-5630.
- Knight, P. G., and Glister, C. 2006. TGF- β superfamily members and ovarian follicle development. *Reproduction*, 132(2), 191-206.
- Kunkel, J.G., and Nordin, J.H. 1985. Yolk proteins. Kerkut, G.A., Gilbert, L.J. (Eds.), *Comprehensive insect physiology, biochemistry and pharmacology*. Oxford, New York, 83-111.
- Laudet, V., and Gronemeyer, H. 2002. The nuclear receptor factsbook. DOI: 10.1016/B978-012437735-6/50026-6
- Lee, J., and Pilch, P. F. 1994. The insulin receptor: structure, function, and signaling. *American Journal of Physiology-Cell Physiology*, 266(2), C319-C334.
- Lenaerts, C., Marchal, E., Peeters, P., and Broeck, J. V. 2019. The ecdysone receptor complex is essential for the reproductive success in the female desert locust, *Schistocerca gregaria*. *Scientific reports*, 9(1), 1-12.
- Li, C. W., and Ge, W. 2011. Spatiotemporal expression of bone morphogenetic protein family ligands and receptors in the zebrafish ovary: a potential paracrine-signaling mechanism for oocyte-follicle cell communication. *Biology of reproduction*, 85(5), 977-986.
- Li, C., Chen, M., Ji, M., Wang, X., Xiao, W., Li, L., Gao, D., Chen, X., and Li, D. 2020. Transcriptome analysis of ripe peach (*Prunus persica*) fruit under low-dose UVB radiation. *Scientia Horticulturae*, 259, p.108757.
- Li, F., Zheng, Z., Li, H., Fu, R., Xu, L., and Yang, F. 2021. Crayfish hemocytes develop along the granular cell lineage. *Scientific Reports*, 11(1), 1-16.
- Li, Q., Agno, J. E., Edson, M. A., Nagaraja, A. K., Nagashima, T., and Matzuk, M. M. 2011. Transforming growth factor β receptor type 1 is essential for female reproductive tract integrity and function. *PLOS Genetics*, 7(10), e1002320.
- Li, Q., Ren, Y., Luan, L., Zhang, J., Qiao, G., Wang, Y., Ye, S. and Li, R. 2019. Localization and characterization of hematopoietic tissues in adult sea cucumber, *Apostichopus japonicus*. *Fish and shellfish immunology*, 84, 1-7.
- Li, W., and Godzik, A. 2006. Cd-hit: a fast program for clustering and comparing large sets of protein or nucleotide sequences. *Bioinformatics*, 22(13), 1658-1659.

- Lima, I. M. T., Brito, I. R., Rossetto, R., Duarte, A. B. G., Rodrigues, G. Q., Saraiva, M. V. A., Costa, J. J. N., Donato, M. A. M., Peixoto, C. A., and Silva, J. R. V. 2012. BMPRII and BMPRII mRNA expression levels in goat ovarian follicles and the in vitro effects of BMP-15 on preantral follicle development. *Cell and tissue research*, 348(1), 225-238.
- Lin, J., Shi, X., Fang, S., Zhang, Y., You, C., Ma, H., and Lin, F. 2019. Comparative transcriptome analysis combining SMRT and NGS sequencing provides novel insights into sex differentiation and development in mud crab (*Scylla paramamosain*). *Aquaculture*, 513, p.734447.
- Liu, Y., Lv, J., Liu, Z., Wang, J., Yang, B., Chen, W., Ou, L., Dai, X., Zhang, Z., and Zou, X. 2020. Integrative analysis of metabolome and transcriptome reveals the mechanism of color formation in pepper fruit (*Capsicum annuum* L.). *Food Chemistry*, 306, p.125629.
- Lou, F., Gao, T. and Han, Z. 2019. Transcriptome analyses reveal alterations in muscle metabolism, immune responses and reproductive behavior of Japanese mantis shrimp (*Oratosquilla oratoria*) at different cold temperature. *Comparative Biochemistry and Physiology Part D: Genomics and Proteomics*, 32, p.100615.
- Lowe, R., Shirley, N., Bleackley, M., Dolan, S., and Shafee, T. 2017. Transcriptomics technologies. *PLoS computational biology*, 13(5), p.e1005457.
- Lu, B., Jiang, Q., Liu, A., Huang, H., and Ye, H. 2020. Stimulatory roles of epidermal growth factor receptor (EGFR) in ovarian development of mud crab *Scylla paramamosain*. *General and Comparative Endocrinology*, 299, 113616.
- Lu, W., Yamamoto, V., Ortega, B., and Baltimore, D. 2004. Mammalian Ryk is a Wnt coreceptor required for stimulation of neurite outgrowth. *Cell*, 119(1), 97-108.
- Lynch, J. W. 2004. Molecular structure and function of the glycine receptor chloride channel. *Physiological reviews*, 84(4), 1051-1095.
- Mangelsdorf, D.J., Thummel, C., Beato, M., Herrlich, P., Schutz, G., Umesono, K., Blumberg, B., Kastner, P., Mark, M., and Chambon, P., et al. 1995. The nuclear receptor superfamily: The second decade. *Cell*, 83, 835–839.

- Martín-Durán, J. M., Vellutini, B. C., and Hejnol, A. 2015. Evolution and development of the adelphophagic, intracapsular Schmidt's larva of the nemertean *Lineus ruber*. *Evodevo*, 6(1), 1-18.
- McBain, C. J., and Mayer, M. L. 1994. N-methyl-D-aspartic acid receptor structure and function. *Physiological reviews*, 74(3), 723-760.
- Meusy, J.J., 1980. Vitellogenin, the extraovarian precursor of the protein yolk in Crustacea: a review. *Reproduction Nutrition Development*, 20, 1-21.
- Meusy, J.J., and Payen, G.G. 1988. Female reproduction in Malacostracan Crustacea. *Zool. Sci.*, 5, 217-265.
- Mikkelsen, L., Moesgaard, K., Hegnauer, M., and Lopez, A. D. 2020. ANACONDA: a new tool to improve mortality and cause of death data. *BMC medicine*, 18(1), 1-13.
- Moss, S. J., and Smart, T. G. 2001. Constructing inhibitory synapses. *Nature Reviews Neuroscience*, 2(4), 240-250.
- Motoh, H., and Kuronuma, K. 1980. Field guide for the edible crustacea of the Philippines. Aquaculture Department, Southeast Asian Fisheries Development Center.
- Mulsant, P., Lecerf, F., Fabre, S., Schibler, L., Monget, P., Lanneluc, I., Pisselet, C., Riquet, J., Monniaux, D., and Callebaut, I. 2001. Mutation in bone morphogenetic protein receptor-IB is associated with increased ovulation rate in Booroola Merino ewes. *Proceedings of the National Academy of Sciences*, 98(9), 5104-5109.
- Munga, C., Ndegwa, S., Fulanda, B., Manyala, J., Kimani, E., Ohtomi, J., and Vanreusel, A. 2012. Bottom shrimp trawling impacts on species distribution and fishery dynamics; Ungwana Bay fishery Kenya before and after the 2006 trawl ban. *Fisheries Science*, 78(2), 209-219.
- Nguyen, N. T., Lin, D. P. C., Yen, S. Y., Tseng, J. K., Chuang, J. F., Chen, B. Y., ... and Ju, J. C. 2009. Sonic hedgehog promotes porcine oocyte maturation and early embryo development. *Reproduction, Fertility and Development*, 21(6), 805-815.
- Nguyen, T.V., R, G.E., Cummins, S.F., Elizur, A., and Ventura, T. 2018. Insights into sexual maturation and reproduction in the Norway lobster (*Nephrops*

- norvegicus) via in silico prediction and characterization of neuropeptides and G protein-coupled receptors. *Frontiers in endocrinology*, 9, 430. DOI: 10.3389/fendo.2018.00430
- Niimi, T., Yoshimi, T., and Yamashita, O. 1993. Vitellin and egg-specific protein as metal-binding proteins of the silkworm, *Bombyx mori*. *J. Seric. Science Council of Japan*, 62, 310-318.
- Nilaweera, K. N., Wilson, D., Bell, L., Mercer, J. G., Morgan, P. J., and Barrett, P. 2008. G protein-coupled receptor 101 mRNA expression in supraoptic and paraventricular nuclei in rat hypothalamus is altered by pregnancy and lactation. *Brain research*, 1193, 76-83.
- Nishizono, H., Darwish, M., Endo, T. A., Uno, K., Abe, H., and Yasuda, R. 2020. Glycine receptor $\alpha 4$ subunit facilitates the early embryonic development in mice. *Reproduction*, 159(1), 41.
- Nuckels, R. J., Ng, A., Darland, T., and Gross, J. M. 2009. The vacuolar-ATPase complex regulates retinoblast proliferation and survival, photoreceptor morphogenesis, and pigmentation in the zebrafish eye. *Investigative ophthalmology and visual science*, 50(2), 893-905.
- Oka, T., and Futai, M. 2000. Requirement of V-ATPase for Ovulation and Embryogenesis in *Caenorhabditis elegans*. *Journal of Biological Chemistry*, 275(38), 29556-29561.
- Parsa, M., Larcombe, J., and Curtotti, R. 2019. Northern prawn fishery. Australian Bureau of Agricultural and Resource Economics and Sciences, Canberra, 62-83.
- Pearson Education. 2006. Receptor types. Available from: https://player.slideplayer.com/90/14797579/slides/slide_29.jpg.
- PÉREZ, I., and Kensley, B. 1997. Penaeoid and sergestoid shrimps and prawns of the world. Keys and diagnoses for the families and genera. *Mémoires du Muséum National d'Histoire Naturelle*, 175, pp.1-233.
- Posiri, P., Ongvarrasopone, C., and Panyim, S. 2013. A simple one-step method for producing dsRNA from *E. coli* to inhibit shrimp virus replication. *Journal of virological methods*. 188(1-2), 64-69.

- Povinelli, B. J., and Nemeth, M. J. 2014. Wnt5a regulates hematopoietic stem cell proliferation and repopulation through the Ryk receptor. *Stem cells*, 32(1), 105-115.
- Powell, D., Knibb, W., Remilton, C., and Elizur, A. 2015. De-novo transcriptome analysis of the banana shrimp (*Fenneropenaeus merguensis*) and identification of genes associated with reproduction and development. *Marine genomics*, 22, 71-78.
- Puengyam, P., Tsukimura, B., and Utarabhand, P. 2013. Molecular characterization of hepatopancreas vitellogenin and its expression during the ovarian development by in situ hybridization in the banana shrimp *Fenneropenaeus Merguensis*. *Journal of Crustacean Biology*, 33(2), 265-274.
- Qian, J. L., Mang, D. Z., Lv, G. C., Ye, J., Li, Z. Q., Chu, Sun, L., Liu, Y., and Zhang, L. W. 2020. Identification and Expression Profile of Olfactory Receptor Genes Based on *Apriona germari* (Hope) Antennal Transcriptome. *Frontiers in physiology*, 11, 807.
- Quinn, R. L., Shuttleworth, G., and Hunter, M. G. 2004. Immunohistochemical localization of the bone morphogenetic protein receptors in the porcine ovary. *Journal of anatomy*, 205(1), 15-23.
- Raafat, A., Goldhar, A. S., Klauzinska, M., Xu, K., Amirjazil, I., McCurdy, D., Lashin, K., Salomon, D., Vonderhaar, B. K., and Egan, S.. 2011. Expression of Notch receptors, ligands, and target genes during development of the mouse mammary gland. *Journal of cellular physiology*, 226(7), 1940-1952.
- Radtke, F., Wilson, A., Stark, G., Bauer, M., van Meerwijk, J., MacDonald, H. R., and Aguet, M. 1999. Deficient T cell fate specification in mice with an induced inactivation of Notch1. *Immunity*, 10(5), 547-558.
- Ramain, P., Khechumian, K., Seugnet, L., Arbogast, N., Ackermann, C., and Heitzler, P. 2001. Novel Notch alleles reveal a Deltex-dependent pathway repressing neural fate. *Current Biology*, 11(22), 1729-1738.
- Rangarajan, A., Talora, C., Okuyama, R., Nicolas, M., Mammucari, C., Oh, H., Aster, J.C., Krishna, S., Metzger, D., and Chambon, P. 2001. Notch signaling is a direct determinant of keratinocyte growth arrest and entry into differentiation. *The EMBO journal*, 20(13), 3427-3436.

- Ratmuangkhwang. n.d. *Fenneropenaeus merguensis*. Available from: <https://www.sealifebase.ca/photos/ThumbnailsSummary.php?Genus=FenneropenaeusandSpecies=merguiensis>.
- Roberts, R. E., Powell, D., Wang, T., Hall, M. H., Motti, C. A., and Cummins, S. F. 2018. Putative chemosensory receptors are differentially expressed in the sensory organs of male and female crown-of-thorns starfish, *Acanthaster planci*. *BMC genomics*, 19(1), 1-13.
- Rothlisberg, P.C., Staples, D.J., and Crocos, P.J. 1985. A review of the life history of the banana prawn, *Penaeus merguensis*, in the Gulf of Carpentaria. Second Australian prawn national semina, NPS2, Cleveland, Australia, 125-136.
- Rothlisberg, P.C., Staples, D.J., and Crocos, P.J. 1985. Review of the life history of the banana prawn, *Penaeus merguensis*, in the Gulf of Carpentaria. Cleveland, Qld., National Prawn Seminar 2.
- Saetan, U., Sangket, U., Deachamag, P., and Chotigeat, W. 2016. Ovarian transcriptome analysis of vitellogenic and non-vitellogenic female banana shrimp (*Fenneropenaeus merguensis*). *PloS one*, 11(10), e0164724.
- Sagi, A., Soroka, E., Chomsky, O., Calderon, J., and Milner, Y. 1995. Ovarian protein synthesis in the prawn *Macrobrachium rosenbergii*: does ovarian vitellin synthesis exist? *Invert. Repro. Development*, 27, 41-47.
- Salic, A., and Mitchison, T. J. 2008. A chemical method for fast and sensitive detection of DNA synthesis in vivo. *Proceedings of the National Academy of Sciences*, 105(7), 2415-2420.
- Sanchez-Duffhues, G., Williams, E., Goumans, M. J., Heldin, C. H., and Ten Dijke, P. 2020. Bone morphogenetic protein receptors: Structure, function and targeting by selective small molecule kinase inhibitors. *Bone*, 115472.
- Sathapondecha, P., and Chotigeat, W. 2019. Induction of vitellogenesis by glass bottom boat in the female banana shrimp, *Fenneropenaeus merguensis* de Man. *General and comparative endocrinology*, 270, 48-59.
- Sato, Y., Tucker, R. P., and Meizel, S. 2002. Detection of glycine receptor/Cl-channel beta subunit transcripts in mouse testis. *Zygote*, 10(2), 105.
- Schlessinger, J., and Ullrich, A. 1992. Growth factor signaling by receptor tyrosine kinases. *Neuron*, 9(3), 383-391.

- Schmierer, B., and Hill, C. S., 2007. TGF β –SMAD signal transduction: molecular specificity and functional flexibility. *Nature reviews Molecular cell biology*, 8(12), 970-982.
- Schneider, M. R., and Wolf, E. 2008. The epidermal growth factor receptor and its ligands in female reproduction: insights from rodent models. *Cytokine and growth factor reviews*, 19(2), 173-181.
- Schuster, S., Miesen, P., and van Rij, R. P. 2019. Antiviral RNAi in insects and mammals: parallels and differences. *Viruses*, 11(5), 448.
- Scitable. 2014. Ion Channel. Available from: <https://www.nature.com/scitable/topicpage/ion-channel-14047658>.
- Sharabi, O., Manor, R., Weil, S., Aflalo, E. D., Lezer, Y., Levy, T., Aizen, J., Ventura, T., Mather, P. B., Khalaila, I., and Sagi, A. 2016. Identification and characterization of an insulin-like receptor involved in crustacean reproduction. *Endocrinology*, 157, 2(1), 928–941. DOI: 10.1210/en.2015-1391
- Sharabi, O., Ventura, T., Manor, R., Aflalo, E. D., and Sagi, A. (2013, April). Dual function of a putative epidermal growth factor receptor in the decapod crustacean *Macrobrachium rosenbergii*. I In *Integrative and Comparative Biology*, 53, E195-E195.
- Sheaves, M., Johnston, R., Connolly, R.M. and Baker, R. 2012. Importance of estuarine mangroves to juvenile banana prawns. *Estuarine, Coastal and Shelf Science*, 114, 208-219.
- Shu, L., Yang, Y., Huang, H., and Ye, H. 2016. A bone morphogenetic protein ligand and receptors in mud crab: A potential role in the ovarian development. *Molecular and cellular endocrinology*, 434, 99-107.
- Siddeek, M.S.M., Fouda, M.M. and Hermosa Jr, G.V. 1999. Demersal fisheries of the Arabian Sea, the Gulf of Oman and the Arabian Gulf. *Estuarine, Coastal and Shelf Science*, 49, 87-97.
- Stone, D. M., Hynes, M., Armanini, M., Swanson, T. A., Gu, Q., Johnson, R. L., ... and Noll, M. 1996. The tumour-suppressor gene patched encodes a candidate receptor for Sonic hedgehog. *Nature*, 384(6605), 129-134.

- Stransky, N., Egloff, A. M., Tward, A. D., Kostic, A. D., Cibulskis, K., Sivachenko, A., Kryukov, G. V., Lawrence, M.S., Sougnez, C., and McKenna, A. 2011. The mutational landscape of head and neck squamous cell carcinoma. *Science*, 333(6046), 1157-1160.
- Sudhagar, A., Kumar, G., and El-Matbouli, M. 2018. Transcriptome analysis based on RNA-Seq in understanding pathogenic mechanisms of diseases and the immune system of fish: a comprehensive review. *International journal of molecular sciences*, 19(1), 245.
- Sugimoto, M., Sasaki, S., Watanabe, T., Nishimura, S., Ideta, A., Yamazaki, M., ... and Sugimoto, Y. 2010. Ionotropic glutamate receptor AMPA 1 is associated with ovulation rate. *PloS one*, 5(11), e13817.
- Tatar, M., Kopelman, A., Epstein, D., Tu, M. P., Yin, C. M., and Garofalo, R. S. 2001. A mutant *Drosophila* insulin receptor homolog that extends life-span and impairs neuroendocrine function. *Science*, 292(5514), 107-110.
- Tatusov, R. L., Fedorova, N. D., Jackson, J. D., Jacobs, A. R., Kiryutin, B., Koonin, E. V., Krylov, D. M., Mazumder, R., Mekhedov, S. L., and Nikolskaya, A. N. 2003. The COG database: an updated version includes eukaryotes. *BMC bioinformatics*, 4(1), 1-14.
- Treerattrakool, S., Panyim, S., Chan, S. M., Withyachumnarnkul, B., and Udomkit, A. 2008. Molecular characterization of gonad-inhibiting hormone of *Penaeus monodon* and elucidation of its inhibitory role in vitellogenin expression by RNA interference. *The FEBS journal*, 275(5), 970-980.
- Tsang, W.S., Quackenbush, L.S., Chow, B.K.C, Tiu, S.H.K., He, J.G., and Chan, S.M. 2003. Organization of the shrimp vitellogenin gene: evidence of multiple genes and tissue specific expression by the ovary and hepatopancreas. *Gene*, 30, 99–109.
- Tse, A. C. K., and Ge, W. 2010. Spatial localization of EGF family ligands and receptors in the zebrafish ovarian follicle and their expression profiles during folliculogenesis. *General and comparative endocrinology*, 167(3), 397-407.
- Tsukimura, B. 2001. Crustacean vitellogenesis: its role in oocyte development. *American Journal of Zoology*, 41, 465- 476.

- Uawisetwathana, U., Leelatanawit, R., Klanchui, A., Prommoon, J., Klinbunga, S., and Karoonuthaisiri, N. 2011. Insights into eyestalk ablation mechanism to induce ovarian maturation in the black tiger shrimp. *PLoS ONE*, 6(9).
- Ullrich, A., and Schlessinger, J. 1990. Signal transduction by receptors with tyrosine kinase activity. *Cell*, 61(2), 203-212.
- Urbanski, H. F., and Ojeda, S. R. 1990. A role for N-methyl-D-aspartate (NMDA) receptors in the control of LH secretion and initiation of female puberty. *Endocrinology*, 126(3), 1774-1776.
- Van de Walle, I., De Smet, G., De Smedt, M., Vandekerckhove, B., Leclercq, G., Plum, J., and Taghon, T. 2009. An early decrease in Notch activation is required for human TCR- $\alpha\beta$ lineage differentiation at the expense of TCR- $\gamma\delta$ T cells. *Blood, The Journal of the American Society of Hematology*, 113(13), 2988-2998.
- Van de Walle, I., De Smet, G., Gärtner, M., De Smedt, M., Waegemans, E., Vandekerckhove, B., Leclercq, G., Plum, J., Aster, J. C., and Bernstein, I. D. 2011. Jagged2 acts as a Delta-like Notch ligand during early hematopoietic cell fate decisions. *Blood, The Journal of the American Society of Hematology*, 117(17), 4449-4459.
- Van de Walle, I., Waegemans, E., De Medts, J., De Smet, G., De Smedt, M., Snauwaert, S., Vandekerckhove, B., Kerre, T., Leclercq, G., and Plum, J. 2013. Specific Notch receptor–ligand interactions control human TCR- $\alpha\beta/\gamma\delta$ development by inducing differential Notch signal strength. *Journal of Experimental Medicine*, 210(4), 683-697.
- Van den Heuvel, M., and Ingham, P. W. 1996. Smoothed encodes a receptor-like serpentine protein required for hedgehog signalling. *Nature*, 382(6591), 547-551.
- Vanorny, D. A., and Mayo, K. E. 2017. The role of Notch signaling in the mammalian ovary. *Reproduction*, 153(6), R187-R204.
- Venkatakrishnan, A.J., Deupi, X., Lebon, G., Tate, C.G., Schertler, G.F., and Babu, M.M. February 2013. "Molecular signatures of G-protein-coupled receptors". *Nature*. 494 (7436), 185–94. DOI: 10.1038/nature11896

- Walker, L., Carlson, A., Tan-Pertel, H. T., Weinmaster, G., and Gasson, J. 2001. The notch receptor and its ligands are selectively expressed during hematopoietic development in the mouse. *Stem Cells*, 19(6), 543-552.
- Wang, C., and Roy, S. K. 2009. Expression of bone morphogenetic protein receptor (BMPR) during perinatal ovary development and primordial follicle formation in the hamster: possible regulation by FSH. *Endocrinology*, 150(4), 1886-1896.
- Wang, W., Yang, S., Wang, C., Shi, L., Guo, H., and Chan, S. 2017. Gill transcriptomes reveal involvement of cytoskeleton remodeling and immune defense in ammonia stress response in the banana shrimp *Fenneropenaeus merguensis*. *Fish and shellfish immunology*, 71, 319-328.
- Wang, Z., Zhou, W., Hameed, M. S., Liu, J., and Zeng, X. 2018. Characterization and expression profiling of neuropeptides and G-protein-coupled receptors (GPCRs) for neuropeptides in the Asian citrus psyllid, *Diaphorina citri* (Hemiptera: Psyllidae). *International journal of molecular sciences*, 19(12), 3912.
- Waxham, M. N. 2014. Neurotransmitter receptors. In *From Molecules to Networks*. Academic Press, 285-321.
- Wagner, D. O., Sieber, C., Bhushan, R., Borgermann, J. H., Graf, D., and Knaus, P. 2010. BMPs: From bone to body morphogenetic proteins. *Science Signaling*, 3(107). DOI: 10.1126/scisignal.3107mr1
- Wilson, C., Gohberdhan, D., and Steller, H. 1993. Dror, a potential neurotrophic receptor gene, encodes a *Drosophila* homolog of the vertebrate Ror family of Trk-related receptor tyrosine kinases. *Proceedings of the National Academy of Sciences*, 90(15), 7109-7113.
- WoRMS. 2019. *Fenneropenaeus merguensis* (de Man, 1888). Available from: <http://www.marinespecies.org/aphia.php?p=taxdetails&id=377435>.
- Wu, H. H., Brennan, C., and Ashworth, R. 2011. Ryanodine receptors, a family of intracellular calcium ion channels, are expressed throughout early vertebrate development. *BMC research notes*, 4(1), 1-17.

- Wu, X., Chen, H., Liu, Z., and Cheng, Y. 2014. Immunorecognition and distribution of progesterone receptors in the Chinese mitten crab *Eriocheir sinensis* during ovarian development. *Journal of Shellfish Research*, 33(1), 35-43.
- Xu, W., Jiang, X., and Huang, L. 2019. RNA interference technology. *Comprehensive Biotechnology*, 560.
- Yan, H., Xue, M., Liu, H., Wang, L., Liu, Q., and Jiang, L. 2017. Energy reserves and gonad steroid levels during the reproductive cycle of the Japanese mantis shrimp *Oratosquilla oratoria* De Haan, 1844 (Stomatopoda: Squillidae) in Pikou Bay, Dalian, China. *Journal of Crustacean Biology*, 37(1), 99–108. DOI:10.1093/jcbiol/ruw016
- Yano, I. 1988. Oocyte development in the kuruma prawn *Penaeus japonicus*. *Marine Biology.*, 99(4), 547-53.
- Yarden, Y., and Ullrich, A. 1988. Growth factor receptor tyrosine kinases. *Annual Review of Biochemistry*, 57, 443–478.
- Yin, X., and Tsukaya, H. 2019. Morphogenesis of flattened unifacial leaves in *Juncus prismatocarpus* (Juncaceae). *New Phytologist*, 222(2), 1101-1111.
- Yoda, A., Oishi, I., and Minami, Y. 2003. Expression and function of the Ror-family receptor tyrosine kinases during development: Lessons from genetic analyses of nematodes, mice, and humans. *Journal of receptors and signal transduction*, 23(1), 1-15.
- Zhao, Y. Y., Li, X. X., Wang, W., Chen, X., Yu, P., Wang, J. J., and Xu, Y. X. 2014. Effect of BMPRII gene silencing by siRNA on apoptosis and steroidogenesis of porcine granulosa cells. *Genetics and Molecular Research*, 13(4), 9964-9975.
- Zheng, H., Zeng, B., Shang, T., and Zhou, S. 2020. Identification of G protein-coupled receptors required for vitellogenesis and egg development in an insect with panoistic ovary. *Insect Science*. DOI: 10.1111/1744-7917.12841
- Zhou, Y. L., Wang, C., Gu, W. B., Zhu, Q. H., Wang, L. Z., Zhou, Z. K., Liu, Z., Chen, Y., and Shu, M. A. 2018. Identification and functional analysis of transforming growth factor- β type I receptor (T β R1) from *Scylla paramamosai*: the first evidence of T β R1 involved in development and

innate immunity in crustaceans. *Developmental and Comparative Immunology*, 88, 144-151.

Zhuo, R. Q., Zhou, T. T., Yang, S. P., and Chan, S. F. 2017. Characterization of a molt-related myostatin gene (FmMstn) from the banana shrimp *Fenneropenaeus merguensis*. *General and Comparative Endocrinology*, 248, 55-68.

APPENDIX A

Appendix 1 Receptor keywords used to identify putative receptors.

3.1 Receptor keywords for G protein-coupled receptor type (the IUPHAR/BPS Guide to pharmacology, 2019):

Orphan and other 7TM receptors

- Class A Orphans
- Class B Orphans
- Class C Orphans
- Opsin receptors
- Taste 1 receptors
- Taste 2 receptors

Other 7TM proteins

5-Hydroxytryptamine receptors

Acetylcholine receptors (muscarinic)

Adenosine receptors

Adhesion Class GPCRs

Adrenoceptors

Angiotensin receptors

Apelin receptor

Bile acid receptor

Bombesin receptors

Bradykinin receptors

Calcitonin receptors

Calcium-sensing receptor

Cannabinoid receptors

Chemerin receptors

Chemokine receptors

Cholecystokinin receptors

Class Frizzled GPCRs
Complement peptide receptors
Corticotropin-releasing factor receptors
Dopamine receptors
Endothelin receptors
G protein-coupled estrogen receptor
Formylpeptide receptors
Free fatty acid receptors
GABAB receptors
Galanin receptors
Ghrelin receptor
Glucagon receptor family
Glycoprotein hormone receptors
Gonadotrophin-releasing hormone receptors
GPR18, GPR55 and GPR119
Histamine receptors
Hydroxycarboxylic acid receptors
Kisspeptin receptor
Leukotriene receptors
Lysophospholipid (LPA) receptors
Lysophospholipid (S1P) receptors
Melanin-concentrating hormone receptors
Melanocortin receptors
Melatonin receptors
Metabotropic glutamate receptors
Motilin receptor
Neuromedin U receptors
Neuropeptide FF/neuropeptide AF receptors
Neuropeptide S receptor
Neuropeptide W/neuropeptide B receptors
Neuropeptide Y receptors
Neurotensin receptors

Opioid receptors
Orexin receptors
Oxoglutarate receptor
P2Y receptors
Parathyroid hormone receptors
Platelet-activating factor receptor
Prokineticin receptors
Prolactin-releasing peptide receptor
Prostanoid receptors
Proteinase-activated receptors
QRFP receptor
Relaxin family peptide receptors
Somatostatin receptors
Succinate receptor
Tachykinin receptors
Thyrotropin-releasing hormone receptors
Trace amine receptor
Urotensin receptor
Vasopressin and oxytocin receptors
VIP and PACAP receptors

3.2 Receptor keywords for receptor-tyrosine kinase type (Ségalliny, Aude I., et al., 2015):

Type I RTKs: ErbB (epidermal growth factor) receptor family

- EGFR (epidermal growth factor receptor)
- HER2 (erb-b2 receptor tyrosine kinase 2)
- HER3 (erb-b2 receptor tyrosine kinase 3)
- HER4 (erb-b2 receptor tyrosine kinase 4)

Type II RTKs: Insulin receptor family

- InsR (Insulin receptor)
- IGF1R (Insulin-like growth factor I receptor)
- IRR (Insulin receptor-related receptor)

Type III RTKs: PDGFR, CSFR, Kit, FLT3 receptor family

- PDGFR α (platelet derived growth factor receptor alpha)
- PDGFR β (platelet derived growth factor receptor beta)
- PDGFR β (platelet derived growth factor receptor beta)
- CSFR (colony stimulating factor 1 receptor)
- FLT3 (fms related tyrosine kinase 3)

Type IV RTKs: VEGF (vascular endothelial growth factor) receptor family

- VEGFR-1 (fms related tyrosine kinase 1)
- VEGFR-2 (kinase insert domain receptor)
- VEGFR-3 (fms related tyrosine kinase 4)

Type V RTKs: FGF (fibroblast growth factor) receptor family

- FGFR1 (fibroblast growth factor receptor 1)
- FGFR2 (fibroblast growth factor receptor 2)
- FGFR3 (fibroblast growth factor receptor 3)
- FGFR4 (fibroblast growth factor receptor 4)

Type VI RTKs: PTK7 (tyrosine-protein kinase-like 7) // CCK4 (colon carcinoma kinase 4) receptor family

- CCK4 (protein tyrosine kinase 7 (inactive))

Type VII RTKs: Neurotrophin receptor // Trk: trkA, trkB and trkC (tropomyosin-related kinase) receptors family

- trkA (neurotrophic receptor tyrosine kinase 1)
- trkB (neurotrophic receptor tyrosine kinase 2)
- trkC (neurotrophic receptor tyrosine kinase 3)

Type VIII RTKs: ROR family

- ROR1 (receptor tyrosine kinase like orphan receptor 1)
- ROR2 (receptor tyrosine kinase like orphan receptor 2)

Type IX RTKs: MuSK // Muscle-Specific Kinase

- MuSK (muscle associated receptor tyrosine kinase)

Type X RTKs: HGF (hepatocyte growth factor) receptor family // c-Met // tyrosine-protein kinase Met

- MET (MET proto-oncogene, receptor tyrosine kinase)

- Ron (macrophage stimulating 1 receptor)

Type XI RTKs: TAM (TYRO3-, AXL- and MER-TK) receptor family // TAM (or AXL) receptor family

- Axl (AXL receptor tyrosine kinase)
- Tyro3 (TYRO3 protein tyrosine kinase)
- Mer (MER proto-oncogene, tyrosine kinase)

Type XII RTKs: TIE family of angiopoietin receptors

- TIE1 (tyrosine kinase with immunoglobulin like and EGF like domains 1)
- TIE2 (TEK receptor tyrosine kinase)

Type XIII RTKs: Ephrin receptor family

- Eph receptors
- EphA1 (EPH receptor A1)
- EphA2 (EPH receptor A2)
- EphA3 (EPH receptor A3)
- EphA4 (EPH receptor A4)
- EphA5 (EPH receptor A5)
- EphA6 (EPH receptor A6)
- EphA7 (EPH receptor A7)
- EphA8 (EPH receptor A8)
- EphA10 (EPH receptor A10)
- EphB1 (EPH receptor B1)
- EphB2 (EPH receptor B2)
- EphB3 (EPH receptor B3)
- EphB4 (EPH receptor B4)
- EphB6 (EPH receptor B6)

Type XIV RTKs: RET

- Ret (ret proto-oncogene)

Type XV RTKs: RYK

- receptor like tyrosine kinase // receptor-like tyrosine kinase
- Related to receptor tyrosine kinase

Type XVI RTKs: DDR (collagen receptor) family

- discoidin domain receptor tyrosine kinase
- DDR1 // CD167a
- Type XVII RTKs: ROS receptors
- c-ros oncogene 1, receptor tyrosine kinase

Type XVIII RTKs: LMR family

- Lmr1 (apoptosis associated tyrosine kinase)
- Lmr2 (lemur tyrosine kinase 2)
- Lmr3 (lemur tyrosine kinase 3)

Type XIX RTKs: Leukocyte tyrosine kinase (LTK) receptor family

- LTK (leukocyte receptor tyrosine kinase)
- ALK (ALK receptor tyrosine kinase)

Type XX RTKs: STYK1

- TK-unique family
- STYK1 (serine/threonine/tyrosine kinase 1)

3.3 Receptor keywords for nuclear receptor type (the IUPHAR/BPS Guide to pharmacology, 2019):

Thyroid Hormone Receptor-like

- Thyroid hormone receptors
- Thyroid hormone receptor- α
- Thyroid hormone receptor- β
- Retinoic acid receptor
- Retinoic acid receptor- α
- Retinoic acid receptor- β
- Retinoic acid receptor- γ
- Peroxisome proliferator-activated receptor
- Peroxisome proliferator-activated receptor- α
- Peroxisome proliferator-activated receptor- β/δ
- Peroxisome proliferator-activated receptor- γ
- Rev-ErbA receptors
- Rev-ErbA α
- Rev-ErbA α

- RAR-related orphan receptor
- RAR-related orphan receptor- α
- RAR-related orphan receptor- β
- RAR-related orphan receptor- γ
- Liver X receptor-like
- Liver X receptor- α
- Liver X receptor- β
- Farnesoid X receptor
- Farnesoid X receptor- β
- Vitamin D receptor-like
- Vitamin D receptor
- Pregnane X receptor
- Constitutive androstane receptor
- NRs with two DNA binding domains

Retinoid X Receptor-like

- Hepatocyte nuclear factor-4
- Hepatocyte nuclear factor-4- α
- Hepatocyte nuclear factor-4- γ
- Retinoid X receptors
- Retinoid X receptor- α
- Retinoid X receptor- β
- Retinoid X receptor- γ
- Testicular receptor
- Testicular receptor 2
- Testicular receptor 4
- TLX/PNR
- Tailless-like receptors
- Homologue of the Drosophila tailless gene
- Photoreceptor cell-specific nuclear receptor
- COUP/EAR
- Chicken ovalbumin upstream promoter-transcription factor I

- Chicken ovalbumin upstream promoter-transcription factor II

COUP-TF-like receptors

Estrogen Receptor-like

- Estrogen-related receptors
- Estrogen-related receptor- α
- Estrogen-related receptor- β
- Estrogen-related receptor- γ
- 3-Ketosteroid receptors
- Glucocorticoid receptor
- Mineralocorticoid receptor
- Progesterone receptor
- Androgen receptor
- Nerve growth factor IB-like receptors
- Nerve Growth factor IB
- Nuclear receptor related 1
- Neuron-derived orphan receptor 1

Fushi tarazu F1-like receptors

Germ cell nuclear factor receptors

DAX-like receptors

Steroidogenic Factor-like receptors

- Steroidogenic factor 1
- Liver receptor homolog-1

3.3 Receptor keywords for nuclear receptor type (the IUPHAR/BPS Guide to pharmacology, 2019):

Ligand-gated ion channels

- 5-HT₃ receptors
- Complexes
- 5-HT_{3AB}
- 5-HT_{3A}
- Subunits

- 5-HT3A
- 5-HT3B
- 5-HT3C
- 5-HT3D
- 5-HT3E
- Acid-sensing (proton-gated) ion channels (ASICs)
- ASIC1
- ASIC2
- ASIC3
- Epithelial sodium channel (ENaC)
- Complexes
- ENaC $\alpha\beta\gamma$
- Subunits
- ENaC α
- ENaC β
- ENaC γ
- ENaC δ
- GABAA receptors
- GABAA receptor α 1 subunit
- GABAA receptor α 2 subunit
- GABAA receptor α 3 subunit
- GABAA receptor α 4 subunit
- GABAA receptor α 5 subunit
- GABAA receptor α 6 subunit
- GABAA receptor β 1 subunit
- GABAA receptor β 2 subunit
- GABAA receptor β 3 subunit
- GABAA receptor γ 1 subunit
- GABAA receptor γ 2 subunit
- GABAA receptor γ 3 subunit
- GABAA receptor δ subunit

- GABAA receptor ϵ subunit
- GABAA receptor θ subunit
- GABAA receptor π subunit
- GABAA receptor $\rho 1$ subunit
- GABAA receptor $\rho 2$ subunit
- GABAA receptor $\rho 3$ subunit
- Glycine receptors
- Complexes
- Glycine Receptor (All subtypes)
- Subunits
- glycine receptor $\alpha 1$ subunit
- glycine receptor $\alpha 2$ subunit
- glycine receptor $\alpha 3$ subunit
- glycine receptor $\alpha 4$ subunit (pseudogene in humans)
- glycine receptor β subunit
- Ionotropic glutamate receptors
- IP3 receptor
- Nicotinic acetylcholine receptors
- P2X receptors
- ZAC

Voltage-gated ion channels

- CatSper and Two-Pore channels
- CatSper1
- CatSper2
- CatSper3
- CatSper4
- TPC1
- TPC2
- Cyclic nucleotide-regulated channels
- Potassium channels
- Calcium- and sodium-activated potassium channels

- Inwardly rectifying potassium channels
- Two P domain potassium channels
- Voltage-gated potassium channels
- Ryanodine receptors
- Transient Receptor Potential channels
- Voltage-gated calcium channels
- Voltage-gated proton channel
- Voltage-gated sodium channels

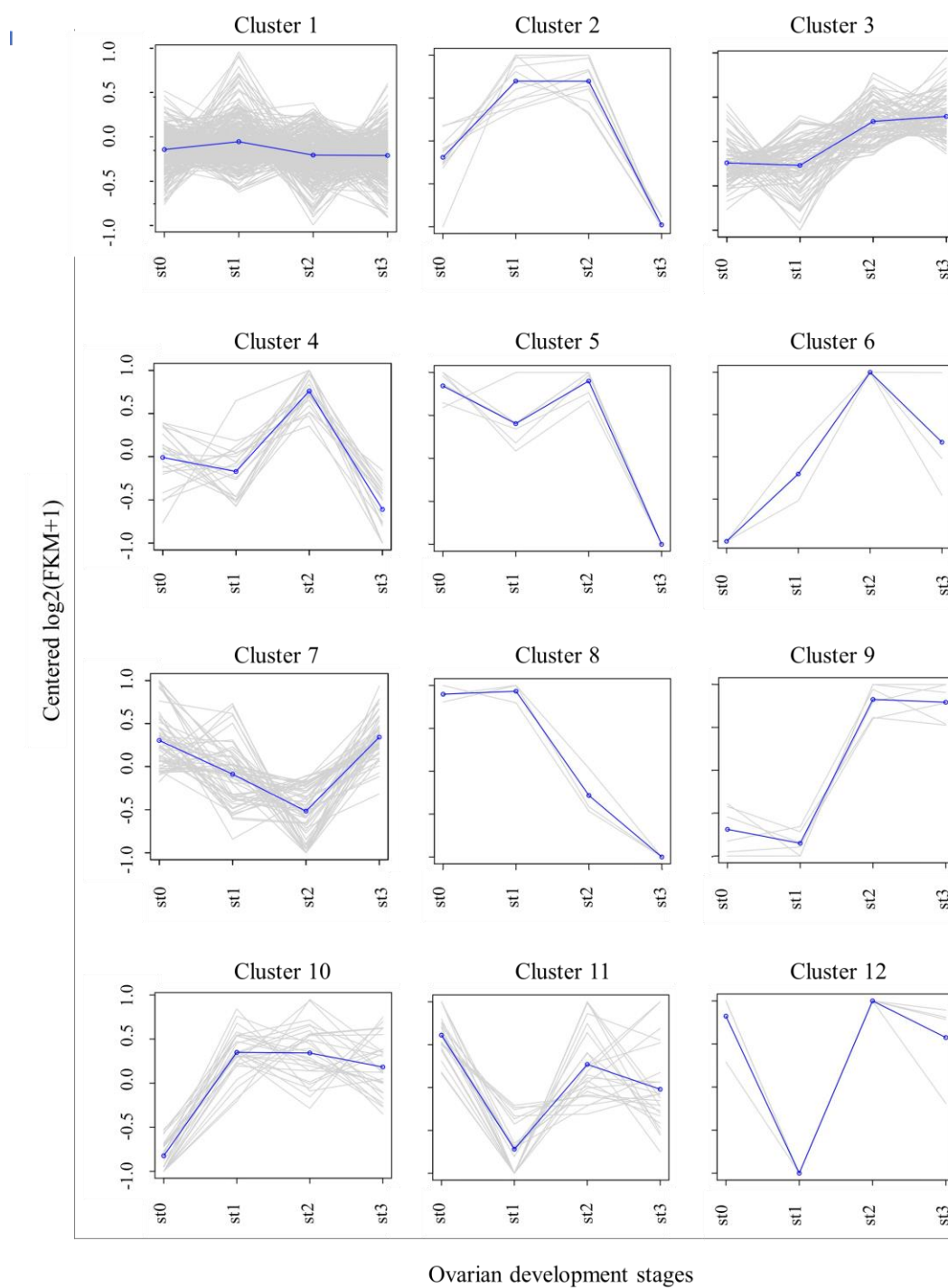
Other ion channels

- Aquaporins
- Chloride channels
- ClC family
- CFTR (Cystic fibrosis transmembrane conductance regulator)
- Calcium activated chloride channel
- Maxi chloride channel
- Volume regulated chloride channels
- Connexins and Pannexins
- Piezo channels
- Piezo1
- Piezo2
- Sodium leak channel, non-selective
- Store-operated ion channels
- Orai channels

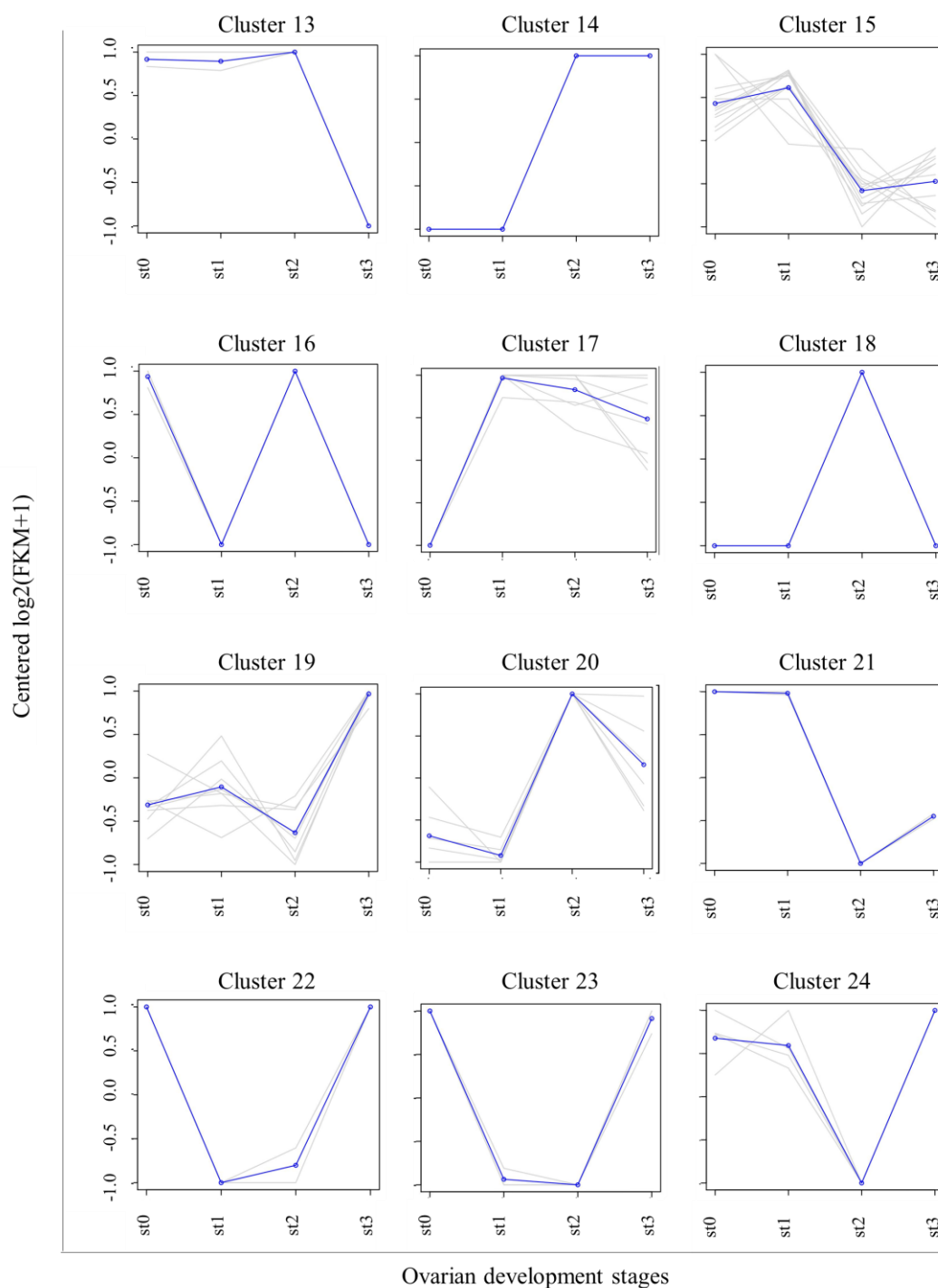
Appendix 2 The efficiency of candidate receptor specific primers.

The candidate receptors	Primer efficiency
Smoothened (Smo) receptor	96 %
G-protein coupled receptor GRL101 (GRL101)	90 %
Renin receptor	98 %
Epidermal growth factor receptor (EGFR)	90 %
Receptor tyrosine kinase-like orphan receptor (ROR)	97 %
Receptor-like tyrosine kinase (RYK)	99 %
Transforming growth factor- β 1 (TGF- β 1) receptor	95 %
Bone morphogenetic protein type 1 receptor (BMPRI) or saxophone (sax)	95 %
Bone morphogenetic protein type 2 receptor (BMPRII)	100 %
Notch receptor	97 %
Insulin receptor	90 %
Glycine- α receptor	98 %
Glycine- β receptor	96 %
Glutamate receptor	90 %
N-methyl-D aspartate (NMDA) receptor	97 %

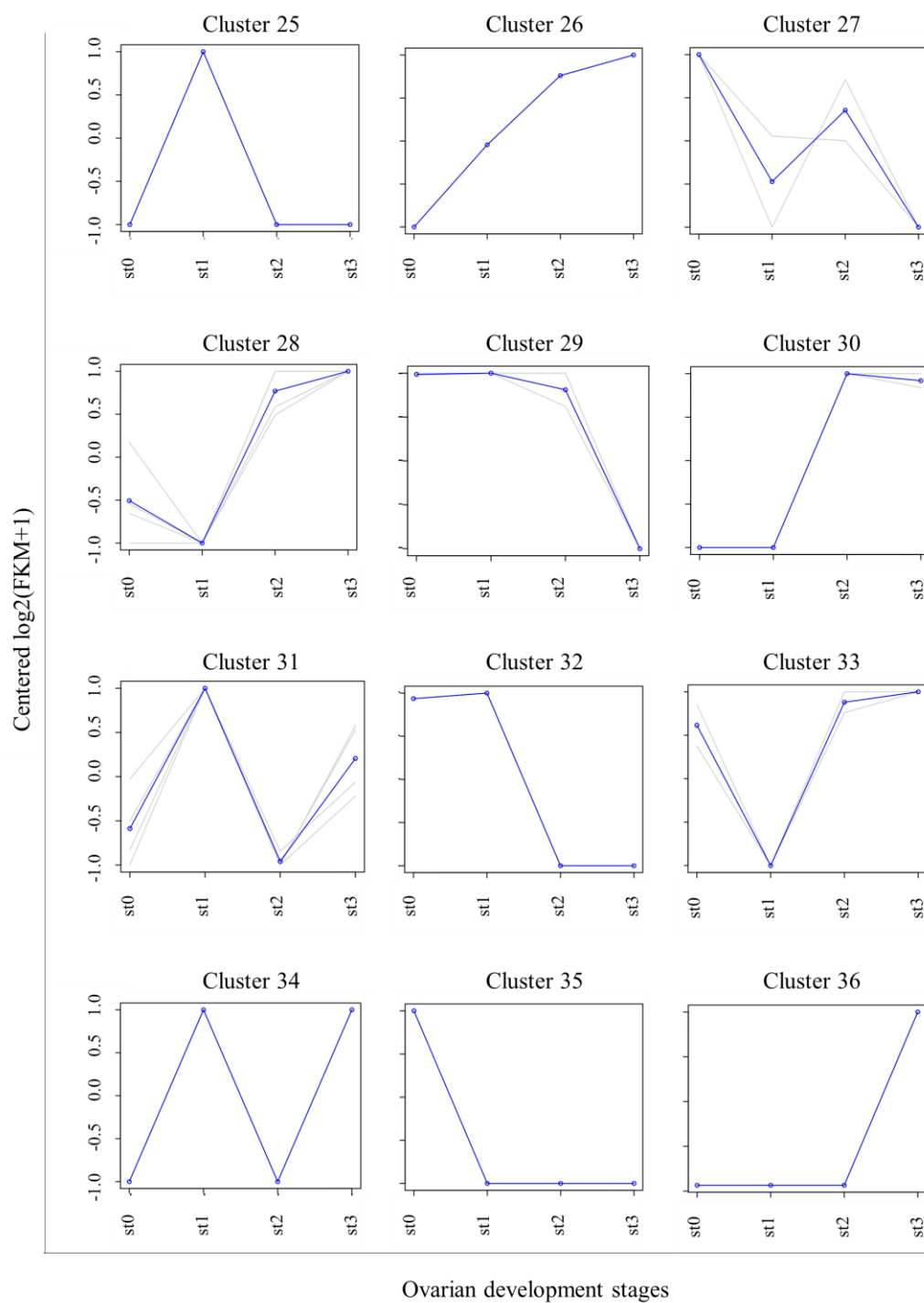
Appendix 3 The dendrogram of differentially expressed receptor genes using the $\log_2(\text{FPKM}+1)$ value. The expression patterns were analyzed into subclusters. Each grey line in a subline chart represented the relative expression value of a gene cluster under ovarian development stages, and the blue line represented the mean value.



Appendix 3 (cont.) The dendrogram of differentially expressed receptor genes using the $\log_2(\text{FPKM}+1)$ value. The expression patterns were analyzed into subclusters. Each grey line in a subline chart represented the relative expression value of a gene cluster under ovarian development stages, and the blue line represented the mean value.



Appendix 3 (cont.) The dendrogram of differentially expressed receptor genes using the $\log_2(\text{FPKM}+1)$ value. The expression patterns were analyzed into subclusters. Each grey line in a subline chart represented the relative expression value of a gene cluster under ovarian development stages, and the blue line represented the mean value.



APPENDIX B



การประชุมวิชาการและนำเสนอผลงานวิจัยระดับชาติและนานาชาติ ครั้งที่ 12
 "Global Goals, Local Actions: Looking Back and Moving Forward 2021"

Transcriptome analysis in ovary of female banana shrimp, *Fenneropenaeus merguensis*: A functional study of *nudel* as a potential gene involved in the ovarian development

Manita Nonsung¹, Unisa Sanget², Ponsit Sathapondacha^{2*}

*Email: ponsit.sat@gmail.com, ponsit.s@psu.ac.th

¹ Master student in Department of Molecular Biotechnology and Bioinformatics, Division of Biological Science, Faculty of Science, Prince of Songkla University, Hat Yai, Songkhla 90110, Thailand

² Assistant Professor in Center for Genomics and Bioinformatics Research, Division of Biological Science, Faculty of Science, Prince of Songkla University, Hat Yai, Songkhla 90110, Thailand

Abstract

Control of ovarian maturation is an important one of problems in the shrimp aquaculture. Several genes involved in control of crucial ovarian development process like vitellogenesis in female crustaceans. In this study, the ovary at each ovarian developmental stage of female banana shrimp, *Fenneropenaeus merguensis*, was analyze for its transcriptome with Illumina HiSeq2500 platform. The *nudel* (*ndl*) was identified for study of characterization and the role of *FmNudel* in vitellogenesis of female banana shrimp. The result suggested that the *FmNudel* expression was significantly highest in ovary compared to other tissues. Its expression was significantly increased in previtellogenic stage (stage 0), then dropped in the other stages. The silencing of *FmNudel* was performed by *nudel*-dsRNA injection on day 10 resulted in significant decrease of *vitellogenin* (*Vg*) expression in ovary.

Keywords *Fenneropenaeus merguensis*, ovarian development, transcriptome

Introduction

Shrimp is one of the widely consumed seafood products all over the world having high economic value (FAO, 2020). However, in recent years the shrimp aquaculture has been interrupted with several problems involved shrimp reproduction. In shrimp aquaculture, the eyestalk ablation was widely used to rapidly stimulate ovarian maturation in female shrimp (Uawisetwathana et al., 2011) because the eyestalks of crustaceans are the source of the gonad-suppressive hormone such as a gonad inhibiting hormone (GIH) (Treerattrakool et al., 2008) but the technique leads to an eventual loss in egg quality, high mortality in spawner



การประชุมวิชาการและนำเสนอผลงานวิจัยระดับชาติและนานาชาติ ครั้งที่ 12
 "Global Goals, Local Actions: Looking Back and Moving Forward 2021"

(Benzie 1998) and risks to impact animal cruelty laws. Therefore, this technique should be replaced with the more effective methods to induce shrimp ovarian maturation.

An understanding of molecular pathway for control of ovarian maturation is necessary. There were several factors involved in the ovarian developmental process. For example, GIH-specific double-stranded RNA in *Penaeus monodon* increased *vitellogenin (Vg)* expression level and led to ovarian maturation and eventual spawning (Treerattrakool et al., 2008, 2011). Serotonin and estradiol and progesterone in *P. monodon* (Wongprasert et al., 2006; Merlin et al., 2015) and insulin-like receptor in *Macrobrachium rosenbergii*, (Sharabi, 2001) could induce ovarian maturation.

In this study, we aimed to identify an ovarian-regulating gene using RNA sequencing and bioinformatic analyses in female banana shrimp, *Fenneropenaeus merguensis*. The differential gene expression of putative gene during ovarian developmental stages was also investigated. The putative ovarian-regulating gene were characterized for its expressions, a candidate gene was studied for its role in the control of vitellogenesis using RNA interference.

Objectives

1. To identify and characterize a candidate gene involved in ovarian development in female banana shrimp.
2. To study an ovarian stimulating function of the *nudel* gene in female banana shrimp.

Research Scopes

1. Transcriptome from shrimp ovary was identified by RNA sequencing and bioinformatics.
2. Differential gene expression was analyzed.
3. A candidate gene, *nudel*, was characterized and studied for its role in ovarian development.

Methodology

1. Animals and acclimatization
 Mature female banana shrimp were reared in 30 ppt seawater for 2-3 days before used.
2. RNA sequencing (RNA-seq) and analysis
 The ovaries isolated from female shrimp at different stages of ovarian development including previtellogenic (stage 0), early vitellogenic (stage 1), late vitellogenic



การประชุมวิชาการและนำเสนอผลงานวิจัยระดับชาติและนานาชาติ ครั้งที่ 12
 "Global Goals, Local Actions: Looking Back and Moving Forward 2021"

(stage 2), and mature stages (stage 3) based on ovarian histology and color (Ayub and Ahmed, 2002). The 3 ovaries from individual shrimp at each stage were pooled and sent to analyze for its transcriptome with the Illumina HiSeq2500 platform (Novogene, Hongkong). The raw reads were filtered to remove the reads containing adapters or reads of low quality. The clean reads were further *de novo* assembled by Trinity software (Grabherr et al., 2011). CD-hit (Fu et al., 2012) performed hierarchical clustering to remove transcripts' redundancy.

3. Gene functional annotation and differentially expressed gene (DEG) analysis

The databases such as NR (the NCBI non-redundant protein), Swiss-Prot, and COG (/KOG) were used to annotate the function of the transcriptome. In addition, the NT (the NCBI non-redundant nucleotide), KEGG, PFAM, and GO (gene ontology) databases were also used. Furthermore, differential gene expression was analyzed using Bowtie, RSEM, and DEGseq software with thresholds of \log_2 -foldchange ≥ 1 for up-regulation or ≤ -1 for down-regulation, and q-value < 0.005 (Li and Dewey, 2011; Wang et al., 2010).

4. RNA extraction and cDNA synthesis

Total RNA extraction was performed using a Trizol reagent (Ambion) according to the manufacturer's protocol. The 1 μg of total RNA was treated with DNase I. The reaction was at 37 °C for 20 min, then the 0.5 μl of 50 mM EDTA was added to the mixture before heating at 65 °C for 5 min. The DNase I-treated RNA was used as a template to construct first stranded cDNA with oligo dT- primer using the Viva cDNA synthesis kit (Vivantis). The profile was at 25 °C for 5 min, 42 °C for 60 min, and 70 °C for 10 min. The cDNA was kept at -20 °C until used.

5. Quantitative realtime PCR (qRT-PCR) analysis

The gene expression was determined by qRT-PCR analysis using a realtime PCR. The PCR mixture was composed of 1X KAPA SYBR® FAST Universal mastermix (Kapa Biosystems), 0.2 μM primer pair, and cDNA. The reaction was at 95 °C for 2 min, 40 cycles of 95 °C for 15 sec, and 60 °C for 30 sec. Then, it was heated at 95 °C for 1 min, 60 °C for 30 sec, and 95 °C for 30 sec. Elongation factor 1 α gene (EF1 α) was used as an internal control. The normalized fold of the gene expression was calculated by the $2^{-\Delta\Delta\text{CT}}$ method (Livak and Schmittgen, 2001). The primer efficiency used in qRT-PCR was about 95-100 % according to the amplification with the serial dilution of the cDNA and calculated by the equation of efficiency = $[10^{(-1/\text{slope})} - 1]$.

6. Determination of the candidate gene expression in shrimp tissues and ovarian developmental stages

The different tissues including eyestalk, brain, thoracic ganglia, gill, hepatopancreas, muscle, and ovary were isolated from 2 previtellogenic shrimp. Also, the



การประชุมวิชาการและนำเสนอผลงานวิจัยระดับชาติและนานาชาติ ครั้งที่ 12
 "Global Goals, Local Actions: Looking Back and Moving Forward 2021"

ovary and hepatopancreas were isolated from 3-7 individual shrimps at each ovarian development stage. Those tissues samples were extracted for their total RNA and subsequently used to synthesize for cDNA as mentioned in 4. The relative quantification of gene expression was evaluated by qRT-PCR analysis as described above.

7. Construction and expression of the gene-specific dsRNA

The recombinant plasmid carrying the inverted repeat sequence of *nudel* was constructed and used to express for *nudel* specific dsRNA (dsNudel). The nucleotides corresponding to a region of the *nudel* sequence, including stem and stem-loop fragments were amplified by PCR with specific primers using the ovarian cDNA as a template. Their fragments were cloned in pET28a plasmid as the expression vector. The sequence was confirmed by DNA sequencing. Afterward, the recombinant plasmid was further transformed in *Escherichia coli* HT115. The bacteria was cultured in LB broth at 37 °C, 180 rpm for overnight. Then, the bacterial starter was inoculated in a new LB broth and cultured until OD₆₀₀ was 0.4-0.8. The bacterial was added with 0.2 mM IPTG and then incubated for 2-3 hours. The bacterial cells were harvested and extracted by the ethanol method (Posiri et al., 2013). The dsRNA was confirmed for its dsRNA features by RNase digestion assay. In addition, a green fluorescent protein (GFP) from pHMGFP plasmid was used to construct GFP-specific dsRNA as a non-specific dsRNA.

8. Effect of the candidate gene knockdown on vitellogenesis in female shrimps

Previtellogenic female shrimps were injected with the 3 µg/g body weight of dsNudel or dsGFP. The 5-8 shrimps were used in each group. On days 7, the shrimps in each group were injected with the same concentration of the dsRNA and cultured for next 3 days. On day 10, their ovaries were determined for *Nudel* and *vitellogenin* expression by qRT-PCR.

9. Data analysis

All results from qRT-PCR analysis were statistically analyzed with one-way ANOVA followed by pair-wise comparison by Scheffe's method. The difference and relationship between groups were considered statistically significant at a *p*-value < 0.05.

Results

1. Sequencing analysis, functional annotation, and DEG analysis

A total of 32,176 transcripts were obtained from *de novo* assembly of raw reads using Trinity. After hierarchically clustered and removed for the redundant transcripts, the 32,160 longest transcripts of each cluster were obtained with assembly statistics (Table 1). Then, the unigenes were annotated against the NR, NT, Swiss-Prot, KOG, KEGG, PFAM, and GO databases. The result showed that the most unigenes were annotated with the NR, GO,



การประชุมวิชาการและนำเสนอผลงานวิจัยระดับชาติและนานาชาติ ครั้งที่ 12
 "Global Goals, Local Actions: Looking Back and Moving Forward 2021"

and PFAM databases (Figure 1A). In addition, a total of 241 unigenes were differentially expressed between ovarian developmental stages as shown in Figure 1B. Some genes can express in more than one group. The number of up-regulated genes in compared stages of 3 and 1, 2 and 0, and 2 and 1, were higher than other groups. On the other hand, the number of down-regulated genes in compared stages of 2 and 0, 2 and 1, and 3 and 2, were higher than other groups (Figure 1B).

Table 1: Summary statistics for the *de novo* assembly of the *F. merguensis*'s transcriptome.

Transcriptome assembly statistics	
Number of transcripts	32,176
Number of unigenes	32,160
• GC (%)	43.12
• Longest contig length (bp)	16,137
• Shortest contig length (bp)	201
• Average contig length (bp)	1,485
• Contig N50 (bp)	6,988
• Total bases	47,775,273

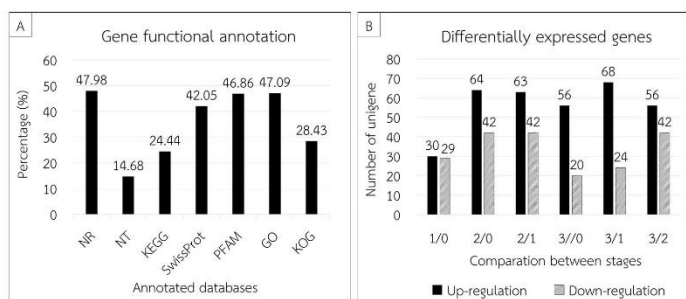


Figure 1: The percentage of unigenes successfully annotated in the databases (A). The number of genes which were uniquely expressed differentially between the stages and some genes expressed in two or more groups (B).

2. Expression profiles of the *nudel* in ovarian developmental stages and tissues

In this study, the *nudel* was selected as a candidate gene due to its expression level was a one of the highest differential expression among ovarian developmental stages. Its expression was up-regulated in mature stage 3 compared with previtellogenic stage. In



การประชุมวิชาการและนำเสนอผลงานวิจัยระดับชาติและนานาชาติ ครั้งที่ 12
 "Global Goals, Local Actions: Looking Back and Moving Forward 2021"

addition, its role is involved in reproductive processes such as dorsal/ventral axis, regulation of Toll signaling pathway, and egg activation. The *nudel* expression was determined in various tissues. The result showed that the *nudel* expression was the significantly highest only in ovary compared to other tissues (Figure 2A), suggesting its specific function in gonads. According to its expression in ovary, the ovarian tissues at each ovarian development stage were determined by qRT-PCR. The result showed that the *nudel* expression was significantly high in stage 0 and rapidly low in stage 1. Then, it slightly increased in stage 2 and gradually decreased in stage 3. However, the *nudel* expression from qRT-PCR was not similar profile to the prediction of DEG derived from transcriptome analysis (Figure 2B).

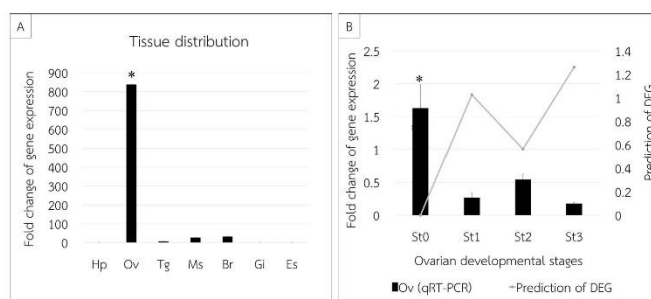


Figure 2: The *nudel* expression in various tissues (A) and ovarian tissue during ovarian developmental stages (B) were performed by qRT-PCR. The tissues including thoracic ganglia (Tg), muscle (Ms), eyestalk (Es), brain (Bn), gills (Gi), hepatopancreas (Hp), and ovary (Ov). The ovarian development stages classified into 4 stages including previtellogenic (st0), early vitellogenic (st1), late vitellogenic (st2), and mature stages (st3). Bars and error bars were means and SEM, respectively. An asterisk indicated significant differences between groups analyzed by one-way ANOVA ($p < 0.05$).

3. Production of the *nudel* specific dsRNA

The inverted repeat nucleotide sequence of *FmNudel* and *GFP* were cloned in the pET28a plasmid, and subsequently transformed in *E. coli* HT115 (DE3). Both dsNudel and dsGFP were produced in bacterial system. For the determination of their feature, their extracted total RNAs were treated using RNase digestion. The RNase A and RNase III specifically digested ssRNA and dsRNA, respectively. At the results, both dsNudel and dsGFP were degraded with RNase III but not with RNase A (Figure 3). The result indicated that that both RNAs were a double-stranded structure.



การประชุมวิชาการและนำเสนอผลงานวิจัยระดับชาติและนานาชาติ ครั้งที่ 12
 "Global Goals, Local Actions: Looking Back and Moving Forward 2021"

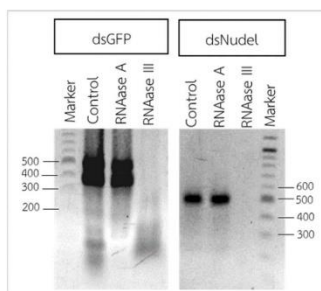


Figure 3: The production and RNase digestion of dsNudel and dsGFP. Both dsNudel and dsGFP produced from *E. coli* were digested with RNase A or RNase III. The result of the digestion was analyzed by agarose gel electrophoresis. The left and right lanes were a DNA ladder.

4. Effect of *FmNudel* silencing on vitellogenesis in female *F. merguensis*

The previtellogenic female shrimps were injected with dsNudel or dsGFP. On 10 days, their ovarian tissue was isolated and determined the effect of *nudel* knockdown on the expression of *nudel* and *vitellogenin* (*Vg*) by qRT-PCR. The result showed that the *nudel* expression was significantly decreased approximately a 2-fold in dsNudel-injected shrimp compared with the dsGFP-injected shrimp, indicating the suppression of *nudel* expression by dsNudel. Interestingly, *Vg* expression was significantly dropped approximately 10-fold in *nudel* knockdown shrimp when compared with dsGFP-injected shrimp. The result suggested that the *nudel* expression involved in control of the *Vg* expression (Figure 4).



การประชุมวิชาการและนำเสนอผลงานวิจัยระดับชาติและนานาชาติ ครั้งที่ 12
 "Global Goals, Local Actions: Looking Back and Moving Forward 2021"

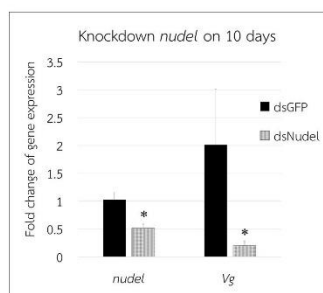


Figure 4: Effect of *FmNudel* knockdown on *Vg* mRNA expression on day 10. The ovary was determined for *FmNudel* and *Vg* expressions by qRT-PCR. Bars and error bars were means and SEM, respectively. An asterisk indicated significant differences between groups analyzed by one-way ANOVA ($p < 0.05$).

Discussion

In this study, the *nudel* was most expressed in ovary in female banana shrimp (Figure 2A), similar to the *nudel* (*ndl*) was reported to be female-specific gene in the ovaries of the *Drosophila* (Hong and Hashimoto, 1996) and shrimp, *Marsupenaeus japonicus* (Callaghan et al., 2010). Furthermore, the *nudel* expression profile during the ovarian development in ovary was significantly increased in previtellogenic stage (st0) compared with other stages (Figure 2B). However, the *nudel* expression from prediction of DEG and from qRT-PCR analysis during the ovarian development was not similar profile (Figure 2B) because our transcriptome having only one biological replicate, this may be provided some unstable data. In addition, the *nudel* was determined the ovarian stimulating role using *FmNudel* injection in shrimp. After the injection 10 days, the *Vg* expression was significantly decreased only in ovaries (Figure 4). These results indicated that *FmNudel* plays roles in the ovarian developmental processes and stimulated vitellogenesis in ovary.

The ovarian developmental role of *nudel* gene in crustacean has not been reported so far. This study may be the first report of *nudel* for ovarian development in shrimp. However, some studies especially in *Drosophila* have been reported that the *nudel* are expressed in ovarian follicle cells and encoded a multi-functional protein with serine protease domain. It requires for the activation of the Toll signaling pathway associated with determination of dorsoventral axis in early embryogenesis. Also, the *nudel* involves in a role in structural integrity of the membrane which is a cross-linking of the vitelline membrane between the follicle cell layer and the embryo (Hong and Hashimoto, 1996; LeMosy et al., 1999; LeMosy and Hashimoto, 2000; Turcotte and Hashimoto, 2002).



การประชุมวิชาการและนำเสนอผลงานวิจัยระดับชาติและนานาชาติ ครั้งที่ 12
 "Global Goals, Local Actions: Looking Back and Moving Forward 2021"

Conclusions

A total of 32,160 unigenes obtained transcriptome analysis were annotated against the NR, NT, Swiss-Prot, KOG, KEGG, PFAM, and GO databases. The unigenes was also analyzed for differential expression level giving a total of 241 differential expression gene. The *nudel* was selected as a candidate gene due to its analysis involved in reproductive processes, had a high expression level, and expressed for up-regulated gene. In experiments, the characterization and functional of *nudel* were investigated in female banana shrimp. The *nudel* was a high expression in ovarian tissue and significantly increased in previtellogenic stage (st0) during ovarian development in ovary. The silencing of *FmNudel* affected the decrease of *Vg* expression in ovary.

Supplement table: Oligonucleotides used in this study

Primer name	Forward sequence (5' → 3')	Purpose
oligo-dT (PRT)	CCGGAATTC AAGCTTCTAGAGGATCCTTTTTTTTTTTTTTTTTT	cDNA synthesis
qFm-Vg-F	TCCATCTGCAGCACCAATCTTCGC	qRT-PCR
qFm-Vg-R	GCAACAGCCTTCATTCTGATGCCA	qRT-PCR
qFm-EF1 α -F	GAACTGCTGACCAAGATCGACAGG	qRT-PCR
qFm-EF1 α -R	GAGCATACTGTTGGAAGTCTCCA	qRT-PCR
Stem-GFP-F	GCG-XbaI-AGCAGACTATGGACCTGACC	Cloning
Stem-GFP-R	GCT-NdeI-ATCTTCTCGGTACTGGGCTC	Cloning
Stem-loop-GFP-F	AA-NotI-AGCAGACTATGGACCTGACC	Cloning
Stem-loop-GFP-R	GCT-NdeI-ACGAAGTGGTAGTCGGGAAG	Cloning
Stem-Nudel-F	GGG-XhoI-GAAAAGTCTCCTCCGCCGAT	Cloning
Stem- Nudel -R	GGG-HindIII-ACGTCTAGCAACCCGT	Cloning
Stem-loop- Nudel -F	GGG-XbaI-GAAAAGTCTCCTCCGCCGAT	Cloning
Stem-loop- Nudel -R	GGG-HindIII-CACCAATTCGTGCAAAGGC	Cloning

References

- Altschul, S. F. et al. (1997). Gapped BLAST and PSI-BLAST: a new generation of protein database search programs. *Nucleic acids research*. 25(17), 3389-3402.
- Ayub, Z., and Ahmed, M. (2002). A description of the ovarian development stages of penaeid shrimps from the coast of Pakistan. *Aquaculture Research*. 33(10), 767-776.
- Benzie, J. A. (1998). Penaeid genetics and biotechnology. *Aquaculture*, 164(1-4), 23-47.
- Buchfink, B., Xie, C., and Huson, D. H. (2015). Fast and sensitive protein alignment using DIAMOND. *Nature methods*. 12(1), 59-60.



การประชุมวิชาการและนำเสนอผลงานวิจัยระดับชาติและนานาชาติ ครั้งที่ 12
 "Global Goals, Local Actions: Looking Back and Moving Forward 2021"

- Callaghan, T. R., Degnan, B. M., and Sellars, M. J. (2010). Expression of sex and reproduction-related genes in *Marsupenaeus japonicus*. *Marine Biotechnology*. 12(6), 664-677.
- Food and Agriculture Organization of the United Nations. (2020). Fisheries Statistical Database, Rome.
- Fu, L. et al. (2012). CD-HIT: accelerated for clustering the next-generation sequencing data. *Bioinformatics*, 28(23), 3150-3152.
- Götz, S. et al. (2008). High-throughput functional annotation and data mining with the Blast2GO suite. *Nucleic acids research*. 36(10), 3420-3435.
- Grabherr, M. G. et al. (2011). Full-length transcriptome assembly from RNA-Seq data without a reference genome. *Nature biotechnology*. 29(7), 644-652.
- Hong, C. C., and Hashimoto, C. (1996). The maternal nude1 protein of *Drosophila* has two distinct roles important for embryogenesis. *Genetics*. 143(4), 1653-1661.
- LeMosy, E. K., and Hashimoto, C. (2000). The nudel protease of *Drosophila* is required for eggshell biogenesis in addition to embryonic patterning. *Developmental biology*. 217(2), 352-361.
- LeMosy, E. K., Hong, C. C., and Hashimoto, C. (1999). Signal transduction by a protease cascade. *Trends in cell biology*. 9(3), 102-107.
- Li, B., and Dewey, C. N. (2011). RSEM: accurate transcript quantification from RNA-Seq data with or without a reference genome. *BMC bioinformatics*. 12(1), 323.
- Livak, K. J., and Schmittgen, T. D. (2001). Analysis of relative gene expression data using real-time quantitative PCR and the $2^{-\Delta\Delta CT}$ method. *Methods*. 25(4), 402-408.
- Merlin, J. et al. (2015). Induction of vitellogenesis and reproductive maturation in tiger shrimp, *Penaeus monodon* by 17β -estradiol and 17α -hydroxyprogesterone: in vivo and in vitro studies. *Invertebrate Reproduction and Development*. 59(3), 166-175.
- Moriya, Y. et al. (2007). KAAS: an automatic genome annotation and pathway reconstruction server. *Nucleic acids research*. 35(suppl_2), W182-W185.
- Posiri, P., Ongvarrasopone, C., and Panyim, S. (2013). A simple one-step method for producing dsRNA from *E. coli* to inhibit shrimp virus replication. *Journal of virological methods*. 188(1-2), 64-69.
- Punta, M. et al. (2012). The Pfam protein families database *Nucleic Acids Res*. 40. D290-D301
 Atom-1 Force Constant Equilibrium Atom-2 Residue Atom (kcal·mol⁻¹·Å⁻²)
 Distance (Å) Residue Atom Y, 397.
- Sharabi, O. et al. (2016). Identification and characterization of an insulin-like receptor involved in crustacean reproduction. *Endocrinology*. 157(2), 928-941.



การประชุมวิชาการและนำเสนอผลงานวิจัยระดับชาติและนานาชาติ ครั้งที่ 12
 "Global Goals, Local Actions: Looking Back and Moving Forward 2021"

- Treerattrakool, S., Panyim, S., and Udomkit, A. (2011). Induction of ovarian maturation and spawning in *Penaeus monodon* broodstock by double-stranded RNA. *Marine biotechnology*. 13(2), 163-169.
- Treerattrakool, S. et al. (2008). Molecular characterization of gonad-inhibiting hormone of *Penaeus monodon* and elucidation of its inhibitory role in *vitellogenin* expression by RNA interference. *The FEBS journal*. 275(5), 970-980.
- Turcotte, C. L., and Hashimoto, C. (2002). Evidence for a glycosaminoglycan on the nudel protein important for dorsoventral patterning of the *Drosophila* embryo. *Developmental dynamics: an official publication of the American Association of Anatomists*. 224(1), 51-57.
- Uawisetwathana, U. et al. (2011). Insights into eyestalk ablation mechanism to induce ovarian maturation in the black tiger shrimp. *PloS one*. 6(9), e24427.
- Wang, L. et al. (2010). DEGseq: an R package for identifying differentially expressed genes from RNA-seq data. *Bioinformatics*. 26(1), 136-138.
- Wongprasert, K. et al. (2006). Serotonin stimulates ovarian maturation and spawning in the black tiger shrimp *Penaeus monodon*. *Aquaculture*. 261(4), 1447-1454.

VITAE

Name: Miss Manita Nonsung
 Student ID: 6110220077
 E-mail: manitan@kkumail.com

Education

2018 – present M.Sc. (Molecular Biology and Bioinformatics), Prince of Songkla University, Thailand
 Thesis title: Identification and Functional Study of Potential Receptors Involved in Vitellogenesis of Female Banana Shrimp *Fenneropenaeus merguensis*

2014 – 2017 B.Sc. (Biology), 2nd Class Honors, Khon Kaen University, Thailand
 Thesis title: Standardized Karyotype and Idiogram of the Long-Whiskered Catfish (*Mystus gulio* Hamilton, 1822) by Conventional Staining and NOR Banding Techniques

Scholarship Awards during Enrolment

Science Achievement Scholarship of Thailand (SAST)

List of Publication and Proceeding

Nonsung, M., Sanget, U., and Sathapondacha, P. 2021. Transcriptome analysis in ovary of female banana shrimp, *Fenneropenaeus merguensis*: A functional study of *nucl* as a potential gene involved in the ovarian development. รายงานการประชุมวิชาการเสนอผลงานวิจัยระดับชาติและนานาชาติ, 1(12), 52.